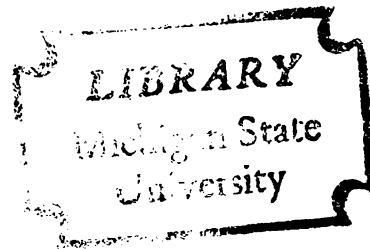EXPERIMENTAL INVESTIGATION OF TRANSIENT
THERMAL PROPERTY CHANGES OF ALUMINUM
2024 - T351

Dissertation for the Degree of Ph. D.
MICHIGAN STATE UNIVERSITY
SAMI RAOUF AL - ARAJI
1973
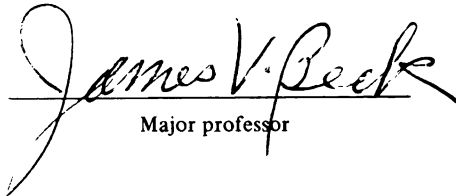
This is to certify that the

thesis entitled

EXPERIMENTAL INVESTIGATION OF TRANSIENT THERMAL
PROPERTY CHANGES OF ALUMINUM 2024-T351

presented by

Sami Raouf Al-Araji

has been accepted towards fulfillment
of the requirements for

___Ph.D.___ degree in _Mechanical_ Engineering

Major professor

Date __October 12, 1973__

O-7639

AA37

120
100   R65

q ——— R53

q ——— 106

ABSTRACT

EXPERIMENTAL INVESTIGATION OF TRANSIENT THERMAL
PROPERTY CHANGES OF ALUMINUM 2024-T351

By

Sami Raouf Al-Araji

When as-received aluminum 2024-T351 is heated to
350 °F, changes in the microstructure take place. These
changes are further enhanced by heating to higher temper-
atures and/or longer times.

This heating results in increases in the thermal
conductivity (k) and specific heat (c_p) values of the
aluminum. A simplified method proposed by Beck was used to
determine the transient values of k and c_p.

It was found that the changes in k can approach 25%
while those for c_p are less. The changes in k follow a
certain pattern. This pattern begins with a value of k
when the specimen arrives at a given temperature (in the
range 350 to 425 °F) then k increases to some maximum value
while it is maintained at that temperature. The rate of
increase depends on the temperature level (the closer the
temperature to 425 °F the faster it arrives at the maximum
value). After it stays at the maximum value for a period

of time (for example, at 425 °F it stays for about 15 to 20 minutes) k starts to drop until it reaches a certain value where it remains relatively constant with time. At this stage the aluminum becomes over-aged.

It was found that the over-aged value of k at room temperature as well as the high temperatures is close to that obtained by the regular annealing process. In order to predict the k values of aluminum 2024-T351 for different temperatures and times, a mathematical model was developed based on the data obtained in this study.

EXPERIMENTAL INVESTIGATION OF TRANSIENT THERMAL

PROPERTY CHANGES OF ALUMINUM 2024-T351

By

Sami Raouf Al-Araji

A DISSERTATION

Submitted to
Michigan State University
in partial fulfillment of the requirements
for the degree of

DOCTOR OF PHILOSOPHY

Department of Mechanical Engineering

1973

ACKNOWLEDGMENTS

TABLE OF CONTENTS

LIST OF TABLES

LIST OF FIGURES

LIST OF SYMBOLS

c_I	integrator constant
c_p	specific heat
c_v	constant ($\frac{°F}{volt}$)
E	length or thickness of specimen
e	half of the washer thickness (in the washer-type thermocouple)
h	contact conductance
k	thermal conductivity
k_{max}	maximum value of thermal conductivity with time, at temperature
k_{min}	value of thermal conductivity as soon as the specimen arrives at the desired temperature
k^+	normalized thermal conductivity, taken to be $\frac{k - k_{min}}{k_{max} - k_{min}}$ for a given temperature.
T	temperature
t	time
t_e	effective time
t_f	final time (end of the test) normally taken to be about 60 seconds
t_{max}	time at which thermal conductivity becomes maximum

t^+ normalized time, taken to be $\dfrac{t}{t_{max}}$

$\dfrac{Q}{A}$ integrated heat flux $\left(\dfrac{Btu}{ft^2}\right)$

$\dfrac{q}{A}$ heat flux $\left(\dfrac{Btu}{hr\ ft^2}\right)$

R^i_j thermal resistance $= \dfrac{\Delta x}{k^i_j}$

α thermal diffusivity

α (phase diagram) solution of copper in aluminum

β thermal linear expansion of a material

Θ (phase diagram) solution of aluminum in the inter-metallic compound $CuAl_2$

ρ density

CHAPTER I

INTRODUCTION

Aluminum 2024-T351 belongs to a class of materials that undergo certain changes in microstructure when subjected to high temperatures (for aluminum 350-400 °F). These microstructure changes result in changes in the thermal properties of the alloy, namely an increase in the thermal conductivity (k) and specific heat (c_p) values. These time as well as temperature dependent thermal properties have not previously been measured for aluminum 2024-T351 or any other material that undergoes similar metallurgical changes. Because of the need of predicting temperature utilizing known thermal properties of materials, a relatively simple experimental method was developed by Beck [1] to measure the thermal properties.

This is a multi-property method capable of measuring the thermal conductivity (k), specific heat (c_p), thermal diffusivity (α), and contact conductance (h) simultaneously over a short period of time for a wide range of temperatures. It can be used to determine the thermal properties

1

of a class of materials that change while held at a given temperature. This implies that the method must be transient. Some of the materials that can be tested using this method are aluminum 2024-T351, ferrous alloys, biological materials, plastics, and other alloys that undergo phase change when heated. Since aluminum 2024-T351 exhibits the unique behavior described earlier, and its importance from a machine design aspect, it was chosen to be the principal material to be investigated.

The problem can be considered to have the following objectives,

    a. Development of the experimental procedures by using a reference material while simultaneously adding needed components to complete the building of the experimental apparatus;

    b. Investigating aluminum 2024-T351 by determining its transient thermal properties, namely the thermal conductivity (k) and specific heat (c_p); and

    c. Development of a mathematical model based on the thermal conductivity data obtained in part b above, and utilizing this model to determine the k values of aluminum 2024-T351 for different temperatures and times.

1.1 Importance of the problem

The problem of developing and applying the new method of thermal property measurement is considered important because of a number of reasons.

1. That the simplified method is a rapid, transient method is in itself important. This is because the method can be used to make measurements that cannot otherwise be made during a single experiment. It is also because rapid measurements result in reduced cost.

2. It is a multi-property determination method which can be used to measure k, c_p, α, and h simultaneously.

3. By knowing the thermal properties of a material, temperatures and heat fluxes can be predicted in situations previously not possible. An example is predicting temperatures of aluminum 2024-T351 after determining its transient thermal conductivity behavior.

4. New data of $k(t,T)$ and $c_p(t,T)$ of aluminum 2024-T351 at different times and temperatures is given for each individual specimen as well as grouped for each selected temperature (example the individual curves and the composite curves respectively). This data is new and has not been reported previously, because rapid transient methods of measuring thermal properties were not available.

5. The effectiveness of the experimental procedure of holding the specimen at a fixed temperature while finding its thermal properties is demonstrated.

6. By providing hitherto non-existent data of the time dependence of k and c_p of aluminum 2024-T351, solid state physicists and material scientists may be aided in understanding such phenomena as stored energy, lattice dislocation, etc.

1.2 Literature review

This section gives a review of various transient methods of thermal property measurement. The difference between these methods and that used herein are particularly noted. Let us begin with a general one-dimensional heat conduction equation which can be written as

$$\frac{1}{r^n} \frac{\partial}{\partial r} (r^n k \frac{\partial T}{\partial r}) = \rho c_p \frac{\partial T}{\partial t} \qquad (1.2.1)$$

If

n = 0	r → x	rectangular coordinates
n = 1	r → r	cylindrical coordinates
n = 2	r → r	spherical coordinates

where

T = temperature

t = time

x = position in rectangular coordinates

r = position in cylindrical or spherical coordinates

ρ = density of material.

The simplest, and usually the preferred, geometry is the flat plate (n = 0).

The following are examples of some transient methods of thermal property measurement.

(1) The line-source method

The line-source method is one of the oldest methods of measuring thermal conductivity. It is based on the equation for temperature rise with time of an infinitely long line heat source which receives energy at a constant rate. The body of material surrounding the line is thermally infinite and the initial temperature is uniform.

Suppose energy is liberated at the rate of $\rho c_p \phi(t)$ per unit time per unit length of a line parallel to the z-axis and through the point (x',y') where ($\phi(t)$ is $q_\ell(\frac{Btu}{ft\ hr})$). If heating starts at $t = 0$ when the solid is at zero temperature, then the temperature at time t is, see [2]

$$T(t) = \frac{1}{4\pi\alpha} \int_o^t \phi(t') e^{-r^2/4\alpha(t-t')} \frac{dt'}{t-t'} \qquad (1.2.2)$$

where $r^2 = (x-x')^2 + (y-y')^2$.

If $\phi(t)$ is set equal to a constant which is designated q_ℓ(Btu/ft-hr), (1.2.2) becomes

$$T(t) = \frac{q_\ell}{4\pi\alpha} \int_{\frac{r^2}{4\alpha t}}^{\infty} \frac{e^{-u} du}{u}$$

where $u = \frac{r^2}{4\alpha(t-t')}$, α = thermal diffusivity; it can also be written as

$$T(t) = -\frac{q_\ell}{4\pi\alpha} Ei\left(-\frac{r^2}{4\alpha t}\right) \qquad (1.2.3)$$

where $-Ei(-x) \equiv \int_x^\infty \frac{e^{-u}}{u} du$ is the exponential integral. For small values of x, $Ei(-x)$ can be approximated by $Ei(-x) = \gamma + \ln x - x + (1/4)x^2 + 0(x^3)$, where γ is Euler's constant, 0.5772156. Thus for large values of time t,

$$T(t) = \frac{q_\ell}{4\pi\alpha} \ln\frac{4\alpha t}{r^2} - \frac{\gamma q_\ell}{4\pi\alpha} \qquad (1.2.4)$$

or

$$T(t) = \frac{q_\ell}{4\pi\alpha} [\ln t + \ln\frac{4\alpha}{r^2} - \gamma].$$

Taylor and Underwood, used this method to determine thermal conductivity values for plastics; for their work and the values they obtained see [3].

An extension of the line-source method is the thermal conductivity probe. It is used to measure k for granular materials, soils, and rocks. The basic equation is

$$\Delta T = \frac{q_\ell}{4\Pi k} \ln \frac{(t_2 - t_c)}{(t_1 - t_c)} \qquad (1.2.5)$$

where t_c (time constant) is called the calibration factor, and is determined experimentally for each probe and it is valid only for use with a specific type of material. Wechsler and Kritz [4], used this method to determine k of several materials by utilizing different designs of probes.

The new method is different from the line-source method and its extensions because

1. The line-source method is quasi-steady state while the new method is transient;

2. The geometries are different; and

3. The line-source method is not a multi-property method.

2. The modified Angstrom method of determining thermal diffusivity.

For the modified Angstrom method of determining thermal diffusivity the sample is in the form of a semi-infinite rod, although the method could be applied to other geometrical shapes. The one-dimensional partial differential equation that gives the temperature T above the ambient temperature at any position x and time t is

$$\alpha \left(\frac{\partial^2 T}{\partial x^2}\right) = \frac{\partial T}{\partial t} + \mu T \qquad (1.2.6)$$

where α is the thermal diffusivity and μ is the coefficient of surface heat loss which takes into account any heat loss by radiation, conduction, and convection. At high temperatures the radiation loss will predominate and μ will vary as the cube of the absolute ambient temperature. Since T is small, only a few degrees at most, the heat loss by radiation, as well as the heat loss by conduction and convection to any gas surrounding the rod, may be assumed to vary linearly with temperature difference (Newton's law of cooling). If radiation is predominant, use of the correct temperature dependence (Stefan-Boltzmann law), in which the radiation varies as the fourth power of the respective temperatures, would not improve the accuracy of the method and would enormously increase the labor of computation.

If a heat source whose temperature varies sinusoidally with time is located at one end of a semi-infinite radiating rod, the boundary conditions for T(x,t) will be

$$T(0,t) = A_0 + A_1 \cos (\omega t + \varepsilon) \qquad (1.2.7)$$

and

$$T(\infty,t) = 0 \qquad (1.2.8)$$

Then the solution of (1.2.6-8) is given by Sidles and Danielson [5] to be

$$T(x,t) = A_0 \exp(-a_0 x) + A_1 \exp(-a_1 x) \cos(\omega t - b_1 x + \varepsilon)$$

$$(1.2.9)$$

where (A_0, A_1, and ε are arbitrary constants), and

$$a_0 = (\frac{\mu}{\alpha})^{1/2} \qquad (1.2.10)$$

$$a_1 = \{(\frac{1}{2\alpha})[(\mu^2+\omega^2)^{1/2} + \mu]\}^{1/2} \qquad (1.2.11)$$

$$b_1 = \{(\frac{1}{2\alpha})[(\mu^2+\omega^2)^{1/2} - \mu]\}^{1/2} \qquad (1.2.12)$$

The temperature oscillations produced at $x = 0$ will be propagated along the rod with a velocity

$$v = \frac{\omega}{b_1} \qquad (1.2.13)$$

and will have an amplitude decrement

$$q = \frac{\exp(-a_1 x_1)}{\exp(-a_1 x_2)} = \exp a_1 L \qquad (1.2.14)$$

The quantity $L = x_2 - x_1$ is the distance between two thermocouples, one placed in the rod at $x = x_1$ and the other placed in the rod at $x = x_2$.

From equations (1.2.13) and (1.2.14),

$$a_1 b_1 = \frac{\omega(\ln q)}{Lv} \qquad (1.2.15)$$

and, from equations (1.2.11) and (1.2.12),

$$a_1 b_1 = \frac{\omega}{2\alpha} \qquad (1.2.16)$$

Eliminating $a_1 b_1$ from equations (1.2.15) and (1.2.16) we get the basic equation for the experimental determination of thermal diffusivity

$$\alpha = \frac{L\nu}{2\ln q} \qquad (1.2.17)$$

If the density (ρ) and specific heat (c_p) of the material are known, then the thermal conductivity (k) of the material can be determined from

$$k = \alpha\rho c_p \qquad (1.2.18)$$

For the experimental determination of (α) and the procedure followed see Sidles and Danielson [5]. The new method is different from the modified Angstrom method since

1. The modified Angstrom method is quasi-steady state while the new method is transient;

2. The geometries are different (semi-infinite and finite); and

3. The modified Angstrom method yields directly only the thermal diffusivity, while the new method is a multi-property method.

3. The Flash Method

    The flash method was first developed and reported by Parker, Jenkins, Butler, and Abbott [6]. This method can be used to measure the thermal diffusivity, heat capacity, and thermal conductivity of a very small specimen. The energy of a high-intensity, short-duration light pulse is absorbed in the front surface of a specimen coated with a few millimeters camphor black. The resulting temperature history of the insulated rear surface is

measured by a thermocouple and recorded with an oscilloscope and camera.

Theory of the method:

If the initial temperature distribution in a thermally insulated plate of uniform thickness (L) is $T(x,0)$, the temperature distribution at any later time (t) is [6]

$$T(x,t) = \frac{1}{L} \int_o^L T(x,0)\,dx + \frac{2}{L} \sum_{n=1}^{\infty} e^{-n^2\Pi^2\alpha t/L^2} \cos\frac{n\Pi x}{L} \int_o^L T(x',0) \cos\frac{n\Pi x'}{L}\,dx'$$

$$(1.2.19)$$

when a pulse of radiant energy $\frac{Q}{A}$ $(\frac{Btu}{ft^2})$ is instantaneously and uniformly absorbed in the small depth g at the front surface $x = 0$ of a thermally insulated solid of uniform thickness L, the temperature distribution at that instant is given by

$$T(x,0) = \frac{\frac{Q}{A}}{\rho c_p g} + T_i \quad \text{for } 0<x<g \qquad (1.2.20)$$

and

$$T(x,0) = T_i \quad \text{for } g<x<L.$$

With this initial condition, equation (1.2.19) can be written as

$$T(x,t) = \frac{\frac{Q}{A}}{\rho c_p L} \left[1 + 2 \sum_{n=1}^{\infty} \cos \frac{n\Pi x}{L} \frac{\sin(n\Pi g/L)}{(n\Pi g/L)} e^{-n^2 \Pi^2 \alpha t/L^2} \right] + T_i$$

$$(1.2.21)$$

where ρ is the density in $\frac{lbm}{ft^3}$ and c_p is the heat capacity in $\frac{Btu}{lbm-F}$. In this application only a few terms are needed. Since g is a very small number for opaque materials, it follows that $\sin \frac{n\Pi g}{L} \approx \frac{n\Pi g}{L}$. At the rear surface where x = L, the temperature history can be expressed by

$$T(L,t) = \frac{\frac{Q}{A}}{\rho c_p L} \left[1 + 2 \sum_{n=1}^{\infty} (-1)^n e^{-n^2 \Pi^2 \alpha t/L^2} \right] + T_i \qquad (1.2.22)$$

Two dimensionless parameters, V and ω, can be defined

$$V(L,t) = \frac{T(L,t) - T_i}{T_M - T_i} \qquad (1.2.23)$$

$$\omega = \frac{\Pi^2 \alpha t}{L^2} \qquad (1.2.24)$$

T_M represents the maximum temperature at the rear surface,

$$T_M = \frac{\frac{Q}{A}}{\rho c_p L} + T_i$$

The combination of (1.2.22), (1.2.23), and (1.2.24) yields

$$V = 1 + 2 \sum_{n=1}^{\infty} (-1)^n e^{(-n^2 \omega)} \qquad (1.2.25)$$

V is plotted versus ω in [6].

Many ways of determining α have been suggested. One of these is the "one-half time" method of analysis. When V is equal to 0.5, ω is equal to 1.38, and so

$$\alpha = (1.38L^2/\Pi^2 t_{1/2}), \qquad (1.2.26)$$

where $t_{1/2}$ is the time required for the back surface to reach one half of the maximum temperature rise.

In another method of analysis the time axis intercept of the extrapolated straight line portion of the curve (V versus ω in [6]) is approximately $\omega = 0.48$, which yields the relationship,

$$\alpha = (0.48L^2/\Pi^2 t_x), \qquad (1.2.27)$$

where t_x is the time axis intercept of the temperature versus time curve. The values of diffusivity determined by equation (1.2.27) are considerably less precise than those determined by equation (1.2.26). The method given by (1.2.27) requires the finding, by eye, of the straight portion of a curve and the extrapolation of this line back to the baseline. This is a subjective method which is rather difficult and one in which a small error in the slope determination results in a relatively large error in the value of the diffusivity. Its advantage is that it is independent of the final height of the curve and does not require that the surface distribution of energy be as uniform as does the half-time method. It is not necessary

to know the amount of energy absorbed in the front surface
in order to determine α. However, this quantity must be
determined if measurements of specific heat or thermal
conductivity are required. The product of the density and
the heat capacity of the material is given by (assuming no
heat losses)

$$\rho c_p = \frac{\frac{Q}{A}}{L(T_M - T_i)} \qquad (1.2.28)$$

and then the thermal conductivity is given by

$$k = \alpha \rho c_p \qquad (1.2.29)$$

The foregoing treatment has neglected the variation
of thermal diffusivity with temperature. The method
produces an effective value of diffusivity for the sample.
The effective value of the corresponding temperature is
arbitrarily picked to be the time average of the mean of
the front and back surface temperatures up to the time that
the rear surface reaches one-half of its maximum value.

The dimensionless parameter $V(L,t)$ at the rear
surface is given by (1.2.25). The dimensionless parameter
$V(0,t)$ at the front surface obtained in a similar manner is
given by

$$V(0,t) = 1 + 2 \sum_{n=1}^{\infty} e^{(-n^2 \omega)}, \qquad (1.2.30)$$

which is observed to be infinite at $\omega = 0$. This is not a realistic physical value. The mean value of $V(L,t)$ and $V(0,t)$ is

$$\frac{V(0,t) + V(L,t)}{2} = 1 + 2 \sum_{n=1}^{\infty} e^{(-4n^2\omega)} \qquad (1.2.31)$$

and the effective value of V is

$$V_e = 1 + \frac{2}{\omega_{1/2}} \int_o^{\omega_{1/2}} \sum_{n=1}^{\infty} e^{(-4n^2\omega)} d\omega \qquad (1.2.32)$$

where $\omega_{1/2} = \frac{\pi^2 \alpha t}{L^2} = 1.38$,

$$V_e = 1 + \frac{2}{4(1.38)} [\sum_{n=1}^{\infty} \frac{1}{n^2} (1 - e^{-4n^2 1.38})] = 1.6 \qquad (1.2.33)$$

Therefore, $T_e - T_i = V_e(T_M - T_i) = 1.6(T_M - T_i)$ (1.2.34)

In this method several simplifying assumptions are made.

1. One-dimensional heat flow is assumed.
2. The energy pulse is assumed to be absorbed in a very thin layer of the specimen surface in a time very short compared with the propagation of the heat wave through the material.
3. α and k are assumed to be independent of the temperature.
4. There are assumed to be no heat losses by conduction or radiation from the faces.

The new method is different from the flash diffusivity method for the following reasons,

1. In the new method the thermal properties are evaluated directly. That is, no curve fitting or visual inspection of the temperature history is needed; in the proposed method only 3 DVM measurements are used. In one way of analysis of the flash method, the thermal properties are evaluated at $t_{1/2}$. $t_{1/2}$ is the time required for the back surface to reach half of the maximum temperature rise. This time requires visual curves fitting.

2. In the flash method, the surface temperature rise is very high, so that sometimes it causes vaporization and energy losses. This is not so in the new method.

3. In the new method, the heat losses by conduction and radiation are smaller than those of the flash method since there are no "free" faces.

In short, the flash method determines the thermal diffusivity by the shape of the temperature versus time curve at the rear surface, the heat capacity by the maximum temperature indicated by the thermocouple, and the thermal conductivity by the product of the heat capacity, thermal diffusivity, and the density.

The flash method was extended and refined by various investigators in the field, and applied to a wide range

of materials over a wide range of temperatures. It is reported to be used in over 80% of the current transient property measurement according to TPRC.

4. Non-linear estimation method (program PROPERTY).

The non-linear estimation method is based on theoretical findings by Beck [7] for the estimation of thermal properties. It is developed into a computer program called "PROPERTY." This program also can predict the temperature at various depths of the specimen. A finite difference method is employed for solving the transient heat conduction equation.

The properties are found by making the calculated temperatures match the measured temperatures in a least-squares sense. The boundary-conditions available in this program are,

1. Temperature boundary condition: in order to determine the thermal diffusivity, only measured temperature boundary conditions are necessary. The program can use temperature histories at two boundaries as boundary conditions in the model to calculate the thermal diffusivity.

2. Heat flux boundary condition: to determine simultaneously the values of thermal conductivity (k), and specific heat (c_p), a nonzero heat flux history at one boundary must be known. In one mode

the program uses heat flux and insulation boundary conditions in the model to calculate k and c_p.

Other input variables include the number of regions, number of nodes in each region, the length of each region, and times for the given transient data of temperatures or heat fluxes.

The program output includes the times, the calculated temperatures "CALTEMP," measured temperatures "ETEMP," and their differences called a residual "DTETC." Printed output also includes the sum of square of residuals "RMS," and sensitivity coefficients symbolized by "BDB."

The values of root-mean-square are a direct measure of agreement between the model and the experiment. For perfect agreement between the calculated and the measured temperature, the value of "RMS" approaches zero. However, "RMS" will never reach zero since there are always sources of errors. The sources of errors may be ascribed to experimental measurement errors, an imperfect model, and finite-difference calculations errors since the partial differential equation model is approximated using difference equations.

The differences between program PROPERTY and the new method are that:

1. The new method is simpler analytically.

2. One can obtain the values of k, c_p, and α immediately after each test when using the new method.

This is not possible at present using program PROPERTY.

3. The new method employs a small electronic integrator to obtain the thermal properties while program PROPERTY is designed for digital computer application.

5. The linear finite rod method

Klein, Shanks, and Danielson [8] used the linear finite rod method to measure the thermal diffusivity (α). In this method, the sample is in the form of a rod with a coaxial radiation guard of the same material and with the heater attached to the sample and guard at one end. Three thermocouples are attached along the length of the rod.

To obtain a data point at a given ambient temperature, the heater is turned "on" and the outputs of the thermocouples are recorded as a function of time. The curve from the first and third thermocouples and an initial estimate of the diffusivity are then used to calculate a curve which is compared with the experimental curve from the second thermocouple. The estimated diffusivity is varied until the difference between the experimental and calculated curves is minimized and the best value for the thermal diffusivity is obtained. In essence, this is what program "PROPERTY" does also. An extension of this method is the radial sample method. In this method, the sample consists of a stack of disks with an axial heater. Three

thermocouples are embedded along the radius of the center disk at three different radii (inner, middle, and outer).

The data are recorded and analyzed in a manner similar to that used in the finite rod method. In other words, the temperature data from the inner and outer radii are used as empirical boundary conditions, and the temperature data from the middle radius are used to obtain (α).

Carter, Maycock, Klein, and Danielson [9] used this method to evaluate (α) of Armco iron in the range 26° to 895 °C, utilizing a computer program to make the calculations by the method of finite differences. The new method is different from these two methods because of geometry, experimental technique, and calculations or analysis. It is similar to the difference between the new method and PROPERTY.

6. Radial heat flow method

McElroy and Moore [10] classified the radial heat flow method into five classes:

Class I: Cylindrical methods with a central source (or sink) of energy in a cylinder that is assumed to be "infinitely long" and does not employ end guards.

Class II: Cylindrical methods with a central energy source (or sink) in a cylinder generally composed of stacked disks and employing end guards to minimize axial flow.

Class III: Spherical and ellipsoidal methods in which the energy source is completely enclosed by the specimen.

Class IV: Comparative methods in which concentric cylinders of materials with known and unknown (k) surround a central energy source (this method is usually not employed on solids).

Class V: Self-heating radial methods involving joule heating of a cylindrical specimen and measurement of the attendant temperature variation along the radius of the cylinder.

Other methods for determining (k) alone have been investigated by

Flynn [11], who used steady-state methods in which the sample is heated directly by passage of an electric current. Also Powell [12], developed and improved the so called "Thermal Comparator methods" to determine k of materials. Laubitz [13], reviewed two experimental systems for measuring (k), the guarded linear-heat flow method and the "generalized Forbes' Bar" method.

Null and Lozier [14], worked on the measurement of the thermal diffusivity (α), using the phase shift method.

Beck, Mitchel, and Pfahl worked on many aspects of thermal conductivity using transient measurements (see references 15-30).

CHAPTER II

EXPERIMENTAL PROCEDURES

This chapter deals with experimental aspects of the problem. The experiment is based on the analysis developed by Beck [1]. The new method necessitated the development of an experimental apparatus and strategy to determine the transient thermal properties of different materials. This chapter is divided into several sections with each one dealing with an important part of the experiment.

2.1 The new method

For detailed analysis of the method, see reference [1]. In this section, the new method is described as it applies to the geometry of the problem, namely the flat plate.

For a flat plate with temperature variable properties which describes transient heat conduction, equation (1.2.1) reduces to

$$\frac{\partial}{\partial x} \left(k \frac{\partial T}{\partial x} \right) = \rho c_p \frac{\partial T}{\partial t} \qquad (2.1.1)$$

Consider the plate to be heated on one side by applying a heat flux $(\frac{q}{A})$ at $x = 0$, and to be insulated on the other which is at $x = E$, see Figure (2.1.1).

Figure 2.1.1 Flat plate geometry of the problem.
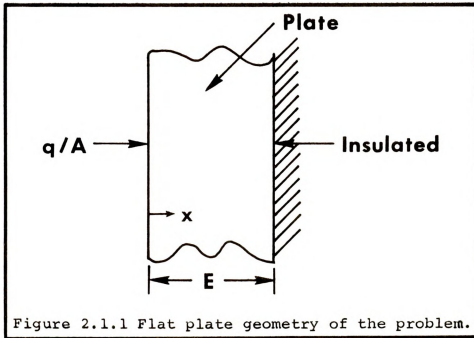
Then the two boundary conditions can be written as

$$\frac{\partial T(E,t)}{\partial x} = 0$$

$$\frac{q}{A} = -k \frac{\partial T(0,t)}{\partial x}$$

(2.1.2a)

and the initial condition can be given as

$$T(x,0) = T_i$$

(2.1.2b)

The following are known: E, ρ, $\frac{Q}{A}$, T_i, T_f where

E = length (or thickness of specimen) (ft)

ρ = density of specimen $(\frac{lbm}{ft^3})$

$\frac{Q}{A}$ = total heat added/area = $\int_o^\infty (\frac{q}{A})$ dt $(\frac{Btu}{ft^2})$

T_i = initial temperature (°F)

T_f = final temperature (°F)

The heat flux $\frac{q}{A}$ and typical temperature histories are shown in Figure 2.1.2.
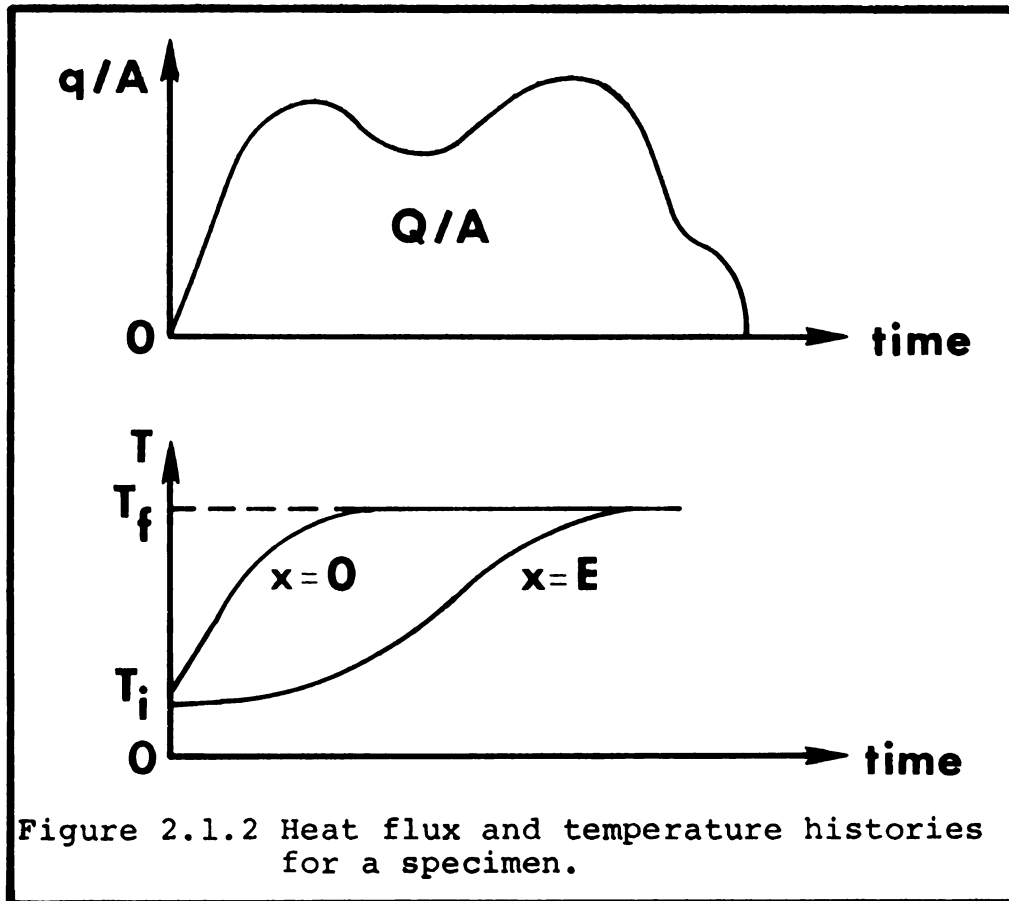
Figure 2.1.2 Heat flux and temperature histories for a specimen.

The objective is to find k and c_p using measurements at two locations, x_1 and x_2 in the plate.

To proceed first integrate equation (2.1.1) over t

$$\int_o^\infty \frac{\partial}{\partial x} (k \frac{\partial T}{\partial x}) \, dt = \int_o^\infty \rho c_p \frac{\partial T}{\partial t} \, dt = \int_{T_i}^{T_f} \rho c_p dT \neq f(x)$$

(2.1.3)

Notice that the boundary conditions result in the right
hand side of (2.1.3) not being a function of x. Now
integrate equation (2.1.3) over x

$$\int_0^\infty [\int \frac{\partial}{\partial x} (k \frac{\partial T}{\partial x}) dx] dt = \int_0^\infty [\int d (k \frac{\partial T}{\partial x})] dt = \int_0^\infty [k \frac{\partial T}{\partial x}] dt =$$

$$\int_0^\infty k \frac{\partial T}{\partial x} dt = x \int_{T_i}^{T_f} \rho c_p dt + c_1 \qquad (2.1.4)$$

Q is defined by the equation,

$$\frac{Q}{A} = \int_0^\infty (\frac{q}{A}) dt$$

Use the boundary condition at x = 0 given in Equation
(2.1.2a) in the above equation to obtain

$$\frac{Q}{A} = - \int_0^\infty [k \frac{\partial T(0,t)}{\partial x}] dt$$

Introducing this equation and the boundary condition at
x = E given by Equation (2.1.2a) in Equation (2.1.4) yields
at x = 0

$$- \frac{Q}{A} = c_1 \qquad (2.1.5)$$

at x = E

$$0 = E \int_{T_i}^{T_f} \rho c_p dT + c_1 \qquad (2.1.6)$$

Substitute Equation (2.1.5) into Equation (2.1.6) to get

$$\int_{T_i}^{T_f} \rho c_p dT = \frac{Q}{AE} \qquad (2.1.7)$$

Use Equations (2.1.5) and (2.1.7) in Equation (2.1.4) to obtain

$$\int_0^\infty k \, \frac{\partial T}{\partial x} \, dt = \frac{Q}{A} \, [\frac{x}{E} - 1] \qquad (2.1.8)$$

Now assume that (k) and (ρ) are constant but let $c_p = f(T)$, and also define

$$\Theta(x) \equiv \int_0^\infty T(x,t) \, dt$$

Then Equation (2.1.8) becomes

$$k \, \frac{d\Theta}{dx} = \frac{Q}{A} \, [\frac{x}{E} - 1] \qquad (2.1.9)$$

Integrating Equation (2.1.9) over x yields

$$k \, [\Theta(x_1) - \Theta(x_2)] = \frac{Q}{A} \, [\frac{x_1^2 - x_2^2}{2E} - x_1 + x_2]$$

solving for the thermal conductivity,

$$k = \frac{\frac{QE}{2A} \, [(\frac{x_1}{E} - 1)^2 - (\frac{x_2}{E} - 1)^2]}{\Theta(x_1) - \Theta(x_2)}$$

or

$$k = \frac{\frac{QE}{A} \, [(\frac{x_1}{E} - 1)^2 - (\frac{x_2}{E} - 1)^2]}{2 \int_0^\infty [T(x_1,t) - T(x_2,t)] \, dt} \qquad (2.1.10)$$

Equation (2.1.10) is the thermal conductivity equation. In Equation (2.1.10), x_1 can be taken as $x = 0$ and x_2 to be $x = E$.

$\frac{Q}{A}$ can be determined from a calorimeter of known thermal properties. OFHC copper can serve as an example

of such material. Then we can derive for a flat plate
calorimeter heated on one side and insulated on the other

$$\frac{Q}{A} = (\rho c_p)_{cal} \; E_{cal} \; (T_i - T_f)_{cal} \qquad (2.1.11)$$

or

$$\frac{QE_{sp}}{A} = (\rho c_p)_{cal} \; E_{cal} \; E_{sp} \; (T_i - T_f)_{cal}$$

where cal means calorimeter and sp means specimen.

Introducing (2.1.11) into (2.1.10) gives the
expression

$$k = \frac{(\rho c_p)_{cal} \; E_{cal} \; E_{sp} \; (T_i - T_f)_{cal}}{2\int_0^\infty [T(x_1,t) - T(x_2,t)] \; dt} \qquad (2.1.12)$$

Next assume that ρ in Equation (2.1.7) to be constant (but
not k), then

$$\rho \int_{T_i}^{T_f} c_p dT = \frac{Q}{AE}$$

or

$$\int_{T_i}^{T_f} c_p dT = \frac{Q}{AE\rho} \qquad (2.1.13a)$$

$$\bar{c}_p = \frac{1}{T_f - T_i} \int_{T_i}^{T_f} c_p dT$$

Therefore Equation (2.1.13a) can be written as

$$\bar{c}_p = \frac{Q}{AE\rho(T_f - T_i)} \qquad (2.1.13b)$$

Equation (2.1.13b) is the specific heat equation.

The contact conductance h can be obtained from the following relation

$$q(t) = h [T_1(t) - T_2(t)]$$

See Figure 2.1.3.

Figure 2.1.3 Two plates in imperfect contact.
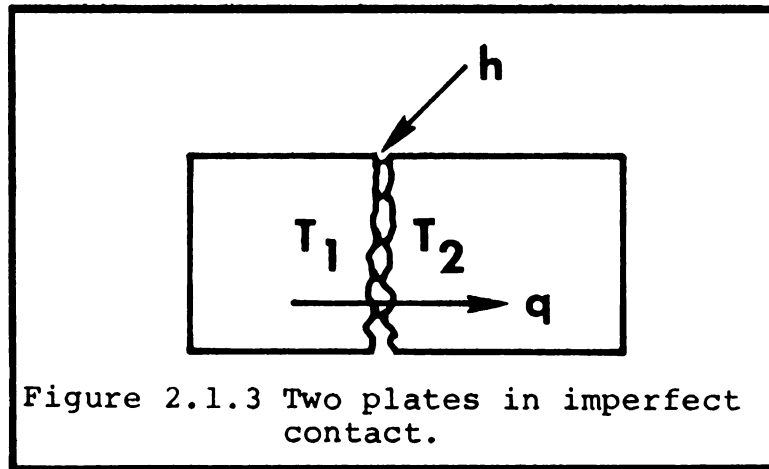
Integrate the above equation over t to get

$$Q = \int_0^\infty h [T_1(t) - T_2(t)] \, dt$$

If h is constant, then

$$h = \frac{Q}{\int_0^\infty [T_1(t) - T_2(t)] \, dt} \qquad (2.1.14)$$

Equation (2.1.14) is the equation for the contact conductance.

2.2 Experimental set-up

The data acquisition system of the Michigan State University Thermal Properties Measurement Facility consists

of a hydraulic system and main testing unit, thermocouple
sensors, computer signal conditioner (CSC), IBM 1800
computer, an electronic integrator, and temperature
controllers. The computer signal conditioner contains a
DC amplifier for each thermocouple (when the integrator
system is used only one amplifier is needed).

The test specimen and the calorimeter are housed
in the main testing unit (or testing assembly). For details
of the testing assembly see Figure 2.2.1. The specimen and
the calorimeter are assembled in exactly the same manner in
their respective cans in the testing assembly. The testing
assembly shown in Figure 2.2.1 consist of two parts
separated by a heater. One part (bottom part) houses the
specimen which sits on three screws 120° apart from each
other. Each screw has a collar that sits on a Transite
block; also each screw has a hole in it that extends from
the tip that carries the specimen to the collar. The
purpose of the holes in the screws is to minimize the heat
losses from the specimen by conduction. Surrounding the
specimen and sitting directly on the Transite block is an
OFHC guard-heater; its purpose is to maintain a constant
temperature zone around the specimen to minimize heat
losses by convection and radiation from the sides and
bottom surface of the specimen. The space between the
outer surface of the guard-heater and the stainless steel
can is filled with Fiberglass insulation to minimize heat
losses from the guard-heater. This whole assembly with the

Figure 2.2.1 Schematic diagram of the testing assembly.
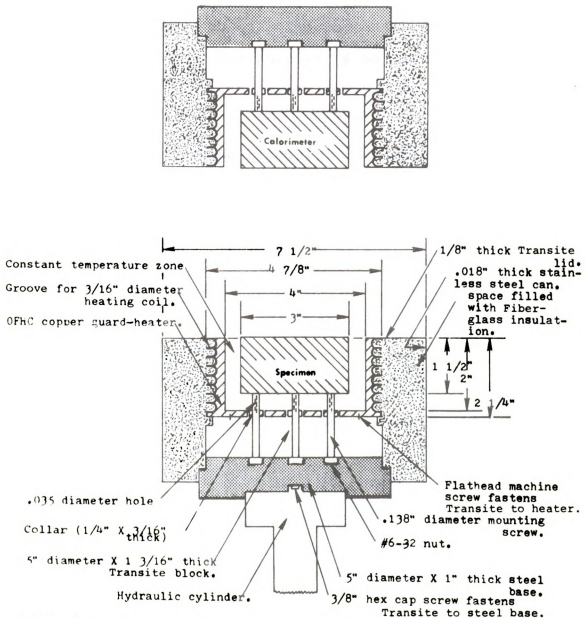
Transite sits on and is fastened to a steel base which in turn is attached to the piston of the hydraulic cylinder. The top part houses the calorimeter, and it is assembled like the bottom part except it does not sit on a piston; instead it is fastened to the loading frame. The heater between the specimen and calorimeter cans is also fixed to the loading frame and its purpose is to heat the mating surfaces of both the calorimeter and the specimen; see Figure 2.2.2.

The following points must be considered during the assembly process of the specimen and the calorimeter.

1. The specimen and calorimeter must have a flat surface and each must be parallel to the steel base in its own can.

2. The specimen and calorimeter must have the same centerline (no offset).

Figure 2.2.2 shows the testing assembly. The bottom can houses the specimen; the top can houses the calorimeter; and the two heaters are between.

Figure 2.2.3 shows the cabinet that houses the temperature controllers and the adjacent hydraulic system. The temperature controllers are made by Leeds and Northrup and are attached (from left to right in Figure 2.2.3) to the

1. specimen surface heater,

2. calorimeter guard-heater,
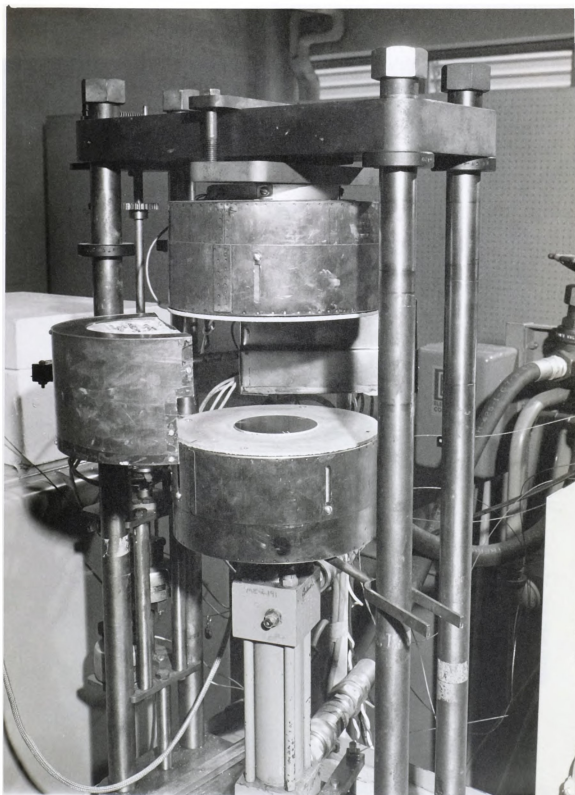
Figure 2.2.2 Photograph of the testing assembly.
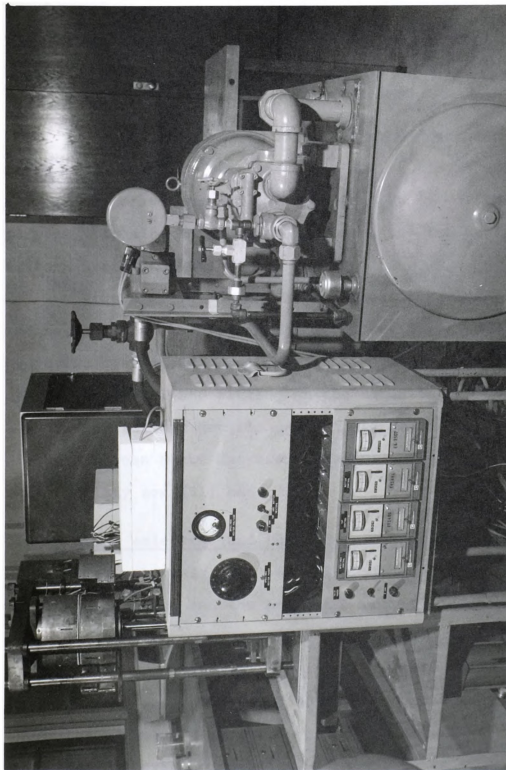
Figure 2.2.3 A cabinet housing the temperature controllers and the adjacent hydraulic system.

3. specimen guard-heater, and

4. calorimeter surface heater.

The temperature controller attached to the specimen surface
heater is the proportional type while the remainder are the
"on-off" type.

Figure 2.2.3 also shows the specimen and the calori-
meter in intimate contact (face to face) during the test
and how the piston brings the specimen can up for this
purpose. It also shows the position of the two surface
heaters during the test.

Figure 2.2.4 concentrates on the operational panel.
The switches on the panel operate the testing assembly,
hydraulic system and surface heaters. To the left of the
operational panel and sitting on the table is the CSC.

For further details on the data acquisition system
of the Michigan State University Thermal Properties Measure-
ment Facility see [31] and [32].

2.3 Specimen selection and thermocouple installation

Two materials have been investigated, one a
reference material and the other the primary material to
be investigated.

The purpose of using a reference material is to
improve and quantify the accuracy of the experimental
apparatus by using a material which has well-known and
established thermal properties. Armco iron is such a
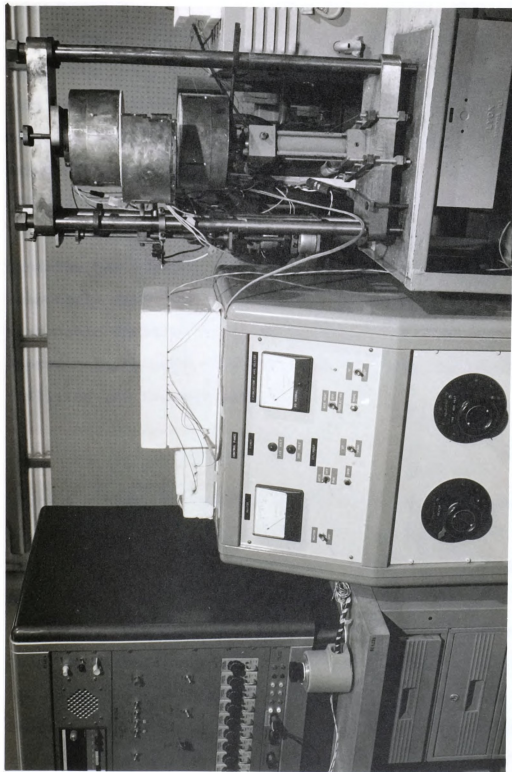
Figure 2.2.4 The operational panel, computer signal conditioner (CSC) and the testing assembly.

material since many investigators have measured its thermal
properties; see [33], and [34].

The primary material investigated is aluminum 2024-
T351. Its transient thermal properties are determined in
this study for different temperatures. Also a mathematical
model is developed to predict the thermal conductivity
values for different times and temperatures (see Chapters
III and IV).

The thickness of the specimen should be chosen to
minimize heat losses from the sides and to maintain a
reasonable duration of the test. It is found that a
reasonable duration is on the order of 30-60 seconds. An
approximate optimum thickness E of the specimen is found by
utilizing the Fourier modulus.

$$\frac{t\alpha}{E^2} \approx 2 \qquad (2.3.1)$$

where t = time, α = thermal diffusivity, and E = thickness
of the specimen. (2.3.1) comes from the solution of the
heat conduction equation for a flat plate (0<x<E), one end
maintained at constant temperature and the other end
insulated. The plate has an initial uniform temperature.
These conditions approximate the experimental conditions of
the tests reported herein. By the time indicated by the
Fourier modulus value given by (2.3.1), the temperature in
the idealized problem just described would be nearly
uniform.

The experiment must be short in duration because the integrator is not accurate after four to five minutes and with longer duration experiments the heat losses become relatively greater. Yet, the duration of the experiment must not be too short because one wishes to visually monitor the ΔT (i.e., $T_{sp_{x=0}} - T_{sp_{x=E}}$) during the experiment. This requires that the duration be about 30-60 seconds minimum. Also, one wants to avoid having the order of the experiment duration be so short as to be on the order of response time of the various components of the system.

As mentioned earlier the specimen's surface must be flat and smooth (as for the calorimeter surface) to insure the best face to face contact with each other. This is done by first grinding and then lapping the surface.

To measure the temperature, type "J" thermocouples were used. They are iron-Constantan, number 30 gage wire which is about 0.010 inches in diameter.

Three thermocouples were used on the heated surface of the specimen, 120° apart from each other. They are embedded in 3 pairs of slots with each slot being 0.010 inch wide, 0.010 inch deep and 0.300 inch long. The distance between the centerline of the slots in each pair is 0.100 inch. See Figure 2.3.1. The centerline slot of 0.010 inch wide and 0.010 inch deep on the specimen's surface was used for another thermocouple, but it was later decided that it was not necessary, and left on all specimens' surface for the sake of consistency.

Figure 2.3.1 Thermocouple locations at the
heated surface of the specimen.
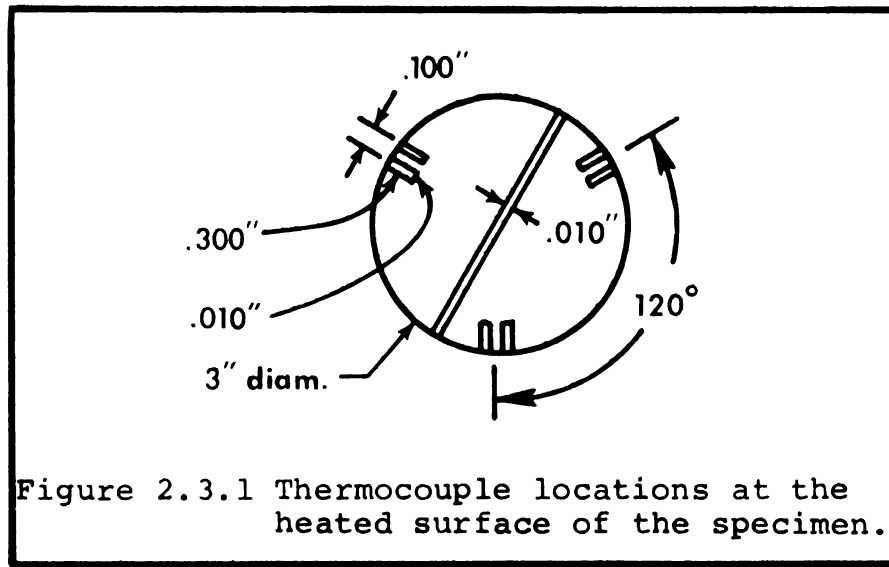
A thermocouple is formed by placing an iron wire in

one slot and an Constantan wire is placed in the adjacent

one. After placing a wire in a slot, the side of the slot

is very carefully peened over to pinch the wire and hold it

in place. A junction between the two dissimilar metals of

the thermocouple wire is not formed before the wire is

attached to the specimen; the metal in the specimen becomes

part of the actual measuring junction. This method elimi-

nates the need for adhesives which add mass and can insulate

the thermocouple from the specimen. An attempt was made to

insulate the slots electrically except at the tip in order

to let the thermocouples measure at 0.3 inches from the

edge of the specimen surface rather than measure the last

point it sees which is the edge. This was done to gain

greater accuracy in the temperature measurement. This

attempt failed because in peening over the edges of the slot the electrical insulation broke down.

A good deal of time was devoted to make the surface thermocouples read uniformly. It was found that two things help make this possible. First, the surface of the specimen must be quite flat. Next it is necessary to provide a uniform layer of silicone grease on the surface which is achieved by utilizing a specially constructed comb to provide a thickness of about 0.015 inch.

To determine the temperature difference across the specimen the temperature at another location beside the heated surface must be measured. This temperature at x_2 was chosen to be E, the insulated surface, for convenience and for greatest accuracy. By measuring the other temperature as far away as possible from the heated surface we can achieve the minimum noise to signal ratio. If the IBM 1800-system is used for data collection from each test, then the thermocouples at x_2 = E (back surface of the specimen) can be installed in exactly the same way they are installed on the heated surface. However, most of our data was collected by using the electronic integrator system, which prevented using the above mentioned method of thermocouple installation on the back surface of the specimen (or referred to as the insulated surface) for electrically conducting materials. This is because the temperature difference in

$$\int_o^\infty [T(x_1,t) - T(x_2,t)] \, dt = \int_o^{t_f} [T(x_1,t) - T(x_2,t)] \, dt$$

required by the integrator was taken by appropriately wiring the thermocouples assuming that the thermocouples were electrically insulated. This posed a considerable problem of selecting the best thermally conducting but electrically insulating adhesive with which to coat the thermocouple and which could also withstand the high temperatures. Many experiments and a great deal of time was devoted to this problem; electrically insulating adhesives vary from one another in their thermal response and the objective was to find the best thermally conducting material to minimize errors in the evaluation of the integral.

Among the many experiments, one in particular deserves some description since through that experiment a suitable adhesive was found. In that experiment a specimen of Armco iron (3 inches in diameter and 1 inch thick) was used. Three thermocouples were installed on the heated surface ($x_1 = 0$) in the manner described above. For the insulated surface ($x_2 = E$) five holes of 0.035 inch diameter and 1/16 inch deep were drilled at different locations, in a circular fashion. The center of each hole is 1.2 inch from the center of the insulated surface. At one location one pair of slots were machined in the same manner and with similar dimensions as those on the heated surface, see Figure 2.3.2.

Figure 2.3.2 Thermocouple locations at the insu-
lated surface (x = E) for an experi-
ment on Armco iron specimen #3.
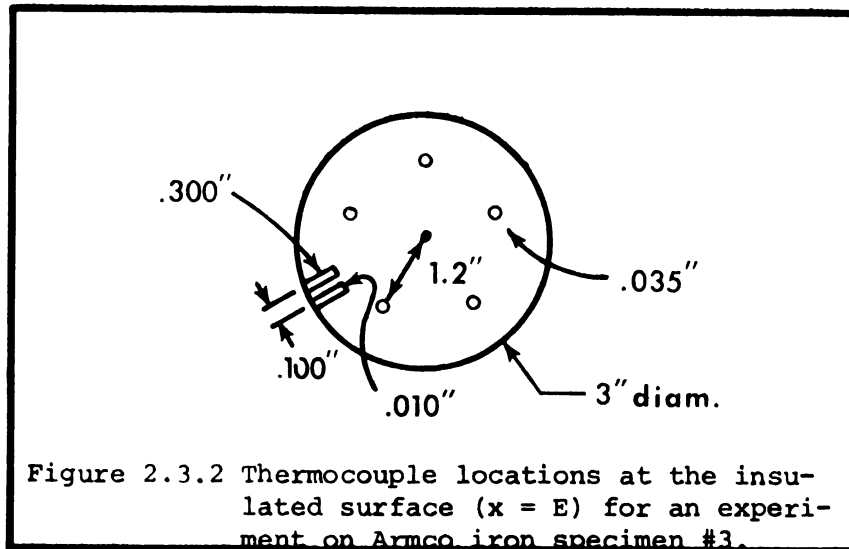
Hole #1 was filled by regular shellac, which is an electrically insulating material. A thermocouple bead was tightly inserted in the hole.

In hole #2 a Mullite tube (ID ≈ .033 inch, OD ≈ 0.035 inch, and length ≈ 1/16 inch) was inserted with the thermocouple bead inserted inside the tube so that it touches the sides of the tube but not the bottom of the hole.

Hole #3 is exactly like hole #2 except the tube was filled with silicone grease before the thermocouple bead was inserted.

Hole #4 was coated using Sauereisen cement number one. The thermocouple bead was also coated with the same material and then it was inserted tightly in the hole.

Hole #5 has exactly the same features as hole #4 except that the insulating material used is Astroceram type A.

In the pair of slots (#6) the two thermocouple wires were installed in a similar manner to those installed on the heated surface.

Several tests were run on this specimen using the IBM 1800-system. The temperature response of all the above mentioned thermocouples were monitored. Since the thermo-couple in #6 touches the metal directly, it had the best thermal response. Next to it was the thermocouple in hole #5 (with the Astroceram insulation). The thermocouples in the #6 and #5 were very close in their temperature measurement and much better than the rest of the thermo-couples. Therefore it was concluded that the Astroceram type A cement is the best thermal conductor and electrical insulator. For many Armco iron and aluminum specimens one thermocouple was used on the insulated surface (x_2 = E) in exactly the same way as that of hole #5 described above.

For the rest of the aluminum specimens a washer in the form of a hollow disk of 1/2 inch outside diameter, a little less than 1/4 inch inside diameter, and 1/16 inch thick was used. Through the side of the washer a hole of 0.035 inch diameter was drilled. This hole was filled with Astroceram type A and the thermocouple bead was inserted in it, see Figure 2.3.3. This washer was placed on the insulated surface and fixed firmly to the surface by a small screw. A small layer of silicone grease was placed between the washer and the specimen to enhance the heat transfer.
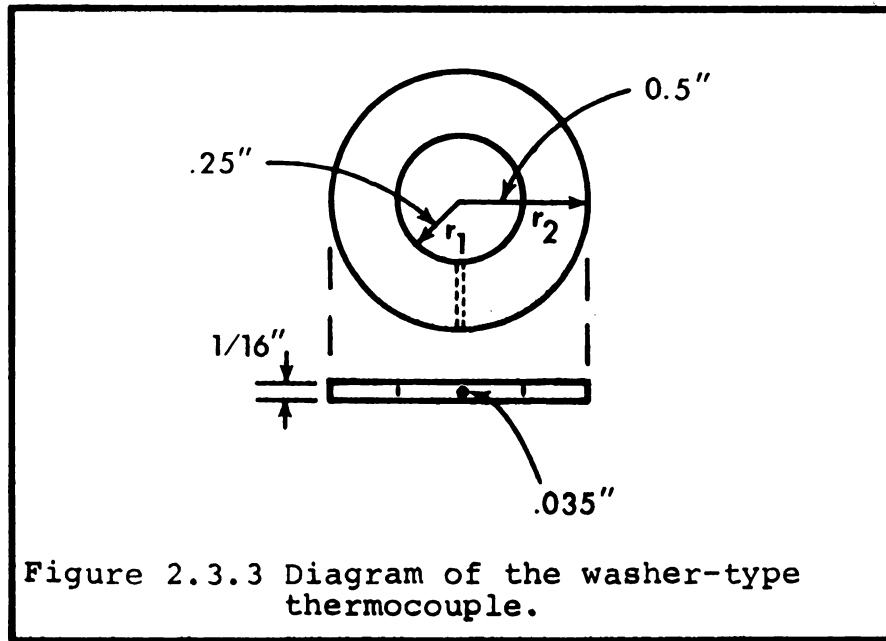
Figure 2.3.3 Diagram of the washer-type
thermocouple.

This washer-type thermocouple introduced a small error in the determination of (k), and a correction was introduced as will be seen later. One washer-type thermocouple was used for several tested specimens. It is important to note that Astroceram type A can withstand temperatures of up to 2000 °F; this is in addition to the desirable qualities mentioned earlier.

As mentioned in section (2.1) there are two boundary conditions used in the integration method, heat flux boundary condition at $x = 0$ and insulation boundary condition at $x = E$. To measure the heat flux at $x = 0$, a standard material with known thermal properties was used. OFHC copper was chosen to be the standard or calorimeter because its properties are very well established and it is often used as a standard material. As mentioned earlier, the calorimeter was a disk of 3 inches diameter and

3/4 inch thick. It was assembled in exactly the same
manner as the specimen and mounted in the loading frame
above the specimen; see Figures 2.2.1 and 2.2.2. To
measure the temperature of the calorimeter, only one
thermocouple was installed in a pair of slots located 3/8
inch from the heated surface and 180° apart; see Figure
2.3.4. The dimensions of the slots are similar to those on
the heated surface of the specimen, namely 0.300 inch long,
0.010 inch wide, and 0.010 inch deep. The thermocouple was
installed in exactly the same way as it was installed on
the heated surface of the specimen with the Constantan wire
in one slot and the iron wire in the other. Since the
calorimeter's thermal properties are known, the heat flux
can be calculated from

$$\frac{Q}{A} = [\rho c_p E (T_i - T_f)]_{calorimeter} \qquad (2.1.11)$$

Figure 2.3.4 Thermocouple location on the side of the OFHC
copper calorimeter.
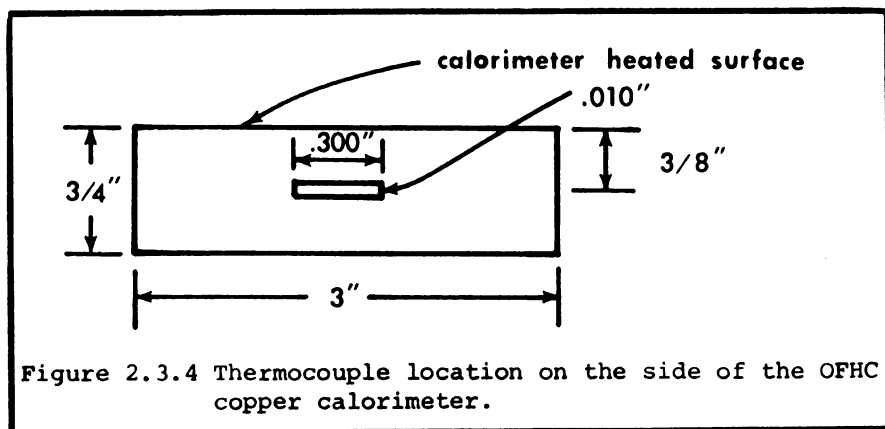
To collect the data all thermocouples were connected to a specially constructed box (which acts as a reference junction). The panel in the box was connected to a rotating switch by plain copper wires that carry the signal or (output) from each thermocouple via the switch to an amplifier. The switch allowed each thermocouple output to be read on a separate channel, see Figure 2.3.5. The amplifier multiplied each signal by a factor of 1000 before being sent to the digital voltmeter (DVM). This digital voltmeter, 10 amplifiers and other auxiliaries comprise what is called the Computer Signal Conditioner (CSC).

The initial and final temperatures of the calorimeter and specimen were read directly (in volts) using a DVM. The ΔT signal (or channel #3 on the rotating switch) after being amplified 1000 times left the CSC and was fed to the electronic integrator. There it was integrated over time for about one minute and the output was read in volts on another DVM.

The integrated temperature difference can be related to the integrated voltage difference by

$$\int_o^\infty \Delta T \, dt \approx \int_o^{t_f} \Delta T \, dt = C_I \int_o^{t_f} C_v \Delta V \, dt$$

using

$$\Delta T = C_v \, \Delta V$$
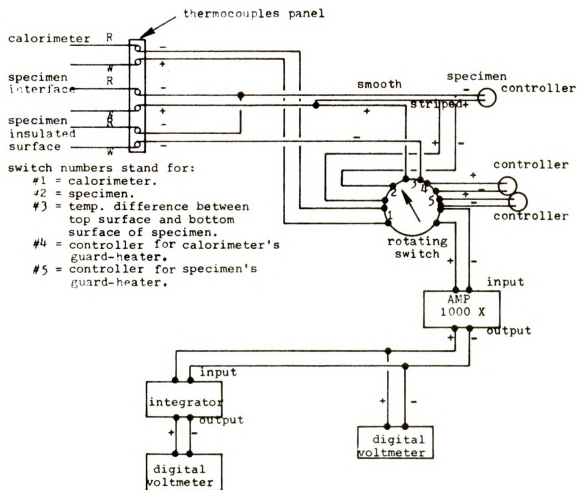
Figure 2.3.5 Wiring diagram for the over-all experimental system.

If $\Delta T = 100$ F° resulting from a temperature rise from 80 to 180 °F then $\Delta V = 4.31 - 1.36 = 2.96$ volts and $C_v = \frac{180-80}{2.95}$. The integrator constant C_I was determined experimentally in the following manner. A constant voltage ΔV_c of 1 mv was applied for 60 seconds to the integrator (see Figure 2.3.6) and the output was read on a digital voltmeter as some number K_1, i.e.,

$$C_I \int_o^{t_f} \Delta V_c \, dt \bigg|_{integrator} = C_I (1 \text{ mv} \times \frac{60}{3600} \text{ hour}) = K_1 \text{ mv-hr}$$

Then solving for C_I gives

$$C_I = \frac{K_1}{1 \text{ mv} \times \frac{1}{60} \text{ hr}}$$

This experiment was repeated several times and the constant was determined to be

$$C_I = 0.00252$$

Figure 2.3.6 One millivolt input over sixty seconds.
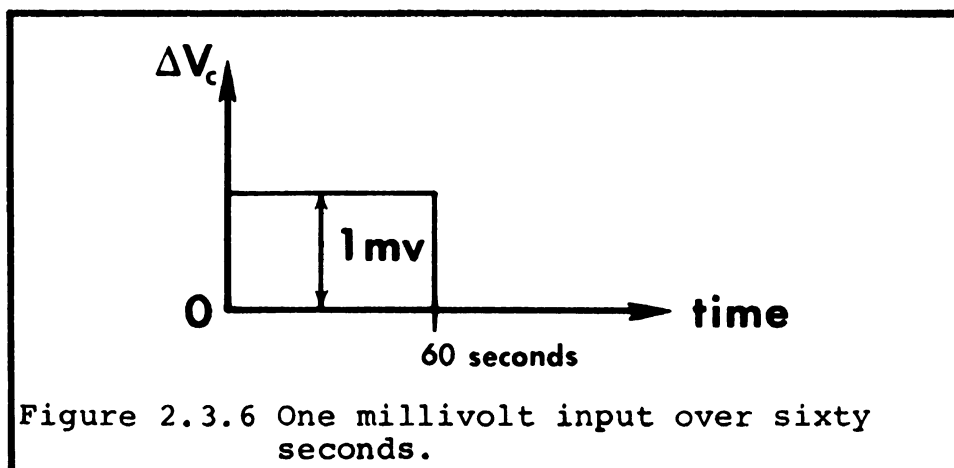
This constant was used in the main equation of thermal conductivity to obtain the value of k as described below.

The specific heat values depend mainly on the initial and final temperatures of the calorimeter and specimen and were read directly in volts from the DVM in the CSC.

2.4 Running a test

Running a test involves several steps which must be put in the following order necessary to produce the optimum experiment.

1. Turn on all the equipment and let them warm up for about 20 minutes. This includes the CSC, electronic integrator, DVM, control panel of the hydraulic system and all temperature controllers.

2. Zero all measuring devices this includes the CSC, electronic integrator and DVM.

3. Clean the heated surface of both the specimen and calorimeter using a clean rag and acetone.

4. Place a film of silicone 0.015 inch thick on the specimen surface by utilizing a comb specially made for this purpose.

5. Heat the specimen and maintain it at the desired temperature by utilizing the surface heater directly above it and the temperature controller connected to it. In the meantime turn on the guard-heater surrounding the specimen and set its temperature

controller at the same temperature as that of the specimen.

6. Heat the calorimeter to constant temperature about 40 to 50 °F above that of the specimen by utilizing the surface heater directly below it and its temperature controller. In the meantime let the guard-heater surrounding the calorimeter to reach the same temperature as that of the calorimeter and hold it there by utilizing the temperature controller. It is important to note that the same "on-off" switch on the cabinet that houses the controllers heats both guard-heaters.

7. After both the specimen and the calorimeter attain equilibrium at their respective temperatures, do the following:

    a. Write down the initial temperature of the calorimeter (channel #1 on the rotating switch).

    b. Write down the initial temperature of the specimen (channel #2 on the rotating switch).

    c. Zero the integrator at (-.104 to -.108 depending on whether the integrator drifts upward or downward), and put the rotating switch on channel #3 (the temperature difference channel).

    d. Turn off the guard-heater for both the calorimeter and the specimen.

    e.   Turn the switches on the control panel of the hydraulic system to the following positions from left to right: "OFF," "AUTO," UP," "insulation," and "OUT."

8. To start the test, push the button on the control panel of the hydraulic system. This causes the bifurcated heater to move out from between the specimen and calorimeter and the hydraulic cylinder to bring the specimen upward into intimate contact with the calorimeter; see Figure 2.2.3. The duration of the test is about 60 seconds.

9. When ΔT decreases to within about 2% of the maximum ΔT (by visually monitoring it on the screen of the CSC), the test should be ended. Then put the integrator back on "HOLD" and

    a.   Record the integrator output from the small digital voltmeter,

    b.   Record the final temperature of the calorimeter, and

    c.   Record the final temperature of the specimen.

10. Put the switch on the control panel of the hydraulic system in the "DOWN" position; this separates the specimen from the calorimeter by bringing the hydraulic cylinder down to its normal position; see Figure 2.2.4.

11. Turn on the guard-heaters for both specimen and calorimeter.

12. Clean the surfaces (interface) of both specimen and calorimeter by using a clean rag and acetone.

13. Repeat the tests by starting from step (4). Also zero the amplifier in the CSC and the integrator prior to each test.

To evaluate k and c_p, substitute in Equations (2.1.12) and (2.1.13b) which reduce to

$$k = (\text{constant})_1 \times \frac{[V(T_i) - V(T_f)]_{\text{calorimeter}}}{0.00252 \int_0^{t_f} [V(T(x_1,t)) - V(T(x_2,t))] \ dt}$$

$$(2.4.1)$$

$$\bar{c}_p = (\text{constant})_2 \times \frac{[V(T_i) - V(T_f)]_{\text{calorimeter}}}{[V(T_f) - V(T_i)]_{\text{specimen}}} \qquad (2.4.2)$$

Note that the constant C_v (section 2.3) cancels in both these equations. Hence no correction is needed to allow for the changing temperature-voltage relation as the temperature is increased. One must, however, take into consideration $(\rho c_p)_{\text{calorimeter}}$ for different temperatures and the thermal linear expansion for both specimen and calorimeter for the different temperatures. These and other corrections are discussed in Chapter III.

2.5 The reference material and typical results

In order to determine the accuracy of the system and develop the testing procedure, a reference material, Armco iron was first chosen to be the specimen.

The type used is called Armco magnetic ingot iron for D-C applications. A great number of tests were conducted at different temperatures using water and silicone films of different thicknesses at the interface.

For room temperature tests, water as well as silicone were used at the interface. The films were placed on the specimen's heated surface just before the test. Silicone films were also placed on the surface of the calorimeter instead of that of the specimen. It was found that the location of the film did not affect the results. Several drops of water were used for room temperature tests with the number of drops varying from 3 to 10 drops. It was found that the optimum number of drops is between 5 to 6 for best results of k and c_p. For the silicone, film thicknesses from 0.010 inch to 0.030 inch were tried and best results for k and c_p were found when the 0.015 inch film thickness was used. Water cannot be used on the interface at the elevated temperatures because it evaporates immediately (at temperatures of 300 °F and above). Hence a 0.015 inch film of silicone was used for all tests. Tables 2.5.1 and 2.5.2 give the k and c_p values of Armco iron (specimen #1) at room temperature. For the values reported in Table 2.5.1 silicone film of 0.015 inch was used on the specimen's surface, while for those reported in Table 2.5.2 three drops of distilled water were used. Specimen #1 was prepared from an Armco iron bar that was purchased some ten years ago.

k and c_p values for room temperature tests of Armco
iron (specimen #3) are reported in Tables 2.5.3 through
2.5.5. Specimen #3 was prepared from a new bar of "Armco
magnetic ingot iron for D-C applications." For the values
reported in Table 2.5.3, three drops of distilled water were
used on the specimen surface, while for those reported in
Table 2.5.4 six drops of distilled water were used. For the
values reported in Table 2.5.5, 0.015 inch silicone film was
used on the specimen's surface. For the k and c_p values
reported in Tables 2.5.3-5 the guard heaters and controllers
were used.

Tables 2.5.6 through 2.5.10 report the average,
variance and standard deviation of the k and c_p values
reported in Tables 2.5.1 through 2.5.5 respectively.

For the old Armco iron specimens one can see that
the average k and c_p values in Table 2.5.6 are close to
those reported in Table 2.5.7. This indicates that using a
silicone film of 0.015 inch thickness on the specimen's
surface is just as accurate as using three drops of
distilled water in room temperature tests. When the
specimen used was prepared from the new bar (Armco magnetic
ingot iron for D-C applications) the agreement of the k
values is not quite as close. As Tables 2.5.8-10 indicate
the average k and c_p values are quite close when using
0.015 inch silicone film or six drops of distilled water
on the specimen's surface for room temperature tests, while

the tests using three drops of distilled water gave values about 6% higher for k.

Table 2.5.11 gives the k and c_p values of Armco iron (specimen #3) for the elevated temperatures of 300 and 400 °F. For these elevated temperature tests only 0.015 inch silicone film was used on the specimen surface because the water evaporates at these temperatures. The average, variance and standard deviation of the k and c_p values given in Table 2.5.11 are reported in Table 2.5.12, while Table 2.5.13 gives a comparison between the present values and those reported by TPRC for room temperature and elevated temperature tests.

Most of these tests were conducted using the integrator method, but some were conducted using the IBM 1800 method to collect the data. A special program (called SIMPL) was used to determine k and c_p and other parameters from the 1800 data. k and c_p values determined by using program "SIMPL" are given in Table 2.5.14. Comparing the value of k obtained by using the integrator method with that by using the IBM 1800 method (using the temperature difference thermocouple readings) for 400 °F we can see a difference of about 5% for the case of heat flow from the calorimeter to Armco and about 9% for the case of heat flow from Armco to the calorimeter. For room temperature tests the difference for the k value is about 7.7% for both methods of heat flow, while the difference for the c_p values is about 5.4% for the heat flow from the calorimeter

Table 2.5.1 Typical values of k and c_p for Armco iron (specimen #1) at room temperature. A silicone film, 0.015 inch thick was used on the interface.

k $(\frac{Btu}{hr-ft-F})$	c_p $(\frac{Btu}{lbm-F})$
41.143	.1098
38.153	.1080
39.87	.1082
40.325	.1085
38.1	.1078
38.658	.1097
38.92	.1078
38.03	.1081
39.596	.1091
40.148	.1086
39.085	.1078
38.471	.1084
38.85	.1078
38.0	.1142
38.502	.1080
38.523	.1078
39.220	.1076
39.012	.1080

56

Table 2.5.2 Typical values of k and c_p for Armco iron
(specimen #1) at room temperature. Three
drops of distilled water were used at the
interface.

$k \ (\frac{Btu}{hr-ft-F})$	$c_p \ (\frac{Btu}{lbm-F})$
39.365	.1096
38.742	.1093
37.6	.1086
39.231	.1086
40.628	.1103
40.247	.1091
39.992	.1082
39.945	.1078
39.935	.1077

Table 2.5.3 Typical values of k and c_p for Armco iron
(specimen #3) a new bar, at room temperature
using 3 drops of distilled water at inter-
face.

$k \ (\frac{Btu}{hr-ft-F})$	$c_p \ (\frac{Btu}{lbm-F})$
45.973	.1085
43.712	.1088
45.389	.1080
47.244	.1074

Table 2.5.4 Typical values of k and c_p for Armco iron (specimen #3) at room temperature using 6 drops of water at interface.

k ($\frac{Btu}{hr-ft-F}$)	c_p ($\frac{Btu}{lbm-F}$)
41.086	.1078
43.889	.1139
43.545	.1083
43.3	.1074
44.118	.1073
42.201	.1075
42.811	.1104
42.5	.1089
43.32	.1085

Table 2.5.5 Typical values of k and c_p for Armco iron (specimen #3) at room temperature using 0.015 inch film of silicone grease at interface.

k ($\frac{Btu}{hr-ft-F}$)	c_p ($\frac{Btu}{lbm-F}$)
42.795	.1087
41.373	.1075
42.493	.1074
42.342	.1070
42.159	.1070
42.915	.1072
41.81	.1072
42.722	.1072
40.4	.1102
40.0	.1085
41.84	.1090
40.2	.1082
43.4	.1080
43.2	.1087

Table 2.5.6   Average, variance and standard of deviation
              for the values obtained at room temperature
              using 0.015 inch silicone film on surface of
              Armco iron (specimen #1).

$\bar{k}$ = 39.0337111	$\bar{c}_p$ = .1086222
Variance = .7754886	Variance = .0000024
Standard Deviation = .8806183	Standard Deviation = .0015338

Table 2.5.7   Average, variance, and standard of deviation
              for values obtained at room temperature using
              3 drops of water on surface of Armco iron
              (specimen #1).

$\bar{k}$ = 39.5205556	$\bar{c}_p$ = .1088000
Variance = .8413818	Variance = .0000007
Standard Deviation = .9172687	Standard Deviation = .0008573

Table 2.5.8   Average, variance, and standard of deviation
              for values obtained at room temperature using
              3 drops of water on surface of Armco iron
              (specimen #3).

$\bar{k}$ = 45.5795000	$\bar{c}_p$ = .1081750
Variance = 2.1497497	Variance = .0000004
Standard Deviation = 1.4662025	Standard Deviation = .0006131

Table 2.5.9   Average, variance, and standard of deviation
for values obtained at room temperature using
6 drops of water on surface of Armco iron
(specimen #3).

$\bar{k}$ = 42.9744556	$\bar{c}_p$ = .1088889
Variance = .8889280	Variance = .0000045
Standard Deviation = .9428298	Standard Deviation =.0021139

Table 2.5.10   Average, variance, and standard of deviation
for values obtained at room temperature using
0.015 inch silicone film on surface of Armco
iron (specimen #3).

$\bar{k}$ = 41.9749071	$\bar{c}_p$ = .1079857
Variance = 1.2324266	Variance = .0000009
Standard Deviation = 1.1101471	Standard Deviation = .0009461

Table 2.5.11   Typical values of k and c_p for Armco iron
(specimen #3) at 300 and 400 °F using 0.015
inch film of silicone grease at the inter-
face.

k ($\frac{Btu}{hr\text{-}ft\text{-}F}$)	c_p ($\frac{Btu}{lbm\text{-}F}$)	Conditions
37.0	.1427	300 °F
38.711	.1412	0.015" film of Si
38.128	.1407	
		Calorimeter
35.90	.1556	400 °F ↓ heat
34.80	.1600	0.015" film of Si Armco flow
		Calorimeter
		↑
33.5	.1190	400 °F heat
35.0	.0953	0.015" film of Si Armco flow

Table 2.5.12 Average, variance, and standard of deviation of the values obtained at 300 and 400 °F of Armco iron (specimen #3) using 0.015 inch silicone film at interface.

For 300 °F (heat flow from calorimeter to Armco iron):	
$\bar{k}$ = 37.946 Variance = 0.7555 Standard Deviation = 0.870	$\bar{c}_p$ = .1415 Variance = 0.1085 x 10^{-5} Standard Deviation = 1.043 x 10^{-3}
For 400 °F (heat flow from calorimeter to Armco iron):	
$\bar{k}$ = 35.35 Variance = 0.6050 Standard Deviation = 0.779	$\bar{c}_p$ = .1578 Variance = 9.68 x 10^{-6} Standard Deviation = 3.115 x 10^{-3}
For 400 °F (heat flow from Armco iron to calorimeter):	
$\bar{k}$ = 34.25 Variance = 1.125 Standard Deviation = 1.062	$\bar{c}_p$ = 0.1072 Variance = 2.78 x 10^{-4} Standard Deviation = 0.0167

Table 2.5.13 Comparison of the present values of k and c_p of Armco iron with those obtained by TPRC.

Temperature	TPRC		Present	
	$k\left(\dfrac{Btu}{hr\text{-}ft\text{-}R}\right)$	$c_p\left(\dfrac{Btu}{lbm\text{-}R}\right)$	$k\left(\dfrac{Btu}{hr\text{-}ft\text{-}F}\right)$	$c_p\left(\dfrac{Btu}{lbm\text{-}F}\right)$
Room temp:	41.5	.1080	42.54 41.56	.1089 (6 drops of water) .1080 (0.015" silicone grease)
300 °F:	36.5	.1200	37.946	.1415
400 °F:	34.0	.1300	35.350	.1578 (calorimeter meter → heat flow) Armco
			34.250	.1072 (calorimeter meter ← heat flow) Armco

Table 2.5.14   k and c_p values obtained from the IBM 1800 data by
utilizing program "SIMPL."

Case	Direction of heat flux	Temp. of specimen	$k\,(\frac{Btu}{hr\text{-}ft\text{-}F})$	$\bar{c}_p\,(\frac{Btu}{lbm\text{-}F})$
4	Armco to calorimeter (hot)	136-113 °F	45.5	.1092
3	Calorimeter to Armco (hot)	87-108 °F	45.35	.1142
2A	Armco to calorimeter (using $T_{x=0}$ & $T_{x=L}$)	415-397 °F	38.5	.1210
2B	Armco to calorimeter (using temp difference TC readings)	"	31.1	
1A	Calorimeter to Armco (using $T_{x=0}$ & $T_{x=L}$ readings)	431-452 °F	39.6	.1331
1B	Calorimeter to Armco (using temp difference TC readings)	"	33.6	

to Armco and about 1.1% for the heat flow from Armco to the
calorimeter. For both methods, the guard-heaters and
controllers were in use. For a description of the experi-
ment using the IBM 1800, see [31]. Since the standard
testing procedure is for the heat flow during the test to
be from the calorimeter to the Armco, we can see that the
two systems are relatively close in determining k and c_p.

As indicated above, Table 2.5.13 compares the
values given by TPRC [33] and the present values. The
present room temperature values of k are about 3.5% higher
using 6 drops of water at the interface and about 1.2%

higher using the 0.015 inch film of silicone grease at the interface. The present c_p values are about 0.9% higher for 6 drops of water while they are nearly the same as those of TPRC when using the 0.015 inch of silicone film.

For the 300 °F values, the present k values are about 3.8% higher while the c_p values are about 15% higher.

For 400 °F with the heat flow during the test from the calorimeter to Armco, the present values are about 3.6% higher in k and about 17.6% higher in c_p. But when the heat flow is from the Armco iron to the calorimeter the difference is about 0.7% higher in k and about 17.5% lower in c_p. We used the method of heat flow from the calorimeter to the specimen (during the test) as our standard testing procedure because it is more consistent in results than that of specimen to calorimeter.

Figures 2.5.1 and 2.5.2 show the results of tests on Armco iron (specimen #3) from the IBM 1800 data by using program "SIMPL."

Figure 2.5.1 shows the temperature history of the calorimeter and specimen during a typical test. It also depicts the actual behavior of the temperature difference between the heated surface and insulated surface of the specimen (ΔT) as well as $\int \Delta T \, dT$ during the test. Figure 2.5.2 shows the integrated heat flux ($\frac{Q}{A}$) and contact conductance (h) history during the test. The k and ρc_p values calculated during a test are also shown. The assymptotic values for "large" times are the desired
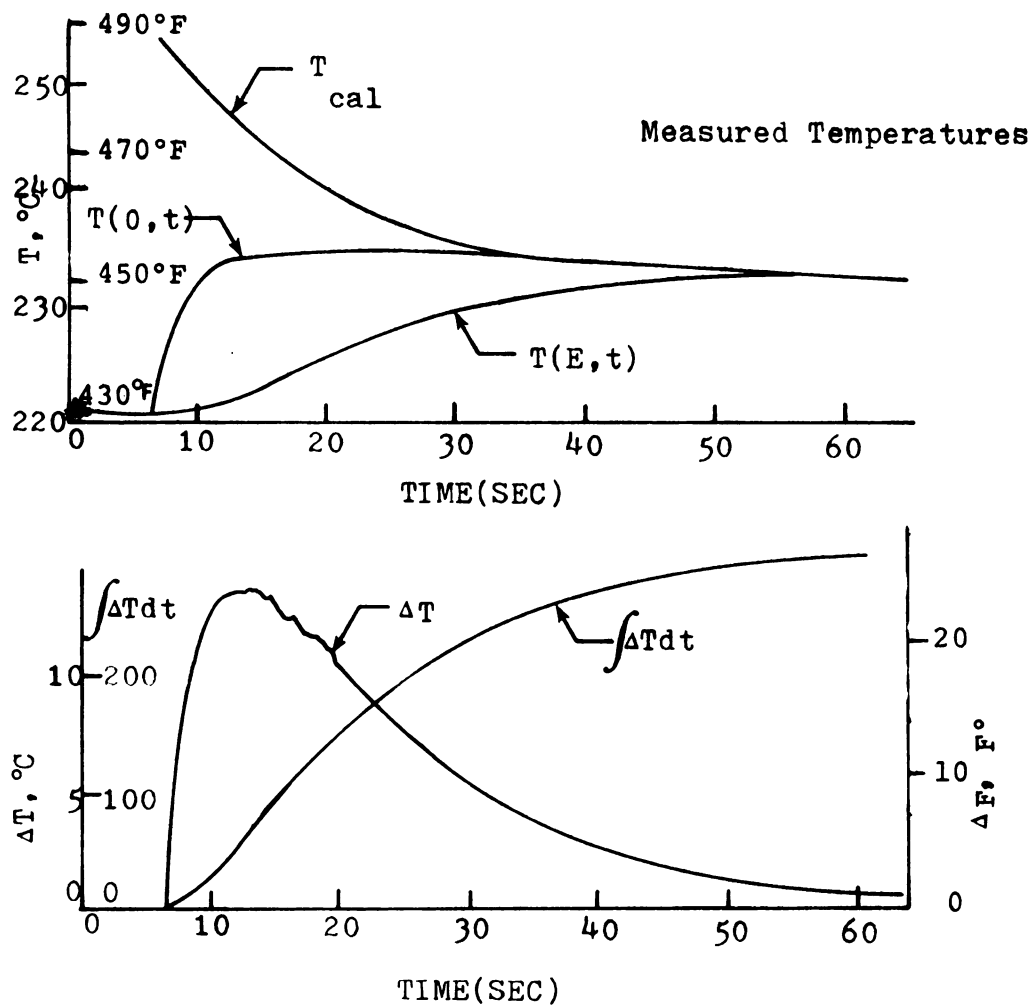
Figure 2.5.1   Temperature history of the calorimeter and specimen during a test on Armco iron.
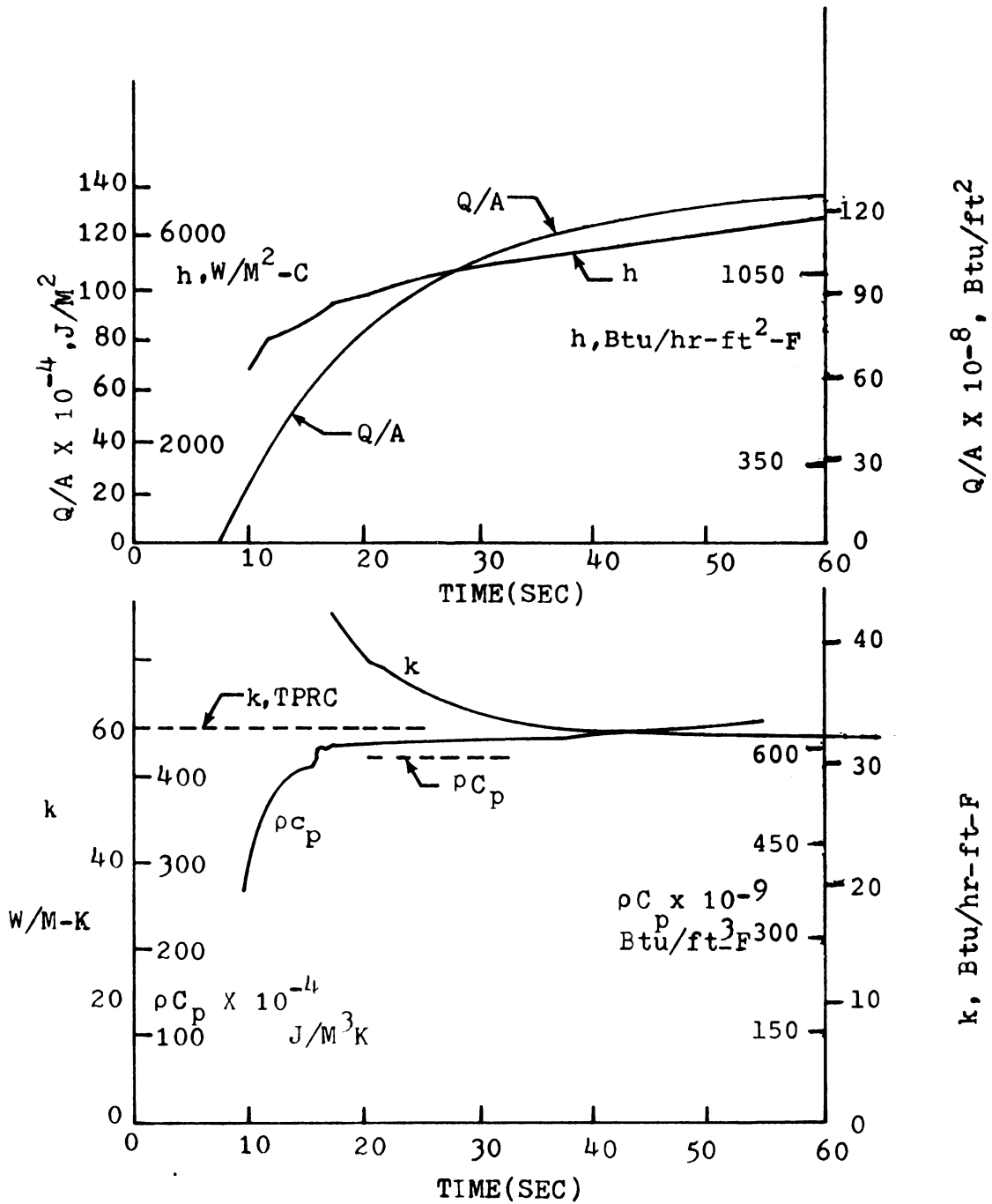
Figure 2.5.2   Typical values of k, ρc_p, h and $\frac{Q}{A}$ during a
given test on Armco iron.

measurements which should be compared with those of TPRC
also indicated.

To minimize the heat losses from the sides and back
surface of the specimen and calorimeter, several insulating
materials were tested as insulators in the system. Many
experiments were performed to determine the best insulating
material or best type of guard-heater. It was found that
the best method (of those tried) of minimizing the heat
losses in the system is to employ an OFHC copper type
guard-heater, one around the calorimeter and another
around the specimen (see Figure 2.2.1). The guard-heaters
must be at the same initial temperatures as those of the
calorimeter and specimen; that is, the guard-heater around
the calorimeter must be at the same temperature as that of
the calorimeter just before the test and the guard-heater
around the specimen must be at the same temperature as that
of the specimen just before the test. It was found that
this procedure gives the best results (see Figure 2.5.5).

Figures 2.5.3, 2.5.4, and 2.5.5 show the results of
some of the experiments that were performed to study the
nature and magnitude of the heat losses. Figure 2.5.3
shows the results of an experiment in which the copper
calorimeter was initially at 425 °F and the Armco iron
specimen was at room temperature initially. Both the
copper and Armco were surrounded by Fiberglass insulation
that fills the whole space in the can. (This test was
performed before the copper guard-heaters were built and

installed.) They were brought into intimate contact and were left in that position for about 50 minutes. The temperatures of both calorimeter and specimen were recorded every minute. The temperature is plotted versus the time in Figure 2.5.3. The same experiment was performed again except this time the specimen (Armco iron) was surrounded by a Transite type guard-heater, this heater was turned off during the test; the temperature history is plotted versus time in Figure 2.5.4. In another experiment the specimen (aluminum 2024-T351) was at 400 °F initially and the copper guard-heater surrounding it was at the same temperature while the calorimeter (OFHC copper) was at 445° initially and the copper guard-heater surrounding it was at 400 °F. Then the specimen was brought into intimate contact with the calorimeter and left in contact for 30 minutes. During this time both guard-heaters were "off," (i.e., the temperature controllers were not used) and the temperature history of both specimen and calorimeter were recorded. This same experiment was repeated exactly with exception of the temperature of the guard-heater around the calorimeter being 445 °F initially (which is the same as the calorimeter's initial temperature) rather than 400 °F. The results of both experiments are plotted in Figure 2.5.5. It is interesting to note that the rate of temperature drop for the case of the calorimeter's guard-heater initial temperature not being the same as that of the calorimeter is about four times higher than that when both the
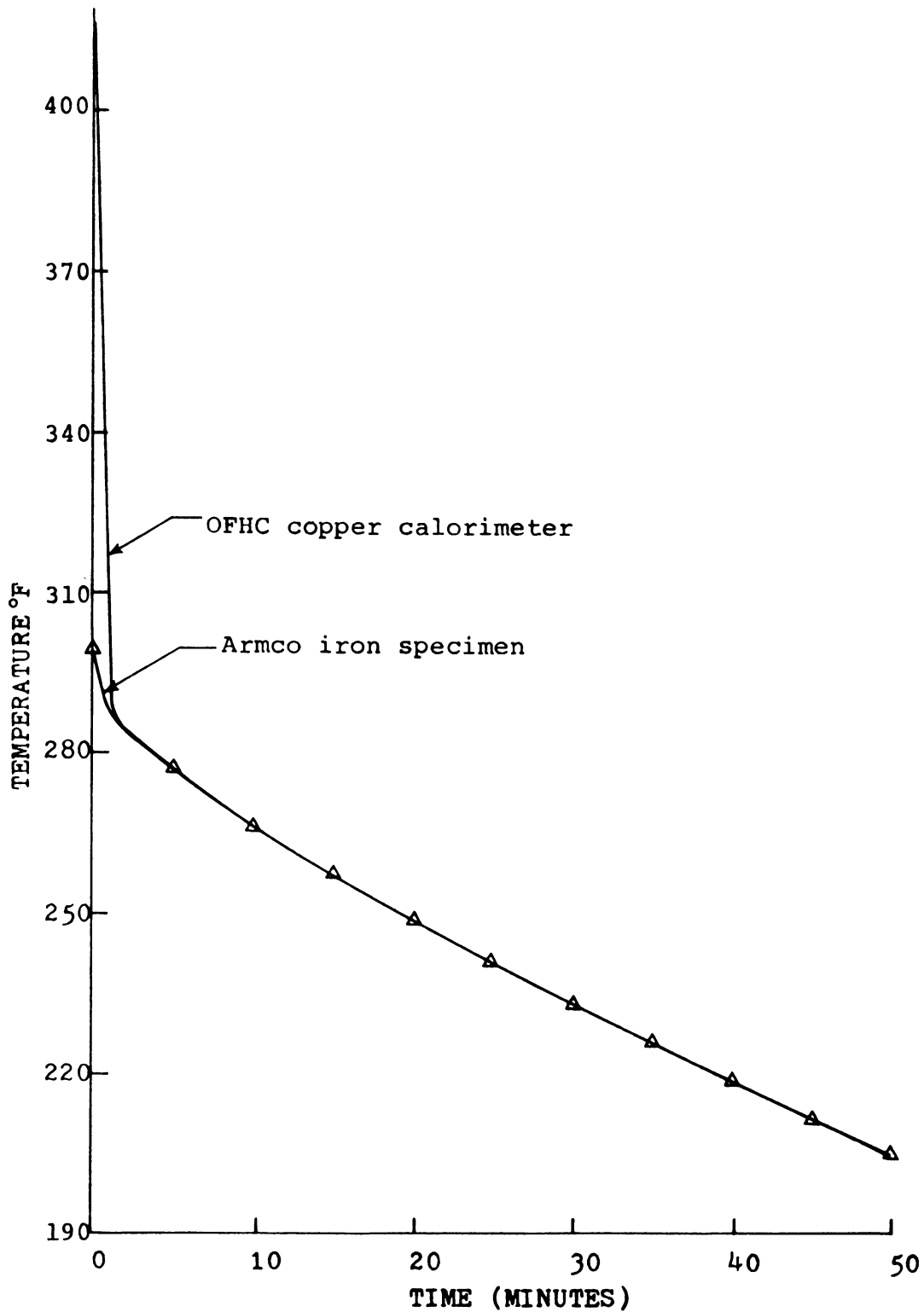
Figure 2.5.3   Copper at elevated temperature and Armco iron at room
temperature initially. Brought into intimate contact,
both copper and Armco are surrounded by Fiberglass
insulation.
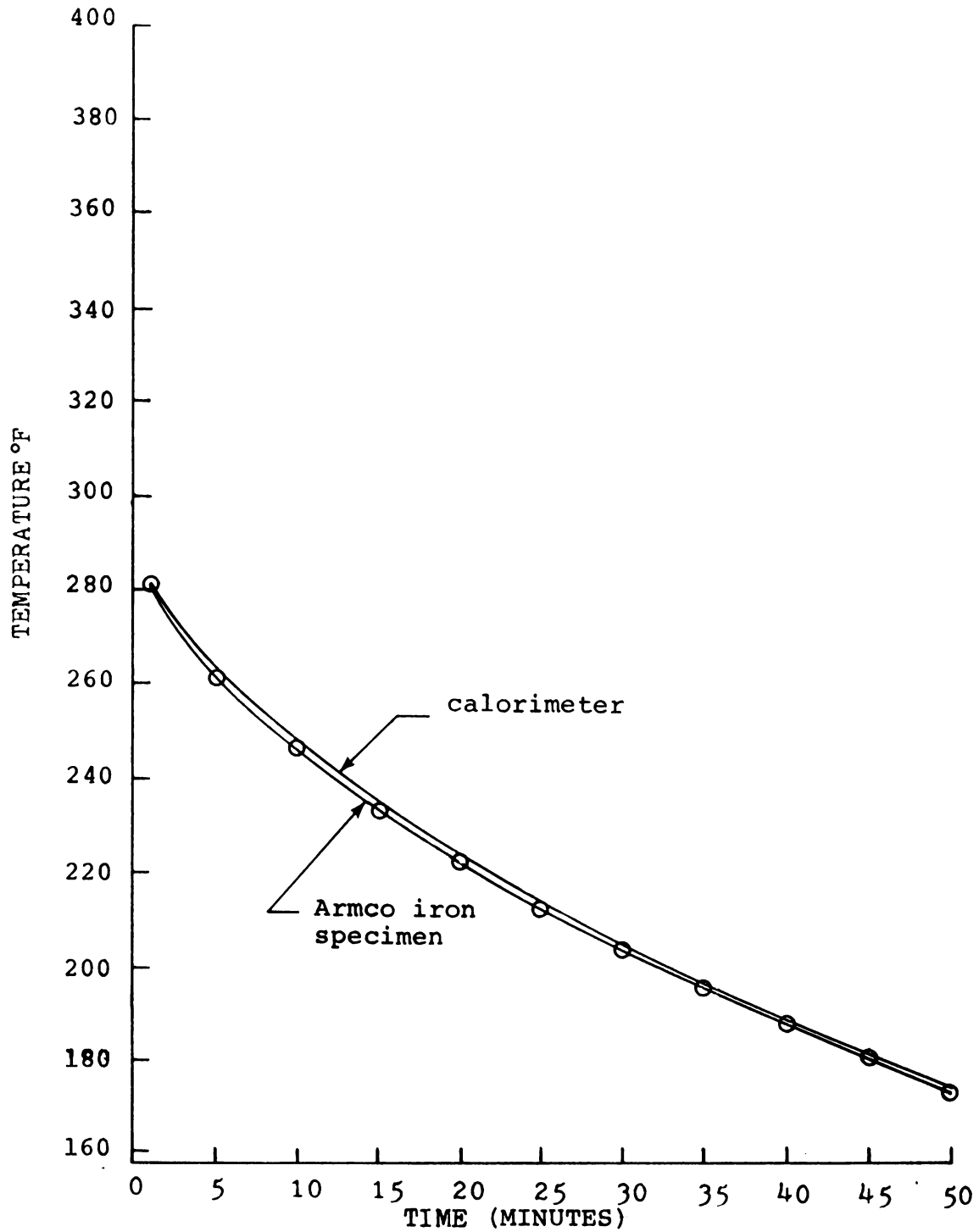
Figure 2.5.4 Copper at elevated temperature and Armco iron
at room temperature initially. Copper is
surrounded by Fiberglass insulation, and Armco
iron is surrounded by Transite guard-heater
(heater was off during test).
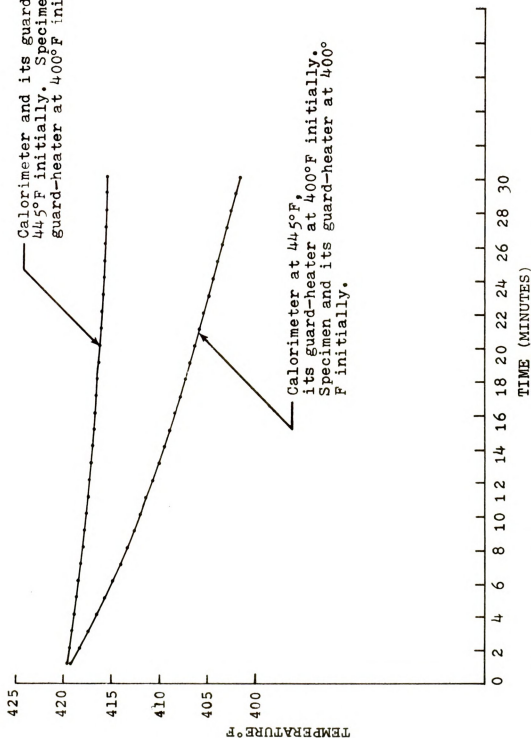
Figure 2.5.5 The temperature history in the present system for two cases.

calorimeter and its guard-heater are at the same temperature just before the test. This indicates that for a minimum of heat losses in the system the temperatures of the specimen and its guard-heater should be equal just before the test and the temperatures of calorimeter and its guard-heater should be the same initially also. (The calorimeter temperature must be 40 to 50 °F higher than the specimen temperature just before the test.) The larger the rate of decrease of the temperatures of a specimen, the greater is the heat losses. Since the rate of temperature decrease shown in Figure 2.5.5 is considerably less than those shown in Figures 2.5.3 and 2.5.4, using an OFHC copper guard-heater around the calorimeter and the specimen is shown to be very effective in minimizing the heat losses in the system.

CHAPTER III

EXPERIMENTAL RESULTS FOR ALUMINUM 2024-T351

Aluminum 2024-T351 is a well-known material which is used in many fields including aircraft construction. It was chosen to be the principal material to be investigated because it undergoes some phase changes with temperature and time. This results in changes of the thermal properties of the material, mainly the thermal conductivity (k).

3.1 Composition of the specimen

The specimen is Aluminum 2024-T351. It is composed of aluminum and 3.8-4.9% copper, 0.50% silicone, 0.50% iron, 0.30-0.9% manganese, 1.2-1.8% magnesium, 0.10% chromium, 0.25% zinc, and 0.15% others. It is solution heat treated and stress-relieved (see Sec. 3.2). Its mechanical and other properties are very well established and tabulated, see reference [36].

3.2 Metallurgical concepts of specimen

The principal alloying element of aluminum 2024-T351 is copper, about 3.8-4.9%. Figure 3.2.1 presents a

portion of the aluminum-copper system. The alloy can be represented on the diagram by the vertical at 4%.

Figure 3.2.1 Partial equilibrium diagram for aluminum-copper alloys.
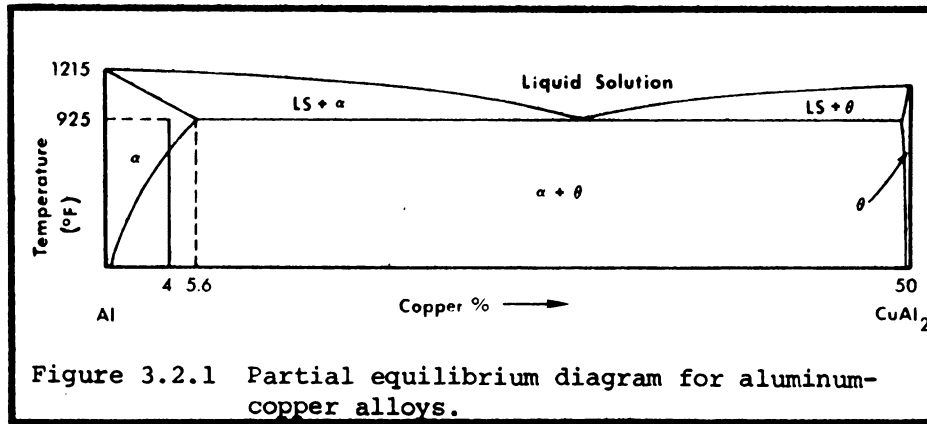
The diagram indicates that if the alloy is heated to 925 °F and maintained at this temperature until an equilibrium composition is reached it will assume the α condition with the complete solution of the Θ-phase. The α condition is a single phase. The Θ phase consists of hard particles based on the intermetallic compound $CuAl_2$ (Θ is a solution of small amount of Al in $CuAl_2$). If the alloy, after holding in the α-condition, is cooled very slowly as in annealing, a precipitation of small spheroids of the Θ-phase will occur. See Figure 3.2.2a which is a photomicrograph. The alloy is in its softest condition when its annealed. In the annealed condition, the alloy has the following mechanical properties, as shown in Table 3.2.1.

The precipitation of the Θ-phase (which involves diffusion) is prevented when the alloy is cooled rapidly by

Table 3.2.1   Mechanical properties of aluminum 2024-T351 in the annealed condition.

Ultimate strength = 27,000 psi

Yield strength = 11,000 psi

Brinell hardness = 47 (500 kg load, 10 mm ball)

Endurance limit = 13,000 psi (based on 500 million cycles of completely reversed stress using R. R. Moore type of machine and specimen)

Modulus of Elasticity = 10.6×10^6 psi

Ultimate shearing strength = 18,000 psi

water-quenching from the α-condition. After quenching in this manner the alloy is said to be in the solution-treated condition and does not exhibit its maximum strength and hardness, see Figure 3.2.2b. Upon holding (after the solution treatment and quenching) either at room temperature or at some elevated temperature in the $\alpha + \Theta$ region, there is a progressive change in the hardness and strength in accordance with the data in Figure 3.2.3. This is because the copper atoms have an extremely strong tendency to precipitate out of solid solution to form a particular crystal pattern of their own with aluminum. This crystal pattern in its first stage of precipitation is called Θ''. When sufficient heat is given for increased atomic mobility, further precipitation takes place, first along the grain boundaries then along the slip planes. In reforming into a separate crystal pattern the copper constituents, in effect,
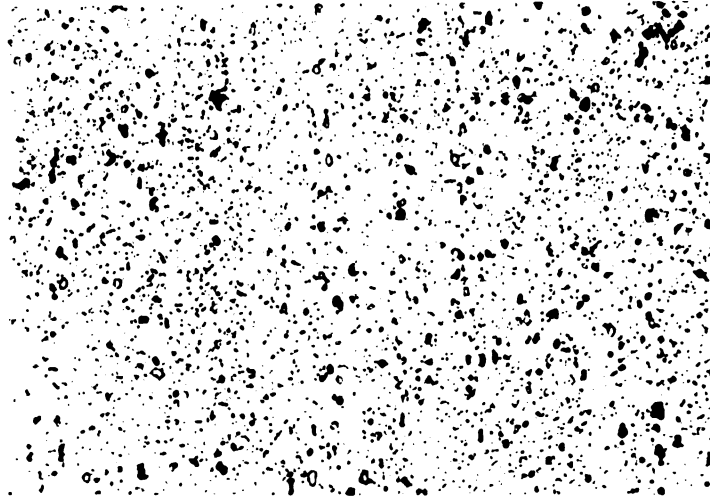
Figure 3.2.2a   Microstructure of aluminum 2024
in the annealed condition.

● Solute atom   O Solvent atom

(a)   (b)

(c)
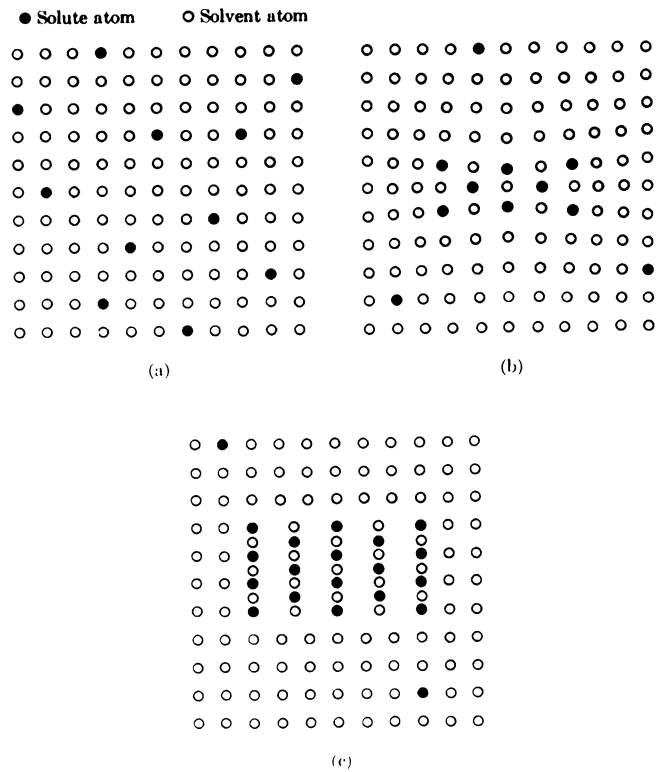
Figure 3.2.2b The stages in the formation of an equilibrium precipitate. (a) Supersaturated solid solution.   (b) Transition lattice coherent with the solid solution.   (c) Equilibrium precipitate essentially independent of the solid solution.

Figure 3.2.3 Aging and over-aging curves for Al-Cu system, over-aging drops the strength and hardness of the alloy.
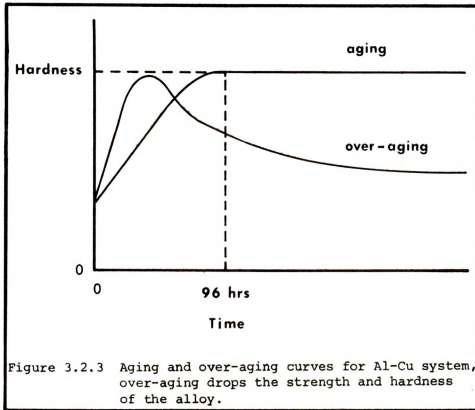
wedge in between the regular crystal pattern and distort the normal lattice structure as shown in Figure 3.2.4.

Figure 3.2.4 Diagram of lattice structure showing distortion caused by precipitated constituent.
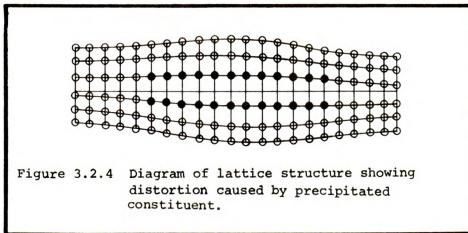
With longer times or higher temperatures more crystals precipitate in the form of θ'. The alloy reaches or achieves its maximum hardness and strength at a precipitation stage between θ" and θ'. This is due to the fact that the distortion of the crystal lattice along the slip planes interfers with smooth slip and thereby increases the strength of the alloy. In accordance with the modern conception of the nature of slip, the precipitated particles and lattice disturbance interfere with the motion of dislocation. The mechanical properties attributed to the alloy in this final aged condition are given in Table 3.2.2.

Table 3.2.2 Mechanical properties of aluminum 2024-T351 in the final aged condition.

Ultimate strength = 68,000 psi

Yield strength = 47,000 psi

Brinell hardness = 120 (based on 500 kg load and 10 mm ball)

Endurance limit = 20,000 psi (based on 500 million cycles of completely reversed stress using R. R. Moore type of machine and specimen)

Modulus of elasticity = 10.6 x 10^6 psi

Ultimate shearing strength = 41,000 psi

If aging were to continue due to higher temperatures or longer times at temperatures or both, then the constituents would combine into larger sizes (θ) and the distortion of

the atomic lattice would be reduced or eliminated. If it
is at room temperature it is called natural aging, however,
if it is at higher temperatures then it is called artificial
aging. At this stage the strength and hardness of the alloy
drops appreciably, and the alloy becomes over-aged, see
Figure 3.2.3. The process of precipitation heat treatment
is schematically shown in Figure 3.2.5. Precipitation heat
treatment plus over heating with appreciable time is called
over-aging and is diagramed in Figure 3.2.6. Θ' and Θ"
represent aging while Θ represent over-aging.

```
                                                        natural
                          quench in                     (at room
                          cold water                    temp)
Solution heat treated     →     super saturated solution → aging
(alloy in α-phase)                                      artificial
                                                        (at high
                                                        temp
                                                        250-300 °F)
```

Figure 3.2.5 Diagram of precipitation heat treatment.

```
                              quench in
                              cold water
Solution heat treatment           →         super-saturated solution
(alloy in α phase)
```

$$\frac{time\ or\ temp}{or\ both} \to \Theta" \frac{further\ temp}{or\ time\ or\ both} \to \Theta' \frac{over\ heating}{with\ appreciable\ time} \to \Theta \to$$

[In this case over-aging had brought the value of the thermal con-
ductivity to approximately the same value obtained by the recommended
annealing procedures]

Figure 3.2.6 Diagram of over-aging

If the alloy to be used in applications such as machine design is in the precipitated-hardened condition, then it is not in equilibrium-state, and is subject to continuing change in microstructure and properties at a rate dependent on service temperature. At room temperature the rate of change is negligible and the mechanical properties will be virtually unaltered in service.

However, if the service temperature is elevated, then changes in structure and properties can become very significant. Such changes can limit the application of the aluminum alloys in machine design.

The mechanical properties of the aluminum alloys after the precipitation hardening heat treatment are frequently enhanced by superimposing hardening and strengthening by plastic deformation or work-hardening. These work-hardening operations also contribute to the unstable condition of the alloy and the work-hardening effects are altered by the elevation of temperature.

The minor constituents such as iron, manganese, zinc, etc. in the composition of the 2024 alloy contribute to the hardening and strengthening of the alloy by simple solution hardening, by altering the composition of the Θ-phase and by forming independent intermetallics.

3.3 Experimental strategy

The experimental strategy consists of:

1. Testing the specimen at room temperature,

2. Heating the specimen to and holding it at the desired temperature and then performing the tests, and

3. Cooling the specimen down to room temperature and test it at that temperature.

After installing the specimen in the experimental apparatus, it must be tested first at room temperature to determine the thermal conductivity and specific heat values of the as-received specimen. Since the purpose of the investigation is to determine the transient k and c_p values of the specimen at the elevated temperatures, then the specimen is heated to the desired temperature and maintained there.

The tests are performed at intervals from the moment it arrived at the desired temperature to the time the alloy is over-aged. (See Section 3.2.)

The time intervals between tests are determined by the temperature level at which the specimen is held. It is important to note that the higher the temperature at which the specimen is maintained, the faster the specimen reaches its over-aged condition. Therefore at temperature levels of 400 °F and above it is recommended that the intervals between tests be as short as possible (on the order of 15 minutes or so) particularly during the first two hours. The intervals can be on the order of an hour or more between tests for temperature levels of 350-375 °F. When the specimen reaches its over-aged condition (experimentally,

the specimen is over-aged when its thermal conductivity values do not change significantly with time anymore) it is cooled down (in air) to room temperature. Tests on the specimen at room temperature are again performed. In this case over-aging brought the thermal conductivity values to approximately the same values obtained by the recommended annealing procedure.

This experimental strategy was applied to all aluminum specimens tested in this investigation. The measured values are given in section 3.4.

3.4 Experimental results

Fourteen specimens of Aluminum 2024-T351 in the as-received condition have been tested at different temperatures to establish transient k and c_p values for this alloy. The test temperatures were 350°, 375°, 400°, and 425 °F.

For test temperatures about 350 °F the alloy undergoes such slow changes that several days are needed to arrive at the over-aged condition. Yet, for temperatures above 425 °F the phase changes take place so rapidly that an accurate picture of these changes is difficult to obtain with the present equipment since the smallest time interval is about 15 minutes. Reasonable experiment durations are possible for those indicated above.

All the data was collected by using the integrator system. As was discussed in Chapter II the insulation

thermocouple was embedded directly into the specimen (after it was insulated with Astroceram) for some of the specimens, and for the others the washer-type thermocouple mounting was used; see Figure 2.3.3.

The results of these tests are given in Tables 3.4.1 to 3.4.13. The thermal conductivity and specific heat values are also plotted versus time in Figures 3.4.1 to 3.4.12.

350° test

Table 3.4.1 gives the results of testing aluminum 2024-T351 (specimen 5H) at the nominal temperature of 350 °F. The specimen was heated to 350 °F and maintained at that temperature for a total of 74 hours. The first test was performed fifteen minutes after it had arrived at 350 °F. (Zero time is the instant at which the specimen arrives at the desired temperature.) As the values of k and c_p indicate, the phase changes at this temperature take place very slowly and it took over three days to establish how the phase changes influence the thermal properties. The k and c_p values given in Table 3.4.1 are plotted versus time in Figures 3.4.1 and 3.4.2. The data points did not provide as a neat pattern as one would desire; yet one can see that it started at an average minimum of 88.0 $\frac{Btu}{hr-ft-F}$ for k and increased to a maximum value of about 103 $\frac{Btu}{hr-ft-F}$ 47 hours later and, then began to drop slightly.

The specific heat values in Figure 3.4.2 do not appear to have a regular pattern. They appear randomly scattered in part because the scale on the vertical-axis covers the small range of .242 to .262--which is about 8%. Note, however, that the largest specific heat value is indicated at an early time.

During a test the temperature of a specimen rises above its nominal temperature by about 15 to 20 °F, this is because the calorimeter is maintained initially at about 40 °F above the specimen's temperature. The duration of the test is about one minute, however. Because the specimen temperature rise above the nominal temperature is not large and is brief, it is believed that the effect upon the properties is not large.

375 °F tests

Tables 3.4.2 and 3.4.3 give the k and c_p values for specimens numbered 4H and 14H which were tested at 375 °F. Specimen 4H was tested over 11.5 hours period. The k values became larger with time until reaching a maximum at about 5.75 hours and then started to drop. See Figure 3.4.3. The specimen then was considered to be over-aged and was allowed to cool in air to room temperature. The specific heat value started with a maximum value as is shown in Figure 3.4.4.

Table 3.4.3 shows data for specimen 14H which was maintained at 375 °F for the long period of 101 hours; see

Figure 3.4.3 also, and note the two time axes. The k value increased with time but at a lower rate than specimen 4H. (Use the 10 hour axes results for this comparison.) From the 100 hour plot on Figure 3.4.3 note that there are two maximums. The first one is 108.4 at 4 hours and the second is at 111.9 $\frac{Btu}{hr-ft-F}$ at 39.75 hours. The latter is the global maximum. This specimen was the last one tested and the continued rise after 10 hours was completely unexpected.

The specific heat had a maximum value (.265) at zero time and it fluctuated in a downward way to about .242 over the 101 hour period. The c_p values given in Tables 3.4.2 and 3.4.3 are plotted versus time in Figure 3.4.4. Again one can see this fluctuation in the specific heat values to be pronounced because the y-axis scale is enlarged. Also one can see from Figures 3.4.3 and 3.4.4 that the k values and c_p values for the two specimen are quite close indicating good precision.

In collecting the data in Table 3.4.3, the washer-type thermocouple mounting (described earlier) was used on the insulated surface.

400 °F tests

Table 3.4.4 gives the 400 °F values of k and c_p for aluminum 2024-T351 specimen 6H. The specimen was maintained at 400 °F for over 8 hours. The k value started with 99.4 ($\frac{Btu}{hr-ft-F}$), went to a maximum of 118.0 ($\frac{Btu}{hr-ft-F}$) in 3.25 hours, and then leveled off and remained relatively

constant until the end of the test. See Figure 3.4.5. The corresponding specific heat values started with a maximum of 0.269 ($\frac{Btu}{lbm-F}$), went down with time to 0.251 ($\frac{Btu}{lbm-F}$), went up to a value of 0.258 ($\frac{Btu}{lbm-F}$) at 3.25 hours, dropped again to a low of 0.249 ($\frac{Btu}{lbm-F}$) and then fluctuated between 0.251 and 0.254 ($\frac{Btu}{lbm-F}$) until the end of the test. See Figure 3.4.6. It is interesting to note that a local maximum of c_p occurred at exactly the same time the k value attained its maximum.

Three additional specimens were tested at 400 °F to establish the pattern and behavior of the alloy at this temperature, to see if different time intervals between tests have any effect on this behavior and to demonstrate the precision of the method. The k and c_p values for the three additional specimens tested at 400 °F are given in Tables 3.4.5, 3.4.6, and 3.4.7, and in collecting these values, the washer-type thermocouple mounting was used on the insulated surface of the specimens. The k and c_p values given in Tables 3.4.5 through 3.4.7 are also plotted in Figures 3.4.5 and 3.4.6. Looking at Figure 3.4.5 one can see that specimen 10H has a maximum k of 109.7 ($\frac{Btu}{hr-ft-F}$) at two hours from zero time while specimens 11H and 12H have a maximum k of 110.62 ($\frac{Btu}{hr-ft-F}$) at two hours and 117.0 ($\frac{Btu}{hr-ft-F}$) at three hours respectively.

The maximum value of k for all four specimens shown in Figure 3.4.5 falls in the range of about 110 to 118 ($\frac{Btu}{hr-ft-F}$), and all four specimens have the same general

behavior, that of starting at a given value and attaining a maximum then leveling off at some constant value. This constant value while lower than the maximum value k attained, is always higher than the initial value at zero time.

The specific heat values for specimens 10H, 11H, and 12H shown in Figure 3.4.6 follow pretty much the same pattern as those of specimen 6H that were described earlier.

425 °F tests

Tables 3.4.8 and 3.4.9 give the k and c_p values of aluminum 2024-T351 (specimens 3H and 13H) at 425 °F and the results are depicted in Figures 3.4.7 and 3.4.8. The k values for the two tests have the same general shape as previously noted for other cases. Again the higher nominal temperature results in a more rapid change with time than for the previous tests which were for lower nominal temperatures. There is a 5 to 8% difference between the values obtained from the two specimens.

Unlike for the other temperatures investigated the specific heat at 425 °F has a time dependence that is similar to that for the thermal conductivity. That is, the initial value is relatively low, a maximum is attained, etc. There is maximum difference in values of c_p in the two tests of 7.6% but most values are less than 4% different.

Composite results

Tables 3.4.10, 3.4.11, and 3.4.12 give the composite
values of k and c_p for the 375°, 400°, and 425 °F temper-
atures. By the composite value we mean an average value
for each data point at a given temperature and time. For
example, the composite value of k 375 °F and one hour is
the average of the k value at one hour from Table 3.4.3
and the interpolated k value at one hour from Table 3.4.2.
The interpolated value is the average of the k values at
0.75 and 1.25 hours. That is, we not only have k and c_p
values for each specimen tested at a given temperature and
time, but we also have the average k and c_p values for all
specimens tested at that temperature and time. These
average values for a given temperature are called the
composite values. The composite values were needed in
developing the mathematical model that is discussed in
Chapter IV.

The k and c_p values given in Tables 3.4.10, 3.4.11,
and 3.4.12 are plotted versus time in Figures 3.4.9 and
3.4.10. Although the k values at zero time in Tables
3.4.10, 3.4.11, and 3.4.12 do not all start at 99.0
$(\frac{Btu}{hr-ft-F})$, they were taken however to be that in Figure
3.4.9 for the sake of uniformity since the average of the
three values is about 98.4 $(\frac{Btu}{hr-ft-F})$.

The values of k at room temperature for over-aged
aluminum 2024-T351 were obtained after the various speci-
mens were cooled in air from their respective nominal

temperatures to room temperature. Table 3.4.13 gives the over-aged values of k at room temperature for all the specimens tested in this study. Table 3.4.14 lists the average room temperature values for over-aged aluminum 2024-T351 as well as a measured value for regular annealing. Note that all the values given in Table 3.4.14 are quite close.

Figures 3.4.11 and 3.4.12 show a comparison of the k and c_p values at different temperatures as given by TPRC and the present study. The lower dashed line in Figure 3.4.11 depicts the initial values (time = zero) of k in the present study. It starts at room temperature (about 540 °R) and goes up to about 885 °R. The final values of k (over-aged values) in the present study are depicted by the upper dashed line, starting at about 885 °R and going down to room temperature. A few of the specific heat values obtained in this study are shown in Figure 3.4.12 by the small dark circles.

3.5 Corrections for errors

To insure accuracy and precision, all sources of potentially significant errors in the experimental values must be considered and corrections made if necessary. The following is a list of corrections that were applied (or considered) to the values given in Section 3.4.

Table 3.4.1 k and c_p values for aluminum 2024-T351
(specimen 5H) at 350 °F.

Time (hrs) at temp	$k(\frac{Btu}{hr\text{-}ft\text{-}F})$	$c_p(\frac{Btu}{lbm\text{-}F})$
.25	89.15	.253
.75	86.7	.251
1.25	88.35	.261
2.25	89.50	.247
3.25	90.40	.249
5.75	88.63	.244
6.75	91.20	.247
7.75	93.74	.252
8.75	91.40	.246
9.75	92.65	.246
10.75	96.45	.249
20.75	94.30	.252
21.75	96.84	.243
22.75	98.91	.244
28.75	97.40	.246
29.75	100.50	.249
30.75	102.0	.245
31.75	102.72	.245
45.0	101.65	.246
46.0	102.65	.247
47.0	103.0	.247
55.0	102.0	.247
73.0	99.82	.243
74.0	101.80	.245

Table 3.4.2   k and c_p values for aluminum 2024-T351
(specimen 4H) at 375 °F.

Time (hrs) at temp	$k(\frac{Btu}{hr-ft-F})$	$c_p(\frac{Btu}{lbm-F})$
0.0	98.0	
.75	104.52815	.249
1.25	107.111	.239
1.75	106.714	.239
2.25	108.547	.241
3.0	108.940	.244
3.75	107.03	.242
4.25	108.05	.245
5.75	110.52	.242
6.25	109.16	.242
6.75	108.75165	.247
7.5	107.35	.244
9.5	104.80	.240
10.5	105.8	.244
11.5	102.93	.245

Table 3.4.3 k and c_p values for aluminum 2024-T351
(specimen 14H) at 375 °F.

Time (hrs) at temp	$k(\frac{Btu}{hr-ft-F})$	$c_p(\frac{Btu}{lbm-F})$
0.0	99.6	.265
1	102.55	.256
2	105.9	.256
3	106.32	.253
4	108.4	.252
5	107.8	.254
6	106.74	.250
8	107.3	.251
9	106.9	.249
10	107.3	.248
11	107.2	.245
24	110.8	.250
25	111.0	.249
39.75	111.9	.248
54.25	111.7	.244
83.25	109.9	.242
101	111.2	.243

Table 3.4.4 k and c_p values for aluminum 2024-T351
(specimen 6H) at 400 °F.

Time (hrs) at temp	$k(\frac{Btu}{hr-ft-F})$	$c_p(\frac{Btu}{lbm-F})$
0.0	99.4	.269
0.5	109.8	.258
1.0	114.5	.255
1.5	112.54	.252
2.0	115.33	.251
2.5	114.35	.251
3.25	118.0	.258
3.75	111.30	.249
4.25	110.70	.251
4.75	110.65	.249
5.25	111.3	.251
5.75	111.21	.254
6.25	112.0	.253
6.75	109.9	.252
7.25	109.7	.252
7.75	110.5	.252
8.25	111.4	.254

Table 3.4.5 k and c_p values for aluminum 2024-T351
           (specimen 10H) at 400 °F.

Time (hrs) at temp	$k(\frac{Btu}{hr-ft-F})$	$c_p(\frac{Btu}{lbm-F})$
0.0	97.8	.272
1.0	104.7	.256
1.5	108.6	.262
2.0	109.7	.267
3.5	105.5	.254
4.5	105.9	.257
5.5	105.4	.254
6.5	105.8	.252
8.0	106.2	.253
9.0	105.3	.254

Table 3.4.6 k and c_p values for aluminum 2024-T351
           (specimen 11H) at 400 °F.

Time (hrs) at temp	$k(\frac{Btu}{hr-ft-F})$	$c_p(\frac{Btu}{lbm-F})$
0.0	98.3	.273
0.5	104.4	.257
1.0	110.55	.254
1.5	110.61	.260
2.0	110.62	.260
3.0	107.8	.256
4.0	107.7	.254
5.0	106.0	.253
6.0	106.7	.253
8.5	106.5	.252

Table 3.4.7 k and c_p values for aluminum 2024-T351
(specimen 12H) at 400 °F.

Time (hrs) at temp	$k(\frac{Btu}{hr\text{-}ft\text{-}F})$	$c_p(\frac{Btu}{lbm\text{-}F})$
0.0	105.3	.278
1.0	114.8	.252
2.0	115.31	.255
3.0	117.0	.258
4.0	115.8	.255
5.0	114.6	.249
6.0	113.34	.248
7.0	113.31	.251
8.0	112.8	.250

Table 3.4.8 k and c_p values of aluminum 2024-T351
(specimen 3H) at 425 °F.

Time (hrs) at temp	$k(\frac{Btu}{hr\text{-}ft\text{-}F})$	$c_p(\frac{Btu}{lbm\text{-}F})$
0.25	91.690	.260
0.75	104.517	.258
1.25	109.471	.281
2.0	109.095	.266
3.0	105.304	.255
4.0	105.481	.252
6.5	101.875	.254
7.5	102.806	.254
8.5	101.890	.252
9.5	102.791	.252
10.5	102.404	.257

Table 3.4.9   k and c_p values of aluminum 2024-T351 (specimen 13H) at 425 °F.

Time (hrs) at temp	$k(\frac{Btu}{hr\text{-}ft\text{-}F})$	$c_p(\frac{Btu}{lbm\text{-}F})$
0.0	102.11	.235
0.75	117.12	.271
1.25	113.8	.262
1.75	113.4	.261
2.75	112.6	.259
3.75	112.6	.259
4.75	113.3	.260
6.0	112.0	.258

Table 3.4.10   Composite (average) values of k and c_p of aluminum 2024-T351 at 375 °F.

Time (hrs) at temp	$k(\frac{Btu}{hr\text{-}ft\text{-}F})$	$c_p(\frac{Btu}{lbm\text{-}F})$
0.0	99	.2650
1	104.2	.2500
2	106.5	.2480
3	107.6	.2485
4	108.0	.2478
5	108.6	.2488
6	108.2	.2460
7	107.3	.2483
8	106.7	.2470
9	106.2	.2450
10	106.3	.2450
11	105.8	.2450

Table 3.4.11 Composite (average) values of k and c_p of
               aluminum 2024-T351 at 400 °F.

Time (hrs) at temp	$k(\frac{Btu}{hr\text{-}ft\text{-}F})$	$c_p(\frac{Btu}{lbm\text{-}F})$
0.0	100.2	.2730
1	111.14	.2543
2	112.7	.2583
3	112.2	.2570
4	110.1	.2540
5	109.3	.2520
6	109.3	.2520
7	108.9	.2522
8	109.1	.2520

Table 3.4.12 Composite (average) values of k and c_p of
               aluminum 2024-T351 at 425 °F.

Time (hrs) at temp	$k(\frac{Btu}{hr\text{-}ft\text{-}F})$	$c_p(\frac{Btu}{lbm\text{-}F})$
0.0	96.0	.2475
0.75	110.66	.2644
1.25	111.65	.2720
2	111.15	.2637
3	109.1	.2571
4	109.1	.2554
5	108	.2560
6	107	.2558

Table 3.4.13   Values of k at room temperature for over-aged
aluminum 2024-T351.

Specimen number and temperature	Over-aged values of k (at room temperature)
3H (425 °F, 10.5 hours)	97.2
4H (375 °F, 11.5 hours)	94.2
5H (350 °F, 74 hours)	96.9
6H (400 °F, 8.25 hours)	99.5
10H (400 °F, 9 hours)	96.0
11H (400 °F, 8.5 hours)	97.5
12H (400 °F, 8 hours)	105.25
13H (425 °F, 6 hours)	102.3
14H (375 °F, 101 hours)	102.8

Table 3.4.14   Composite (average) values of k at room
temperature for over-aged aluminum 2024-T351.

Process	k value ($\frac{Btu}{hr\text{-}ft\text{-}F}$)
Regular annealing	97.0
350 °F-nominal temperature	96.9
375 °F-nominal temperature	98.5
400 °F-nominal temperature	99.56
425 °F-nominal temperature	99.75

Figure 3.4.1 Thermal conductivity as a function of time at 350°F for aluminum 2024-T351, specimen 5H.
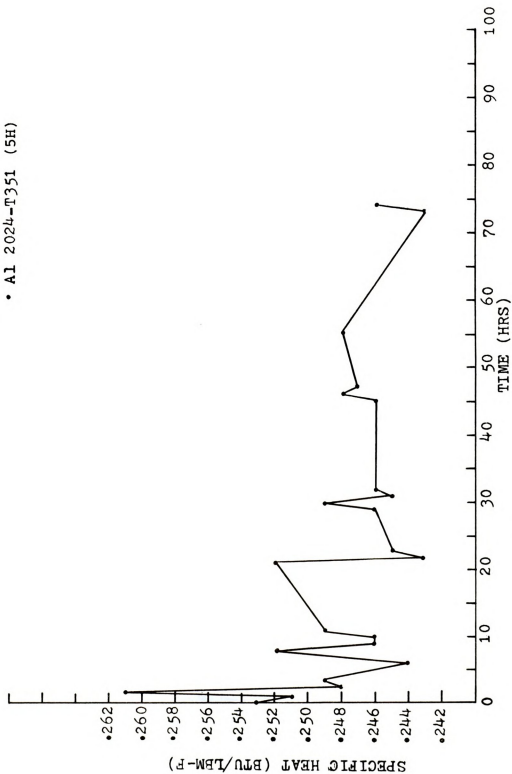
Figure 3.4.2   Specific heat as a function of time at 350 °F for aluminum 2024-T351, specimen 5H.
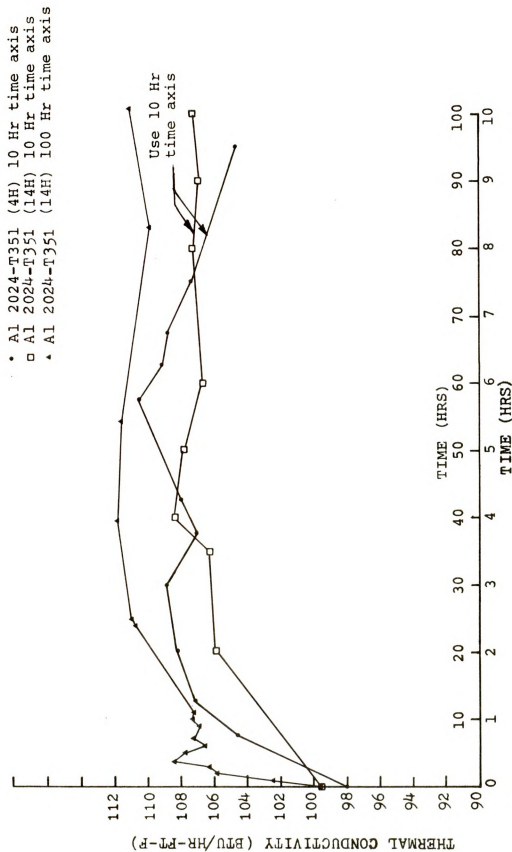
Figure 3.4.3 Thermal conductivity as a function of time at 375 °F for aluminum 2024-T351, specimen 4H and 14H.
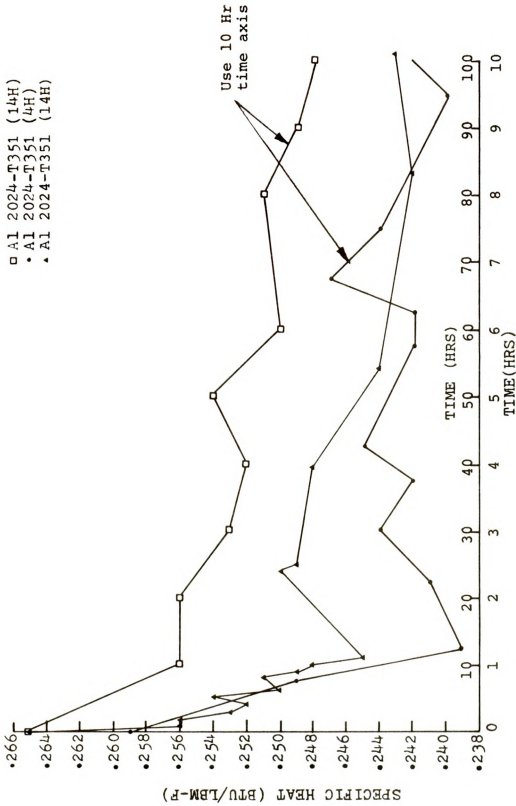
Figure 3.4.4   Specific heat as a function of time at 375 °F for aluminum 2024-T351, specimen 4H and 14H.
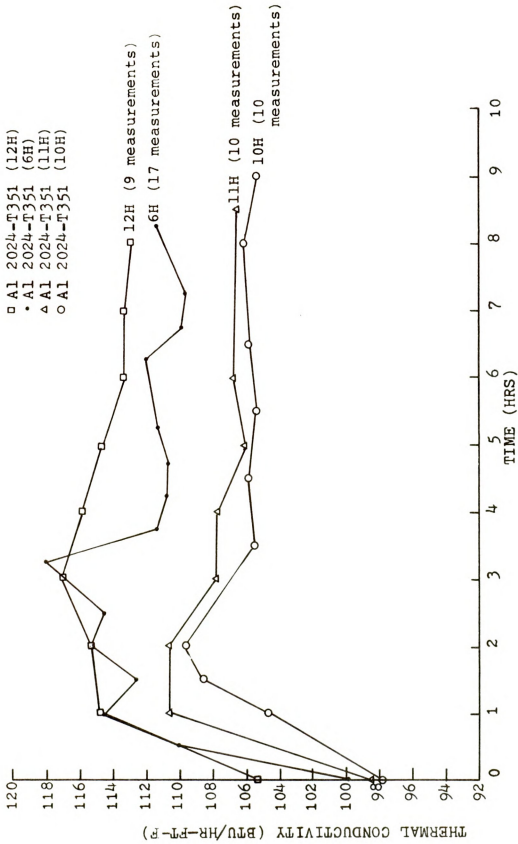
Figure 3.4.5 Thermal conductivity as a function of time at 400 °F for aluminum 2024-T351, specimens 6H, 10H, 11H, and 12H.
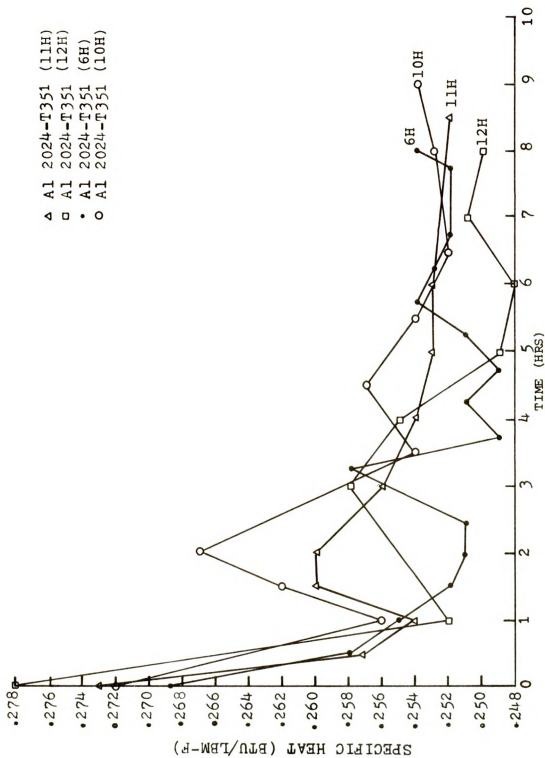
Figure 3.4.6 Specific heat as a function of time at 400 °F for aluminum 2024-T351, specimens 6H, 10H, 11H, 12H.
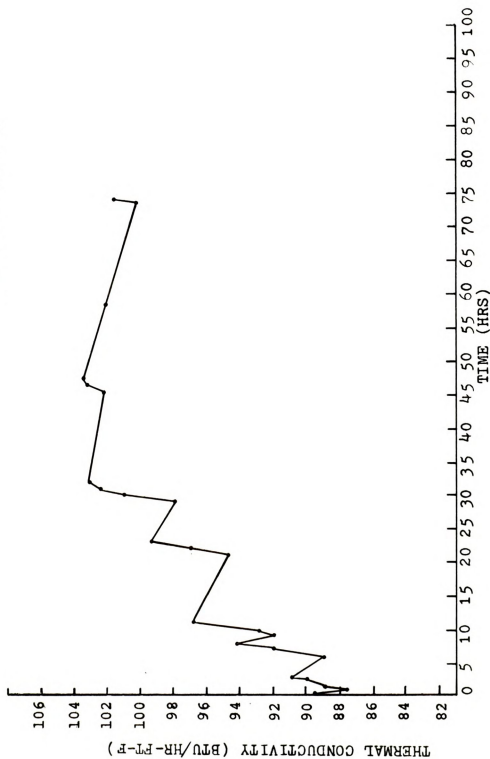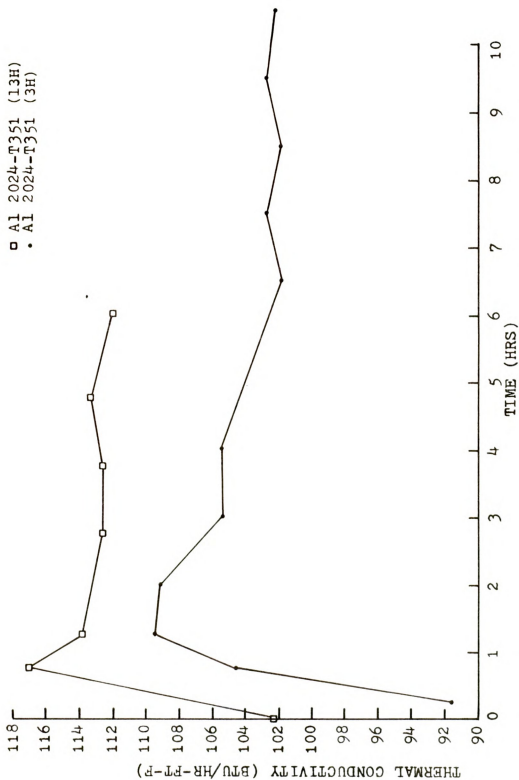
Figure 3.4.7 Thermal conductivity as a function of time at 425 °F for aluminum 2024-T351, specimens 3H and 13H.
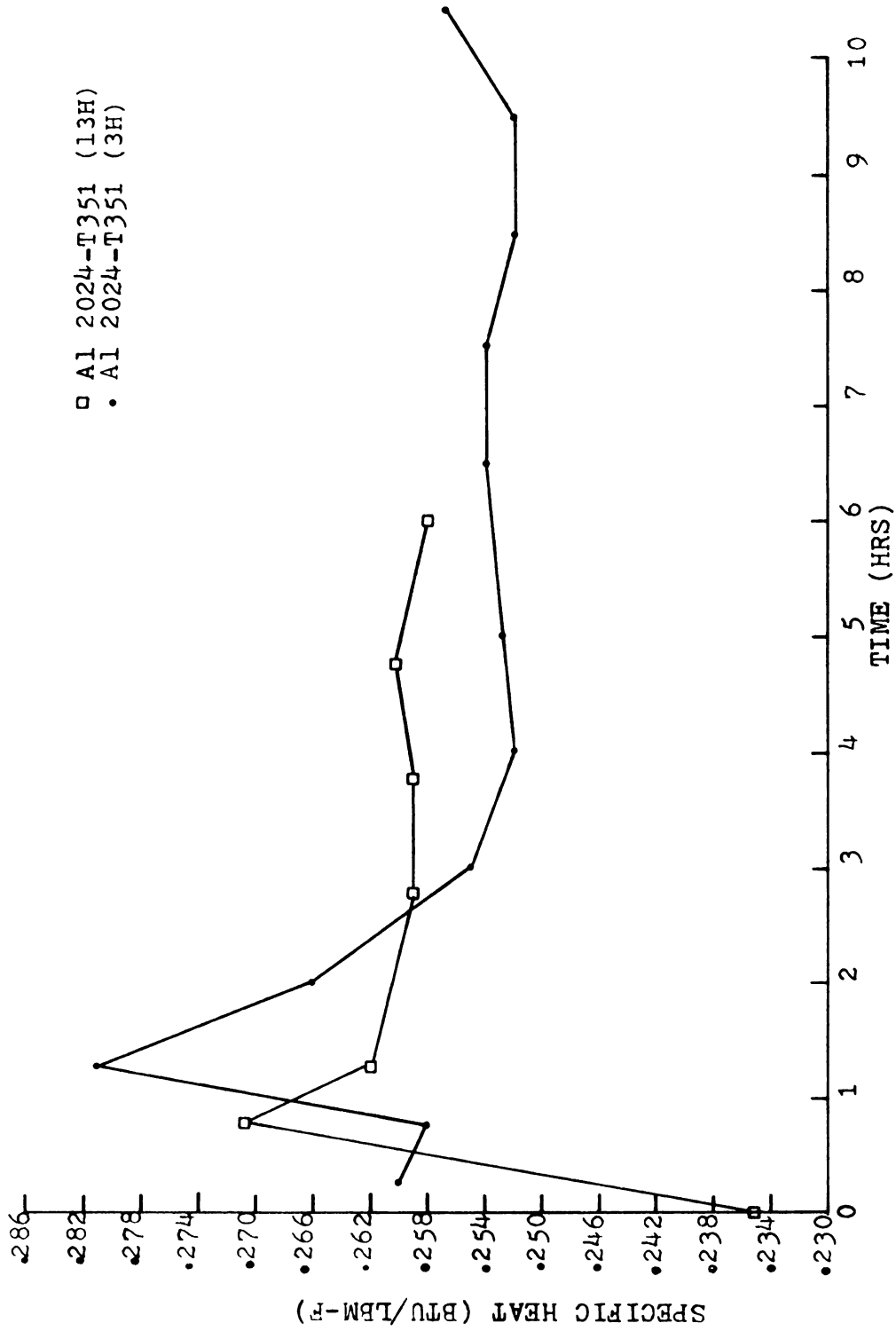
Figure 3.4.8 Specific heat as a function of time at 425 °F for aluminum 2024-T351, specimens 3H and 13H.
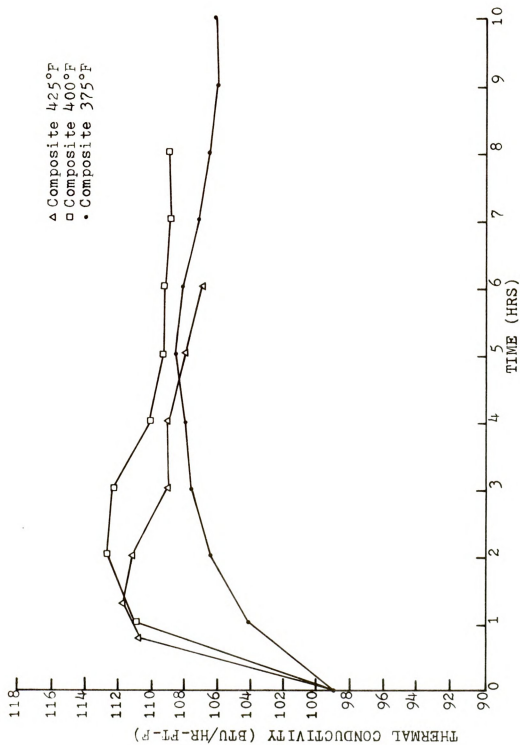
Figure 3.4.9 Thermal conductivity as a function of time for composite curves at 375°, 400°, and 425 °F for aluminum 2024-T351.
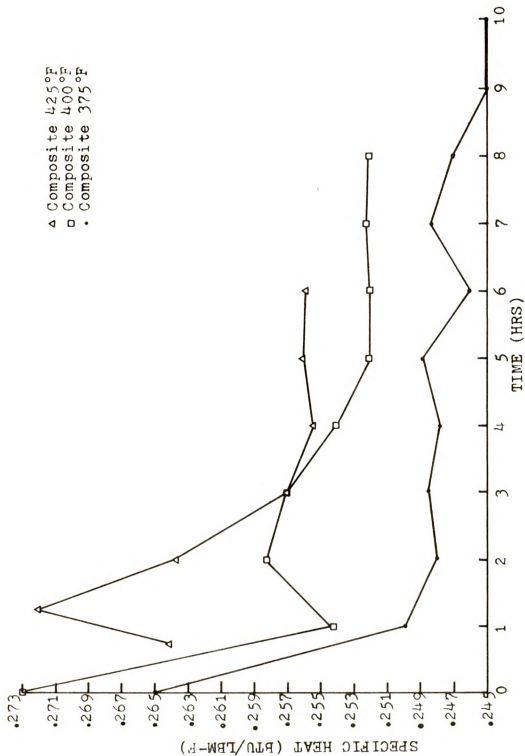
Figure 3.4.10 Specific heat as a function of time for composite curves at 375°, 400°, and 425 °F for aluminum 2024-T351.

108

Figure 3.4.11 Thermal conductivity as a function of temperature given by TPRC.
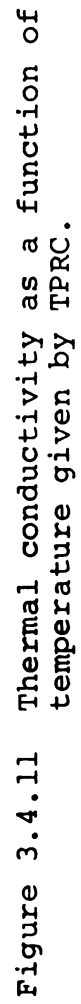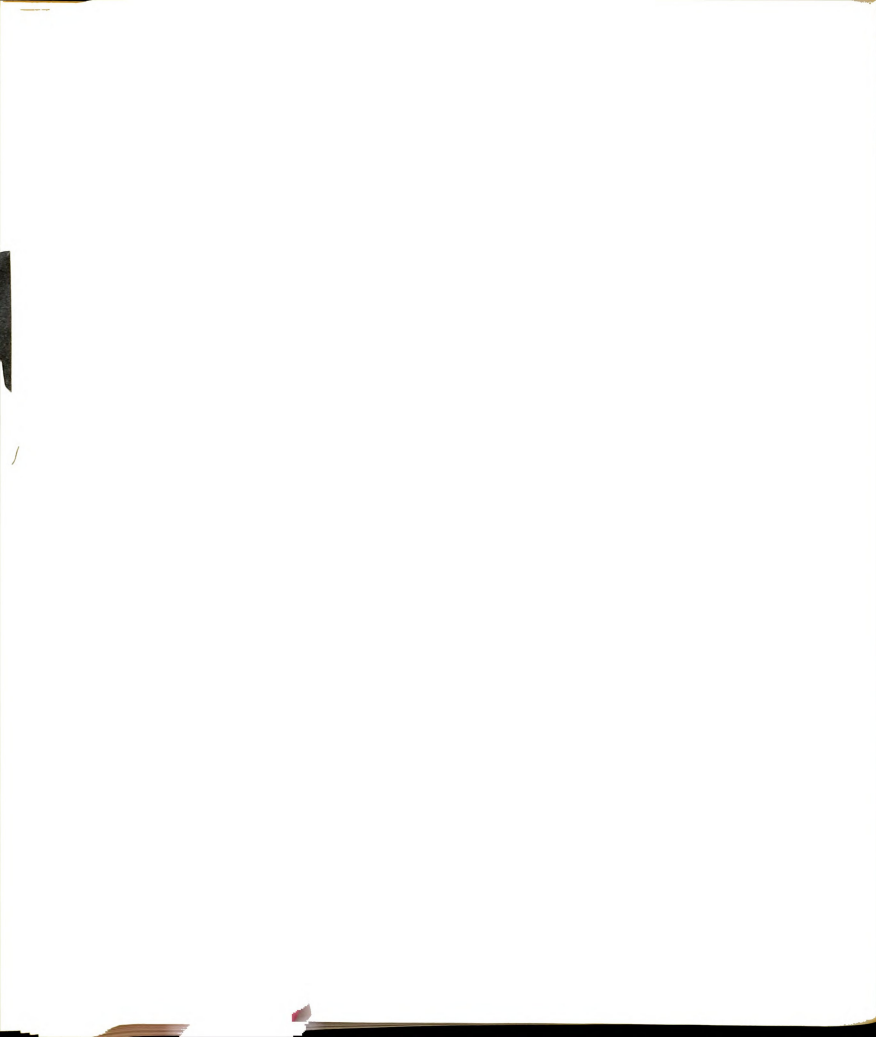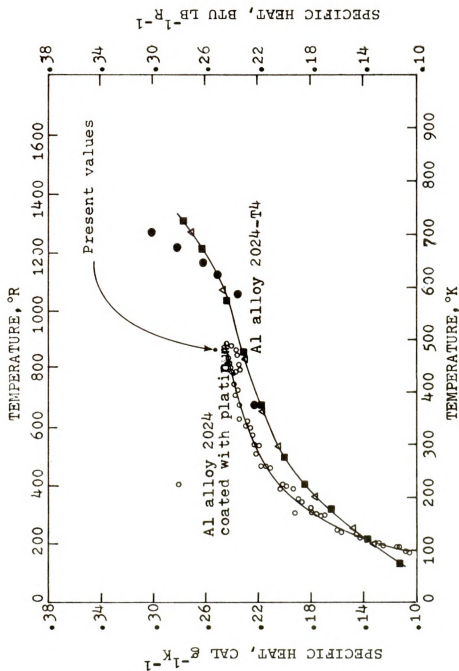
Figure 3.4.12 Specific heat as a function of temperature given by TPRC.

1. Corrections applied to k:

a. Correction due to the changes in the specimen length E_{sp} and $(\rho E c_p)_{cal}$ in Equation (2.1.12) because of the high temperatures. This correction is given by the equation

$$E_{sp}(E\rho c_p)_{cal} = (E_o)_{sp} (E_o \rho_o c_p)_{cal} [1 + \beta_{sp}(T_{sp} - T_o) -$$

$$-2\beta_{cal}(T_{cal} - T_o)] \qquad (3.5.1)$$

where the subscript (o) indicates a room temperature value, and β is thermal linear expansion of the material.

That is, Equation (3.5.1) must be substituted in Equation (2.1.12) for the high temperatures, or simply evaluate

$$[1 + \beta_{sp}(T_{sp} - T_o) - 2\beta_{cal}(T_{cal} - T_o)]$$

and multiply it by the uncorrected k values.

b. Multiply the uncorrected values of k by 0.5% to take into account the absorption of energy by the silicone film on the aluminum surface when heated by the calorimeter during the test.

c. Multiply the uncorrected values of k by 2% when using the washer-type thermocouple mounting on the insulated surface of the specimen. This is because the actual thickness of the specimen where the insulated surface thermocouple is located is not 1.5 inches but rather at 1.5" + 1/16". The reason for taking 2% correction is because the thermocouple is located at half way of the

washer's thickness, that is at 1/32 inch from either end
of the washer where

$$\frac{e}{E} = \frac{\frac{1}{32}}{\frac{3}{2}} = \frac{2}{32 \times 3} = \frac{1}{48} \approx 2\%$$

2. Corrections applied for $\bar{c}_p$:

A correction was applied to the $\bar{c}_p$ values of
aluminum to take into account changes in $(\rho c_p)_{cal}$ at the
high temperatures.

3. Corrections not required

The following corrections were considered for both
k and $\bar{c}_p$ but not applied.

1. No correction is necessary for the iron-constantan
thermocouple calibration. Note that the constant C_v cancels
in both Equations (2.4.1) and (2.4.2).

2. No correction was applied for the heat losses
because it is not clear how to do this at the present time.
The measured specific heat (which is more affected by the
heat losses) of aluminum was about 8% higher than that
reported by TPRC, while that of Armco iron was about 16%
higher.

As it was shown in Chapter II, Armco iron was
tested in two ways; one way was for the heat flow during
the test to be from the calorimeter to Armco and the other
way was to reverse the heat flow.
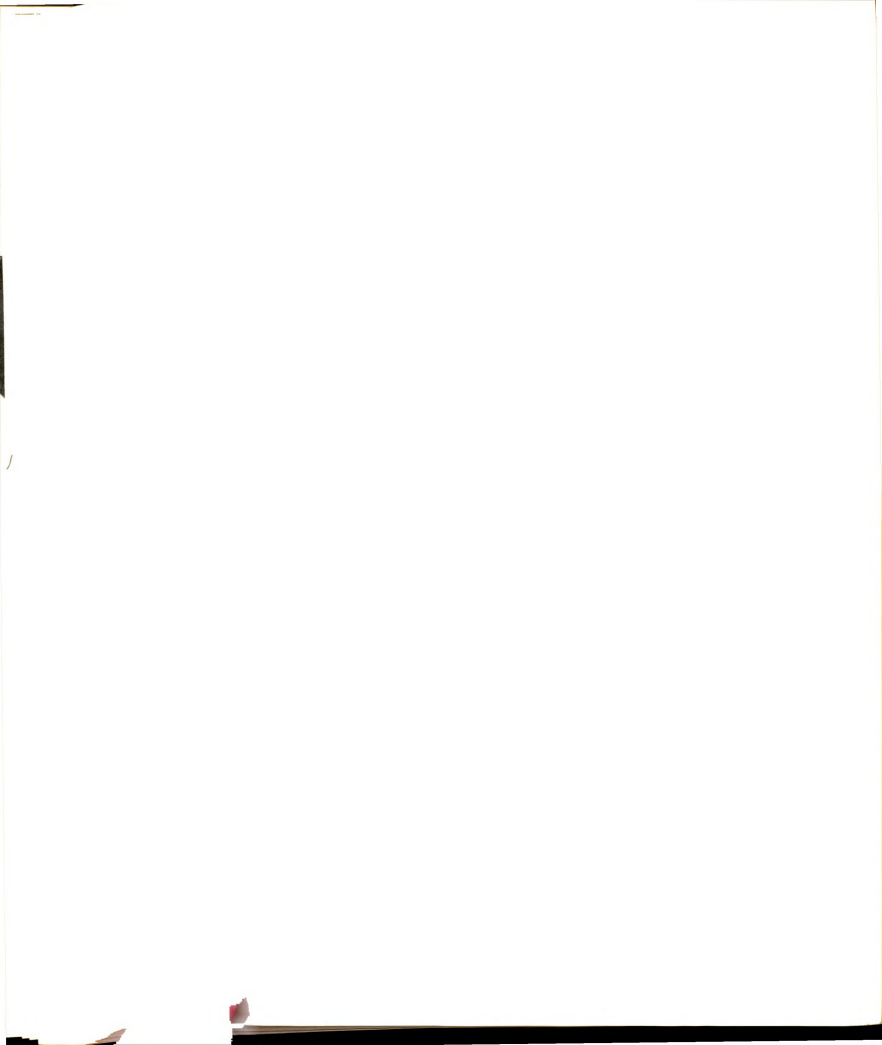
It was found that c_p of Armco at the elevated temperatures (400 °F for example) is about 16% higher than that given by TPRC, if the heat flow is from the calorimeter to the specimen while it is about 16% lower than that reported by TPRC if the heat flow is reversed. If an average value is taken for both tests at the same temperature, one can see that the c_p value becomes almost identical to that given by TPRC for the same temperature.

This process of averaging results for the heat flow in both directions was not performed for the aluminum because the thermal conductivity was of primary interest and the heat flow direction did not significantly affect the k values. All the aluminum values were obtained with the heat flow from the calorimeter to the specimen.

3. No correction was needed for the calorimeter to account for the thermal linear expansion. The specific heat expression is

$$\bar{c}_p = \frac{(\rho E)_{cal} \; (c_p \Delta T)_{cal}}{(E\rho)_{sp} \; (T_f - T_i)_{sp}}$$

At the elevated temperatures $(\rho E)_{cal}$ and $(\rho E)_{sp}$ should be modified in the following manner

$$\bar{c}_p = \frac{(\rho_o E_o)_{cal} \; (1 - 2\beta_{cal} \; (T_{cal} - T_o)) \; (c_p \Delta T)_{cal}}{(\rho_o E_o)_{sp} \; (1 - 2\beta_{sp} \; (T_{sp} - T_o)) \; (T_f - T_i)_{sp}}$$

However,

$$(1 - 2\beta_{cal} (T_{cal} - T_o)) \approx (1 - 2\beta_{sp} (T_{sp} - T_o)$$

Therefore

$$\frac{(\rho E)_{cal} (c_p \Delta T)_{cal}}{(\rho E)_{sp} (T_f - T_i)_{sp}} \approx \frac{(\rho_o E_o)_{cal} (c_p \Delta T)_{cal}}{(\rho_o E_o)_{sp} (T_f - T_i)_{sp}}$$

which means a correction to account for the thermal linear expansion for the calorimeter is not needed.

4. Since the thermocouples on the heated surface do not measure the temperature at the surface but rather at 0.005 inch below the surface (that is, the measurement is done at the center of the wire) some form of correction for k is needed. However, since there is no perfect contact between the thermocouple wire and the surrounding metal, the thermocouple then reads somewhat higher than it should be. Therefore there are two mechanisms in operation, one lowers the temperature measurement by measuring at 0.005 inch below the surface and the other raises the temperature measurement because of the imperfect contact between the thermocouple wires and the surrounding metal. These effects cancel each other out, and a correction for k is not applied. For further information on the possible thermocouple groves effect on the heat transfer see Henning and Parker [37].

CHAPTER IV

MODELING

In order to utilize for design purposes the data
delineated in Chapter III (especially those of the thermal
conductivity) a mathematical model is needed to describe it.
This model would enable one to predict the thermal con-
ductivity values for different temperatures and times.
This chapter deals with (1) formulation of the mathematical
model, (2) predicting the thermal conductivity values for
different times and temperatures by using the model, and
(3) describing an example using the ideas presented in (1)
and (2) above.

4.1. The development of a mathematical model

The thermal conductivity values presented in Section
(3.4), were determined at the four different temperatures
of 350°, 375°, 400°, and 425 °F. To enable the designer
to predict the values of thermal conductivity at temper-
atures other than the ones given above and for transient
conditions, it is necessary to develop a mathematical
model that describes the general behavior of thermal con-
ductivity in the temperature range 350-425 °F. As

114

mentioned earlier, for temperatures below 350 °F the thermal conductivity does not change significantly with time. Yet, for temperatures higher than 425 °F it changes so rapidly that accurate measurements were not possible. The figures presented in Section (3.4) show that thermal conductivity values have a certain pattern; each starts with a relatively small value, attain a maximum value at a given time (depending on the temperature level) and then begin to fall slightly with time before reaching some constant value. It appears that most of the significant changes take place between $t = 0$ and $t = t_{max}$ (where t_{max} is the time at which the thermal conductivity value becomes maximum for a given temperature). The thermal conductivity data between $t = 0$ and t_{max} for all four temperatures (350°, 375°, 400°, and 425 °F) were normalized and plotted versus their normalized time; see Figure 4.1.1. Normalized thermal conductivity, k^+, is defined by

$$k^+ \equiv \frac{k_i - k_{min}}{k_{max} - k_{min}}$$

where

k_i = thermal conductivity values at times t_i in the range $t = 0$ to t_{max}

k_{min} = thermal conductivity value at time zero for a given temperature (time zero means the time at which the specimen arrives at the desired nominal temperature).
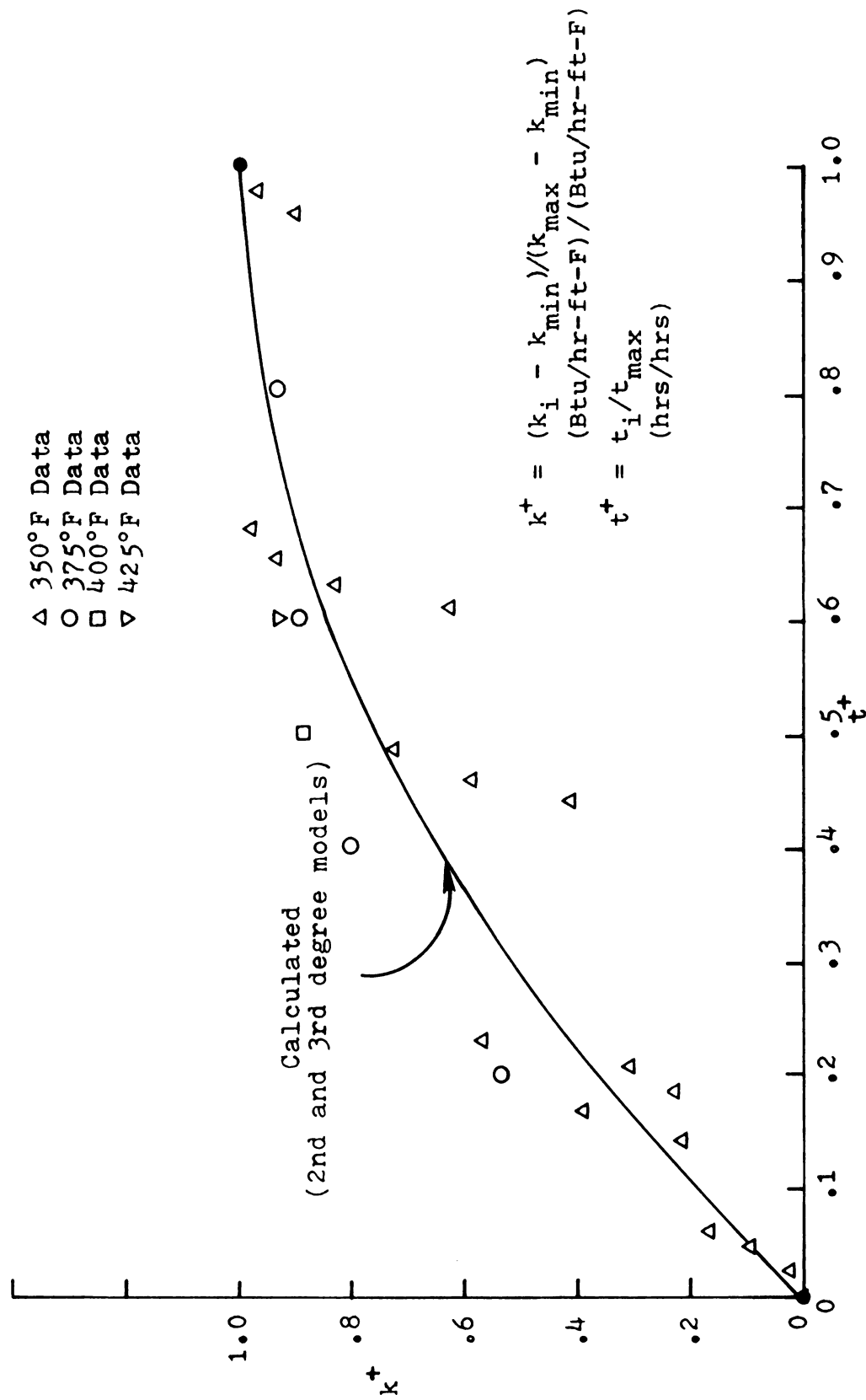
Figure 4.1.1 Values of normalized thermal conductivity of aluminum 2024-T351 for the temperatures 350°, 375°, 400°, and 425 °F versus normalized time. Data points are for the time range t=0 to t=t_{max}.

k_{max} = maximum value of thermal conductivity for a given nominal temperature. The time at which k_{max} is measured is called t_{max}. Normalized time t^+ is defined by

$$t^+ \equiv \frac{t_i}{t_{max}}$$

The data in Figure 4.1.1 can be approximated by a curve. This curve could be described by a number of functions including,

1. second degree polynomial with

   a. fixed end points (at $t = 0$ and $t = t_{max}$) and zero slope at t_{max},

   b. fixed end points (at $t = 0$ and $t = t_{max}$) but not the slope, and

2. third degree polynomial with the same conditions as in 1(a) and 1(b).

For model 1(a) the curve between $t = 0$ and t_{max} is described by

$$k^+ = \beta_1 + \beta_2 t^+ + \beta_3 (t^+)^2 \qquad (4.1.1a)$$

where β_1, β_2, β_3 are parameters. The three conditions are

$$k^+ = 0 \quad at \quad t^+ = 0 \qquad (4.1.1b)$$

$$k^+ = 1 \quad at \quad t^+ = 1 \qquad (4.1.1c)$$

$$and \quad \frac{dk^+}{dt^+} = 0 \quad at \quad t^+ = 1 \qquad (4.1.1d)$$

Substitute (4.1.1b) in (4.1.1a) to get

$$\beta_1 = 0$$

and (4.1.1c) in (4.1.1a) to get

$$1 = \beta_2 + \beta_3 \quad \text{or} \quad \beta_3 = 1 - \beta_2$$

Substitute (4.1.1d) in (4.1.1a) to get

$$0 = \beta_2 + 2\beta_3$$

or

$$0 = \beta_2 + 2(1 - \beta_2)$$

Then

$$\beta_2 = 2, \text{ and } \beta_3 = -1$$

Model 1(a) then becomes

$$k^+ = 2t^+ - (t^+)^2 \qquad (4.1.2)$$

which has no unknown parameters.

For model 1(b) the curve is again given by (4.1.1a) but with the boundary conditions being only

$$k^+ = 0 \quad \text{at} \quad t^+ = 0 \qquad (4.1.3a)$$

$$k^+ = 1 \quad \text{at} \quad t^+ = 1 \qquad (4.1.3b)$$

Substitute (4.1.3a) in (4.1.1a) to get

$$\beta_1 = 0$$

and substitute (4.1.3b) in (4.1.1a) to find

$$1 = \beta_2 + \beta_3 \quad \text{or} \quad \beta_3 = 1 - \beta_2$$

Then model 1(b) becomes

$$k^+ = \beta_2 t^+ + (1 - \beta_2)(t^+)^2 \qquad (4.1.4)$$

which has only one unknown parameter, namely β_2. To estimate β_2 one can minimize the sum of squares (least squares)

$$S = \sum [y_i^+ - k_i^+]^2 \qquad (4.1.5)$$

where

y_i^+ = normalized observed thermal conductivity values (experimental points)

k_i^+ = normalized calculated thermal conductivity values

where $k_i^+ = \beta_2 t^+ + (1 - \beta_2)(t^+)^2$

Introduce (4.1.4) in (4.1.5) to find

$$S = \sum [y_i^+ - \beta_2 t^+ - (1 - \beta_2)(t^+)^2]^2 \qquad (4.1.6)$$

Taking the derivative of S with respect to β_2 and setting the result equal to zero yields a β_2 estimate which minimizes S; then

$$\left. \frac{\partial S}{\partial \beta_2} \right|_{\beta_2 = b_2} = \sum 2[y_i^+ - b_2 t^+ - t^{+^2} + b_2 t^{+^2}][-t^+ + t^{+^2}] = 0$$
$$(4.1.7)$$

or

$$\sum t^{+^3}(t^+ - 1)b_2 - \sum t^{+^2}(t^+ - 1)b_2 = \sum t^{+^3}(t^+ - 1) - \sum t^+(t^+ - 1)y_i^+$$

(4.1.8)

The estimate of β_2 is b_2,

$$b_2 = \frac{\sum t^+(t^+ - 1)(t^{+^2} - y_i^+)}{\sum t^{+^2}(t^+ - 1)^2}$$

(4.1.9)

To find b_2, substitute all y_i^+'s at their respective t_i^+'s ($i = 1, 2, \ldots, n$ observed data points) in Equation (4.1.9). To obtain the calculated values of thermal conductivity, substitute the value obtained for b_2 in Equation (4.1.4).

For model 2(a), the curve can be described as:

$$k^+ = \beta_1 + \beta_2 t^+ + \beta_3 t^{+^2} + \beta_4 t^{+^3}$$

(4.1.10a)

where β_1, β_2, β_3, and β_4 are parameters to be determined. The conditions are

$$k^+ = 0 \quad \text{at } t^+ = 0$$

(4.1.10b)

$$k^+ = 1 \quad \text{at } t^+ = 1$$

(4.1.10c)

$$\frac{dk^+}{dt^+} = 0 \quad \text{at } t^+ = 1$$

(4.1.10d)

Substituting (4.1.10b) in (4.1.10a) yields

$$\beta_1 = 0$$

and substitute (4.1.10c) in (4.1.10a) to find

$$1 = \beta_2 + \beta_3 + \beta_4 \qquad (4.1.11)$$

Differentiating (4.1.10a) and using (4.1.10d) gives

$$0 = \beta_2 + 2\beta_3 + 3\beta_4 \qquad (4.1.12)$$

Then solving (4.1.11) and (4.1.12) simultaneously yields

$$\beta_4 = \beta_2 - 2 \qquad (4.1.13)$$

$$\beta_3 = 3 - 2\beta_2 \qquad (4.1.14)$$

Therefore (4.1.10a) becomes

$$k^+ = \beta_2 t^+ + (3 - 2\beta_2)t^{+2} + (\beta_2 - 2)t^{+3} \qquad (4.1.15)$$

and there is only one parameter to evaluate which is β_2. Substitute (4.1.15) in (4.1.5) and follow in the same manner described earlier to obtain an estimate of β_2, namely b_2, that is

$$b_2 = \frac{\sum(3t^{+2} - 2t^{+3} - y_i^+)(-t^+ + 2t^{+2} - t^{+3})}{\sum(t^+)^2(t^+ - 1)^4} \qquad (4.1.16)$$

and find k_i for a given temperature as discussed earlier.

For model 2(b), the curve can be described by Equation (4.1.10a) and conditions (4.1.10b) and (4.1.10c) only; then the result will be an equal number of unknown

parameters and equations which can be solved simultaneously to obtain these parameters, see Beck [38].

To avoid tedious and error-prone operations in finding the parameters in the models described in this section, a computer program has been used. This program was written by Nicely and Dye [39] of the Department of Chemistry at Michigan State University. It is capable of determining the desired parameters by utilizing a subroutine that is programmed to give the desired mathematical model.

It was found that the parameters in the second degree polynomial model (Equation (4.1.4)) and the third degree polynomial model (Equation (4.1.15)) are nearly the same. For the second degree model b_2 was calculated to be 2.02371 and for the third degree model $b_2 = 2.06447$. Both values are nearly 2.0.

Since the two models are nearly similar in describing the experimental data in Figure 4.1.1, it is easier from a computational point of view to use the second degree polynomial model. Hence, by letting $\beta_2 = 2$ in Equation (4.1.4) yields

$$k^+ = 2t^+ - (t^+)^2 \qquad (4.1.17)$$

or

$$\frac{k_i - k_{min}}{k_{max} - k_{min}} = 2\left(\frac{t_i}{t_{max}}\right) - \left(\frac{t_i}{t_{max}}\right)^2$$

It is interesting to note that Equation (4.1.17) is identical to Equation (4.1.2).

4.2 Obtaining thermal conductivity values from the mathematical model

To obtain thermal conductivity values at a given temperature by using Equation (4.1.17), one must know k_{max}, k_{min}, and t_{max} at that temperature.

The thermal conductivity value at zero time (the time at which the specimen arrives at the desired temperature) is designated k_{min}. The k_{min} values are determined from the composite curves given in Figure 3.4.9 and also from Figure 3.4.1 for 350°, 375°, 400°, and 425°F. These values are plotted versus their respective temperatures in Figure 4.2.1. For k_{min} values between room temperature (about 80 °F) and 350 °F, values were obtained by linear interpolation; the values are 78 and 88.5 $\frac{Btu}{hr-ft-F}$ for 80 and 350 °F respectively.

The maximum values that the thermal conductivity attains (k_{max}) for the temperatures 350°, 375°, 400°, and 425 °F are determined from Figure 3.4.9 and Figure 3.4.1. They are plotted versus their respective temperatures in Figure 4.2.2. It was found that a second degree polynomial curve describes the data. Using the Nicely and Dye program (KINFIT) the model was found to be

$$k_{max} = -0.00244T^2 + 2.006T - 299.835 \qquad (4.2.1)$$
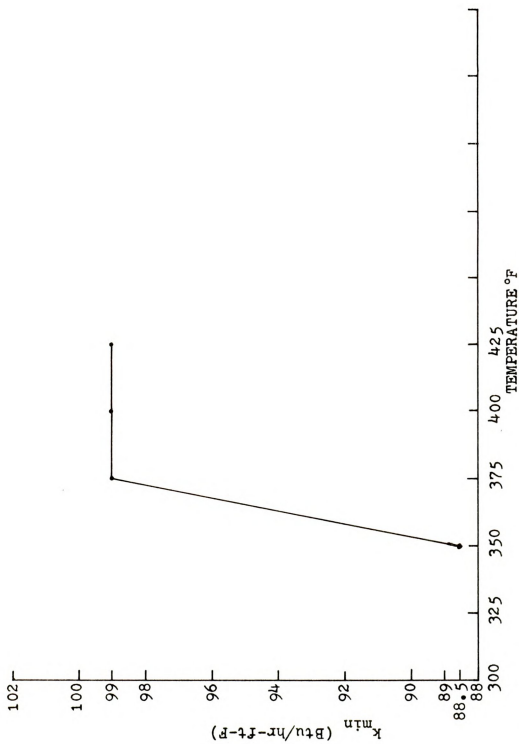
Figure 4.2.1   Graph of thermal conductivity values of aluminum 2024-T351 at zero time (k_{min}) versus temperature.

The model is

$$k_{max} = -.00244 \; T^2 + 2.006 \; T - 299.835$$
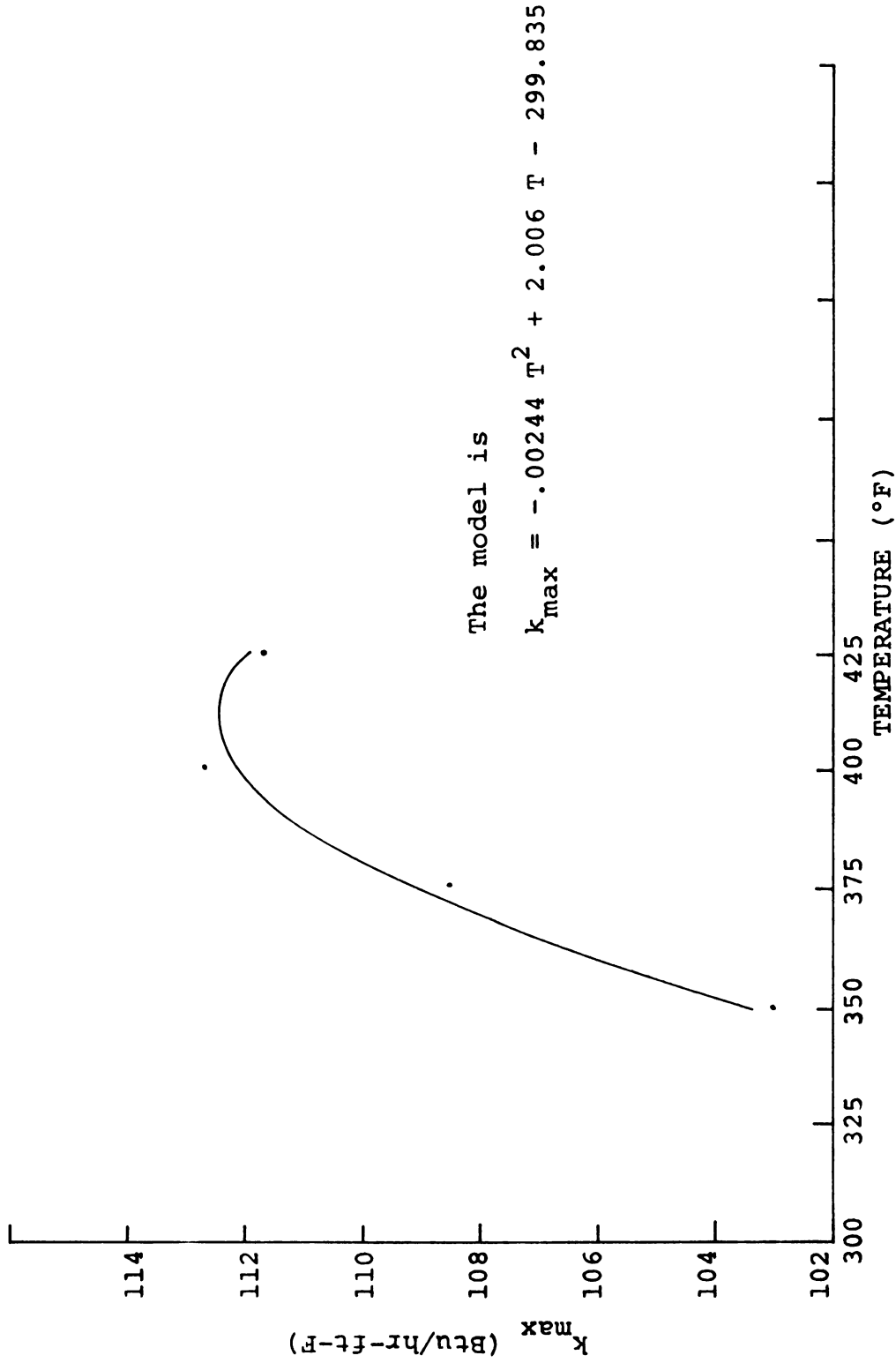
Figure 4.2.2   Maximum values of thermal conductivities of aluminum 2024-T351 (k_{max}) versus their respective temperatures.

Equation (4.2.1) is based on four data points in the temperature range 350° to 425 °F.

The time at which the thermal conductivity attains its maximum value for a given temperature is designated t_{max}. It is also determined from the composite curves in Figure 3.4.9 and Figure 3.4.1 for the temperatures of 350°, 375°, 400°, and 425 °F. These values are plotted versus their respective temperatures in Figure 4.2.3.

A mathematical model suggested by Frame [40] describes the data very well in the temperature range 350°-425 °F; see Figure 4.2.3. The model using KINFIT is found to be

$$t_{max} = \frac{47.0}{1 + 8.4158 \left(\frac{T - 350}{25}\right)^{1.38}} \qquad (4.2.2)$$

Using the equations for k_{min}, k_{max}, and t_{max} given above, k_i can be obtained by using Equation (4.1.17) for the temperature range 350 to 425 °F. To use Equation (4.1.17) the following conditions must be met:

1. The time must be less than t_{max}.

2. For any specific temperature, one must use k_{min} and k_{max} at that temperature, whether one is heating or cooling the specimen to arrive at that desired temperature, regardless of the length of time taken to reach it.

3. It is necessary to use $\frac{t}{t_{max}}$ as an expression of percent precipitation of the (θ) phase, i.e., 47

The model is

$$t_{max} = \frac{47.0}{1 + 8.4158 \left(\frac{T - 350}{25}\right)^{1.38}}$$
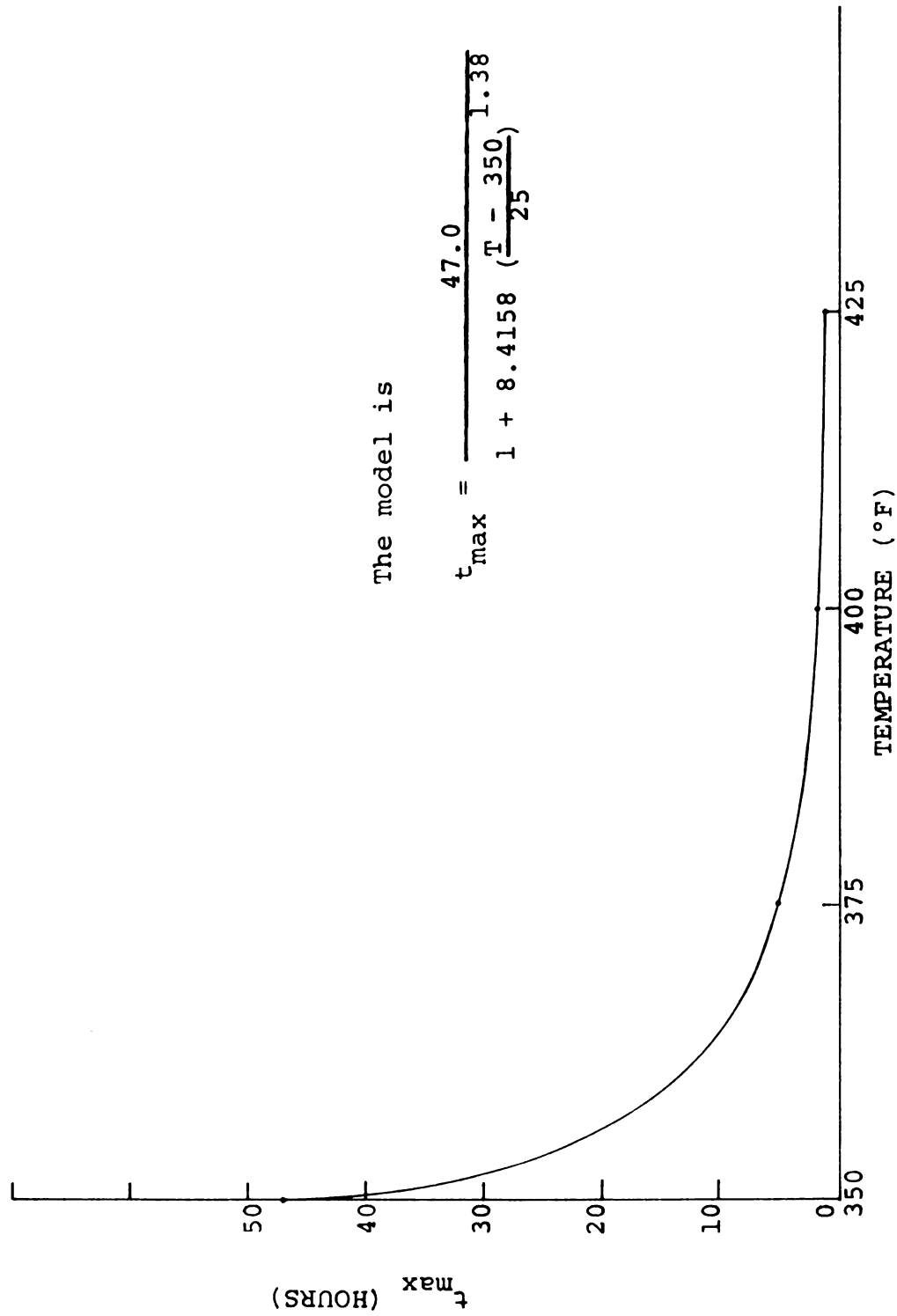
Figure 4.2.3 Time at which the thermal conductivity of aluminum 2024-T351 attains its maximum value (t_{max}) versus temperature.

hours at 350 °F corresponding to 5 hours at 375 °F, 2 hours at 400 °F, etc.

Hence holding the specimen for 23 1/2 hours at 350 °F is assumed to be equivalent in the progress of precipitation of the (θ) phase to holding it for 2 1/2 hours at 375 °F, for 1 hour at 400 °F, etc. Further experimental work should be done to check this assumption with respect to a non-constant temperature history of the specimen. To illustrate the above points consider the case of a specimen which is initially at room temperature and has a step increase in temperature to 375 °F. After two hours the temperature is abruptly increased to 400 °F and held there. The thermal conductivity history is needed for the temperature history depicted in Figure 4.2.4.

Figure 4.2.4   Aluminum 2024-T351 specimen maintained at 375 °F for two hours then heated to and maintained at 400 °F.
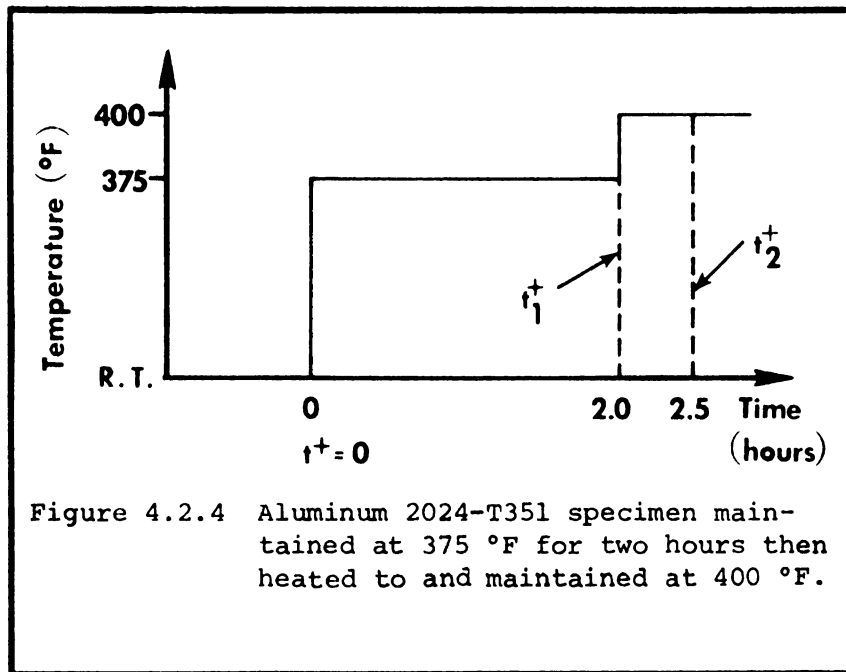
For real times from zero to 2 hours the required constants are

$$k_{min} = k_{min,375} = 99.0 \ (\frac{Btu}{hr\text{-}ft\text{-}F})$$

$$k_{max} = k_{max,375} = 108.6 \ (\frac{Btu}{hr\text{-}ft\text{-}F})$$

$$t_{max} = t_{max,375} = 5.0 \ hours$$

The t^+ values required are simply found using

$$t^+ = \frac{t}{t_{max,375}} \ where \ o<t<2 \ hours$$

For real times greater than 2 hours the k_{min}, k_{max}, and t_{max} values are evaluated at 400 °F, i.e.,

$$k_{min} = k_{min,400} = 99.0 \ (\frac{Btu}{hr\text{-}ft\text{-}F})$$

$$k_{max} = k_{max,400} = 112.7 \ (\frac{Btu}{hr\text{-}ft\text{-}F})$$

$$t_{max} = t_{max,400} = 2.0 \ hours$$

The t^+ range must now be found associated with 400 °F. An important assumption that we shall make is that the t^+ value at the end of 375 °F period is the beginning value for the 400 °F range. This assumption should be investigated experimentally in a later study.

The t^+ value at the end of the 375 °F period shall be called t_1^+ as shown in Figure 4.2.4, this value is given by

$$t_1^+ = \frac{t_{e_1}}{t_{max,375}} = \frac{2.0}{5.0} = 0.4$$

where t_{e_1} is equal to the effective time based on the nominal temperature of 375 °F. To illustrate for 400 °F, the k value is to be given for time 2.5 hours. The t_2^+ value is given by

$$t_2^+ = t_1^+ + \frac{t_{e_2}}{t_{max,400}} = 0.4 + \frac{.5}{2} = 0.65$$

where t_{e_2} is equal to the effective time for which the specimen is held at 400 °F only. The k value then is given by

$$\frac{k - k_{min,400}}{k_{max,400} - k_{min,400}} = 2(t_2^+) - (t_2^+)^2$$

$$\frac{k - 99.0}{112.7 - 99.0} = 2(0.65) - (0.65)^2 = 0.8775$$

$$k = 111.0 \ (\frac{Btu}{hr-ft-F})$$

If we have a continuous case of heating (or cooling) say from 350 to 430 °F, then to find k we can approximate the temperature history by a series of steps as shown in Figure 4.2.5.

Figure 4.2.5 Temperature history of an aluminum 2024-T351 specimen.
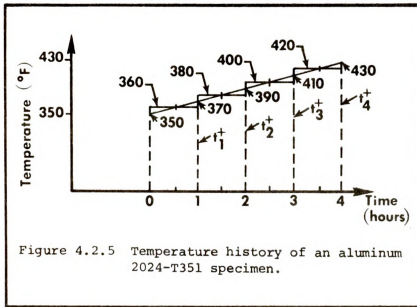
4.3 Example

To demonstrate the application of the findings mentioned in sections 4.1 and 4.2 to some practical engineering problems, the following example is given.

Consider a 1 1/2" thick aluminum 2024-T351 plate held on one side (x = 0) at 420 °F and on the other side (x = L) at 300 °F. The objective is to find (a) thermal conductivity (k) as a function of time, and the (b) temperature history. The problem is illustrated by Figure 4.3.1.

Solution: The general heat conduction equation can be written as [41]

$$\frac{\partial}{\partial x}\left(k\,\frac{\partial T}{\partial x}\right) = \rho c_p \frac{\partial T}{\partial t} \qquad (4.3.1)$$

Figure 4.3.1 Aluminum 2024-T351 plate maintained at 420 °F on one side and at 300 °F on the other.
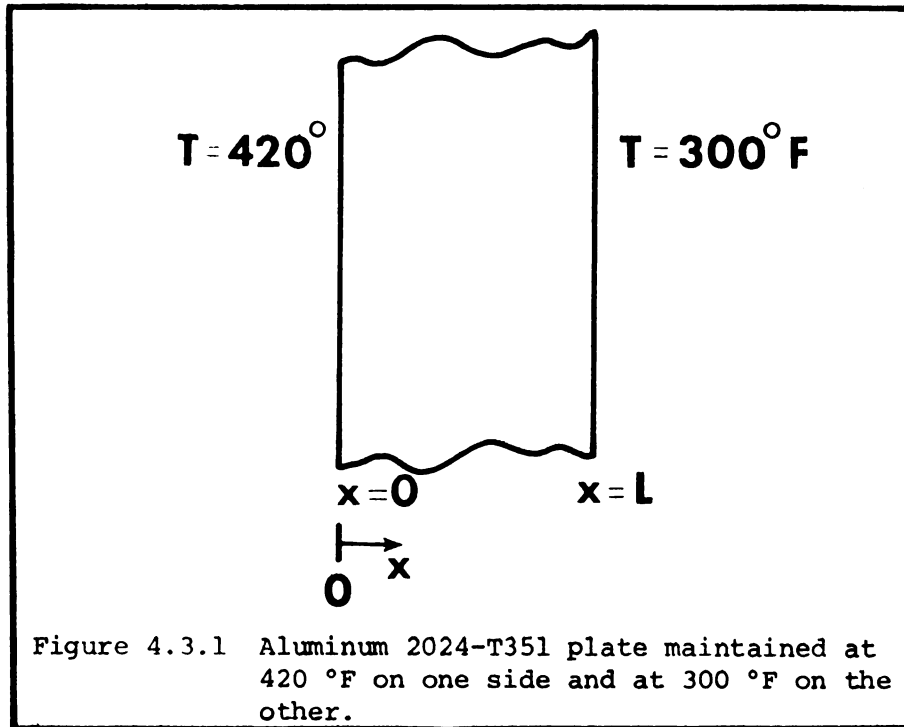
Since the time changes in temperature in the plate are very slow, Equation (4.3.1) can be modified for a quasi-steady state condition and therefore can be written as

$$\frac{\partial}{\partial x} \left(k \frac{\partial T}{\partial x}\right) \approx 0 \qquad (4.3.2)$$

Integrating (4.3.2) yields

$$\frac{q(t)}{A} = - k \frac{\partial T}{\partial x} \qquad (4.3.3)$$

where $\frac{q(t)}{A}$ is the heat flux in the positive x-direction. Consider now an approximate solution of (4.3.3).

Let the plate be divided into an arbitrary number of equal regions, say six. See Figure 4.3.2. Then Equation (4.3.3) can be approximated at time t_i by

$$\frac{q^i}{A} = k_1^i \frac{T_1 - T_2^i}{\Delta x} = k_2^i \frac{T_2^i - T_3^i}{\Delta x} = k_3^i \frac{T_3^i - T_4^i}{\Delta x} = k_4^i \frac{T_4^i - T_5^i}{\Delta x} =$$

$$k_5^i \frac{T_5^i - T_6^i}{\Delta x} = k_6^i \frac{T_6^i - T_7}{\Delta x} \qquad (4.3.4)$$

Figure 4.3.2   Geometry for thermal analysis of an aluminum 2024-T351 plate.

or
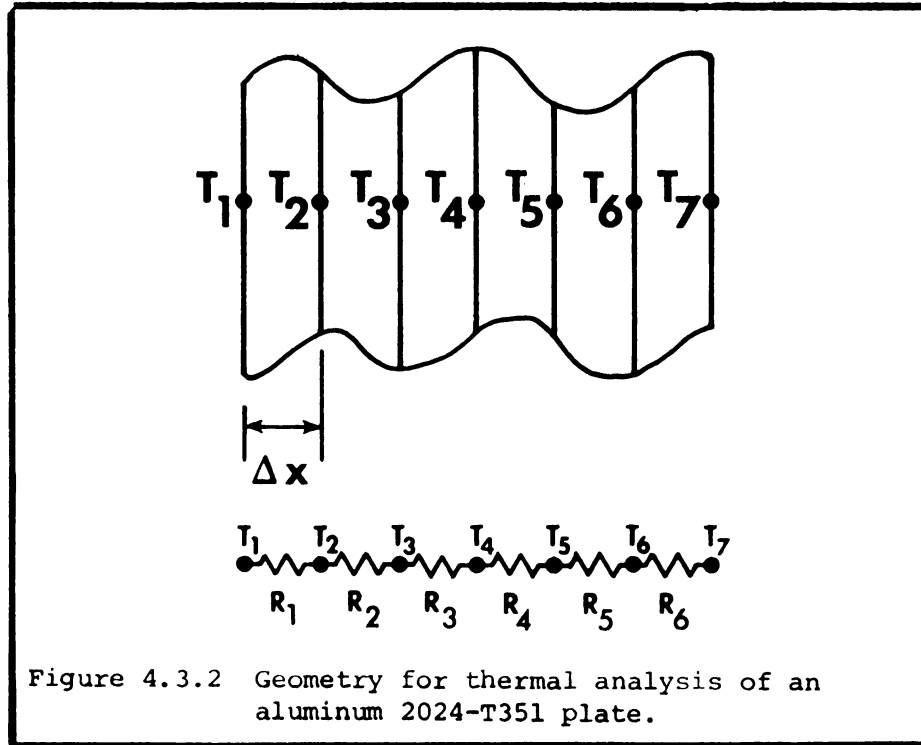
$$\frac{q^i}{A} = \frac{T_1 - T_2^i}{R_1^i} = \frac{T_2^i - T_3^i}{R_2^i} = \frac{T_3^i - T_4^i}{R_3^i} = \frac{T_4^i - T_5^i}{R_4^i} = \frac{T_5^i - T_6^i}{R_5^i} =$$

$$\frac{T_6^i - T_7}{R_6^i} \qquad (4.3.5)$$

where R_j^i is a thermal resistance defined by

$$R_j^i = \Delta x / k_j^i$$

Equation (4.3.5) can also be written as the set of equations

$$R_1^i \left(\frac{q^i}{A}\right) = T_1 - T_2^i$$

$$R_2^i \left(\frac{q^i}{A}\right) = T_2^i - T_3^i$$

$$R_3^i \left(\frac{q^i}{A}\right) = T_3^i - T_4^i \qquad (4.3.6)$$

$$R_4^i \left(\frac{q^i}{A}\right) = T_4^i - T_5^i$$

$$R_5^i \left(\frac{q^i}{A}\right) = T_5^i - T_6^i$$

$$R_6^i \left(\frac{q^i}{A}\right) = T_6^i - T_7$$

If the elements in Equation (4.3.6) are added then

$$(R_1^i + R_2^i + R_3^i + R_4^i + R_5^i + R_6^i) \frac{q^i}{A} = (T_1 - T_7)$$

or

$$\frac{q^i}{A} = \frac{T_1 - T_7}{R_1^i + R_2^i + R_3^i + R_4^i + R_5^i + R_6^i} \qquad (4.3.7)$$

To obtain an initial estimate for time zero evaluate $R_1^{0,\ell}$, $R_2^{0,\ell}$, ..., $R_6^{0,\ell}$ by first assuming that the temperature in the plate to be linear, i.e., assuming constant R_j. The ℓ superscript is an iteration index and starts at $\ell = 0$. Since the plate is divided into six equal regions of $\Delta x = 1/4''$ then one can take

$$T_1 = 420 \ ^\circ F$$

$$T_2^{0,0} = 400 \ ^\circ F$$

$$T_3^{0,0} = 380 \ ^\circ F$$

$$T_4^{0,0} = 360 \ ^\circ F$$

$$T_5^{0,0} = 340 \ ^\circ F$$

$$T_6^{0,0} = 320 \ ^\circ F$$

$$T_7 = 300 \ ^\circ F$$

For region one

$$R_1^{0,0} = \frac{\Delta x}{k_1^{0,0}}$$

Evaluate $k_1^{0,0}$ at the temperature at $\frac{\Delta x}{2}$ or at $\frac{T_1 + T_2^{0,0}}{2} = \frac{420 + 400}{2} = 410 \ ^\circ F$. Similarly evaluate $k_2^{0,0}$ at $390 \ ^\circ F$, etc.

The model (Equation (4.1.17)) must be used to evaluate the different k values. One must specify the

length of time that the plate is held at the above mentioned conditions.

For simplicity let calculations be performed at the zero, 0.5 and 1.0 hour times.

1. At time zero the temperature in the plate can be found in a relatively straightforward manner.

The mathematical model is

$$k^+ = 2t^+ - (t^+)^2$$

but since the time is zero

$$t^+ = \frac{t_i}{t_{max}} = 0$$

which results in

$$k^+ = \frac{k_i - k_{min}}{k_{max} - k_{min}} = 0$$

or

$$k_i = k_{min}$$

A first approximation for time zero uses the linear temperature profile given above. The k_{min} curve, Figure 4.2.1, is used in the following typical manner,

$$R_1^{0,0} = \frac{\Delta x}{k_1} = \frac{\frac{1}{4} \text{ in } \times \frac{1}{12} \frac{ft}{in}}{99 \frac{Btu}{hr\text{-}ft\text{-}F}} = 2.105 \times 10^{-4} \frac{ft^2\text{-}hr\text{-}F}{Btu}$$

and the rest of the values are given in Table 4.3.1. For temperatures below 350 °F k_{min} is evaluated in the manner described in Section 4.2. Substitute the initial estimates of $R_i^{0,0}$ given in Table 4.3.1 in Equation (4.3.7) to get

$$\frac{q^{0,1}}{A} = \frac{420 - 300}{13.502 \times 10^{-4}} = 8.885 \times 10^{+4} \ \frac{Btu}{hr \ ft^2}$$

Use the values $\frac{q^{0,1}}{A}$, $R_1^{0,0}$, ..., and $R_6^{0,0}$, in the elements of Equation (4.3.6) to obtain the more accurate values, $T_2^{0,1}$, $T_3^{0,1}$, ..., and $T_6^{0,1}$; since T_1 is known,

$$R_1^{0,1} \frac{q^{0,1}}{A} = T_1 - T_2^{0,1}$$

which can be solved for $T_2^{0,1}$,

$$2.105 \times 8.885 = 420 - T_2^{0,1}$$

$$T_2^{0,1} = 401.28 \ °F$$

The other temperatures for time zero and the first and second iterations are given in Table 4.3.2. There is little difference between the first and second iterations; hence the iterations are terminated.

2. Next find the temperature distribution at time 1 which is to be at 1/2 hour. During the time interval between time zero and 1/2 hour the aluminum alloy is undergoing metallurgical changes causing k to change. These changes are relatively small, however.

Table 4.3.1   Initial and 1st corrected estimates at time
              zero.

initial estimates at time 0				1st corrected estimates at time 0		
No.	Temp	$k_i^{0,0}$	$R_i^{0,0} \times 10^4$	Temp	$k_i^{0,1}$	$R_i^{0,1} \times 10^4$
1	410	99.0	2.105	410.64	99.0	2.105
2	390	99.0	2.105	391.92	99.0	2.105
3	370	96.90	2.157	372.99	98.0	2.126
4	350	88.5	2.355	352.97	88.8	2.346
5	330	87.6	2.378	331.97	87.6	2.378
6	310	86.74	2.402	310.71	86.74	2.402

Table 4.3.2   Temperatures at time zero.

Node No.	Estimate Temp., $T_i^{0,0}$	1st Corrected Temp., $T_j^{0,1}$	2nd Corrected Temp., $T_j^{0,2}$
1	420	420	420
2	400	401.28	401.28
3	380	382.56	382.56
4	360	363.42	363.67
5	340	342.52	342.83
6	320	321.42	321.70
7	300	300	300

Using the mathematical model for the thermal conductivity

$$\frac{k_i - k_{min}}{k_{max} - k_{min}} = 2(\frac{t_i}{t_{max}}) - (\frac{t_i}{t_{max}})^2$$

or

$$\frac{k_i - 99}{110 - 99} = 2(\frac{.5}{1.59}) - (\frac{.5}{1.59})^2 \quad at \quad 410.64 \ °F$$

where k_{min}, k_{max}, and t_{max} are obtained from Figures 4.2.1, 4.2.2, and 4.2.3 at 410.64 °F. Then

$$k_1^{1,1} = 104.82 \ \frac{Btu}{hr \ ft \ °F}$$

and the other values are given in Table 4.3.3. Therefore

$$R_1^{1,1} = \frac{\Delta x}{k_1^{1,1}} = \frac{\frac{1}{4} \ in \ x \ \frac{1 \ ft}{12 \ in}}{104.82 \ \frac{Btu}{hr \ ft \ °F}}$$

$$= 1.99 x 10^{-4} \ \frac{ft^2 \ hr \ °F}{Btu}$$

and the other values are given in Table 4.3.3.

Substituting in Equation (4.3.7) yields

$$\frac{q^{1,2}}{A} = \frac{420 - 300}{13.290 x 10^{-4}} \ \frac{Btu}{hr \ ft^2}$$

$$= 9.04 x 10^{+4} \ \frac{Btu}{hr \ ft^2}$$

Since $\frac{q^{1,2}}{A}$, $R_1^{1,2}$, $R_2^{1,2}$, ..., and $R_6^{1,2}$ are known, sub-stitute in the elements of Equation (4.3.6) to obtain the more accurate values of $T_2^{1,2}$, $T_3^{1,2}$, ..., $T_6^{1,2}$, i.e.,

$$R_1^{1,2} \frac{q^{1,2}}{A} = T_1 - T_2^{1,2}$$

$$1.99 \times 9.04 = 420 - T_2$$

$$T_2^{1,2} = 402.02 \ °F$$

and the other values are given in Table 4.3.4.

3. The aluminum plate is held for one hour at the above described conditions. Further metallurgical changes take place in the time interval 0.5 to 1 hour which causes k to change more. Again, use the mathematical model for k

$$\frac{k_i - k_{min}}{k_{max} - k_{min}} = 2(\frac{t_i}{t_{max}}) - (\frac{t_i}{t_{max}})^2$$

or for the temperature at $\Delta x/2$,

$$\frac{k_i - 99}{112.46 - 99} = 2(\frac{1}{1.58}) - (\frac{1}{1.58})^2 \quad \text{at } 411.01 \ °F$$

where, k_{min}, k_{max}, and t_{max} are obtained from Figures 4.2.1, 4.2.2, and 4.2.3 at 411.01 °F; then

$$k_1^{2,1} = 107.61 \ \frac{Btu}{hr \ ft \ °F}$$

The other values are given in Table 4.3.5 and the temperatures are given in Table 4.3.6.

Table 4.3.3 Estimates for 0.5 hour time.

No.	Temp	$k_i^{1,1}$	$R_i^{1,1} \times 10^4$
	1st corrected estimate at time 0.5 hour		
1	410.64	104.82	1.99
2	391.92	102.16	2.04
3	373.16	100.14	2.08
4	353.25	89.0	2.34
5	332.26	87.60	2.38
6	310.85	86.74	2.40

Table 4.3.4 Temperatures at time 0.5 hour.

Node No.	Estimate Temp., $T_j^{1,1}$	1st corrected Temp., $T_j^{1,2}$
1	420	420
2	401.28	402.02
3	382.56	383.58
4	363.67	364.78
5	342.83	343.63
6	321.70	322.11
7	300	300

Table 4.3.5 Estimates for 1.0 hour time.

	1st corrected estimate at time 1.0 hour		
No.	Temp	$k_i^{2,1}$	$R_i^{2,1} \times 10^4$
1	411.01	107.61	1.94
2	392.8	107.06	1.95
3	374.18	102.53	2.03
4	354.21	90.50	2.30
5	332.87	87.60	2.38
6	311.06	86.74	2.40

Table 4.3.6 Temperatures at time 1.0 hour.

Node No.	Estimate Temp., $T_j^{2,1}$	1st corrected Temp., $T_j^{2,2}$
1	420	420
2	402.02	402.09
3	383.58	384.09
4	364.78	365.35
5	343.63	344.12
6	322.11	322.15
7	300	300

As can be seen from this example, the thermal conductivity can be obtained by utilizing the mathematical model given by Equation (4.1.17) for a wide range of times and temperatures.

By knowing k one can predict the temperature history of the material which is very important in machine design applications.

This example was solved on the basis of the problem being a quasi steady-state since the changes take place very slowly.

If the property changes are to be very rapid under given conditions, then one can extend this example to the fully transient case by solving the following equation,

$$\frac{\partial}{\partial x} \left(k \frac{\partial T}{\partial x} \right) = \rho c_p \frac{\partial T}{\partial t} \ .$$

Notice, however, that a key assumption is that the thermal conductivity is a function of its composition which is discussed in Section 4.2.

CHAPTER V

SUMMARY AND CONCLUSIONS

The transient thermal properties (namely thermal
conductivity k and specific heat c_p) of aluminum 2024-T351
have been determined for the temperature range of 350 to
425 °F. These values have not previously been measured.
Due to the metallurgy of the alloy, precipitation occurs
above 350 °F. This causes changes in the properties with
time. No existing method and procedure was available for
measurement of the properties at the beginning of the
research. A method had been theoretically derived, however
[1]. Hence one task was the development of experimental
apparatus and procedures for measurement of the transient
thermal properties.

In order to determine the accuracy of the experi-
mental apparatus and testing procedure, a reference
material (Armco iron) was tested. It was found that the
measured k and c_p values of Armco iron were close to those
given in the literature [33].

It was also found that when aluminum 2024-T351 is
subjected to a high temperature in the range 350 to 425 °F,

certain changes in the microstructure take place and these changes influence the values of k and c_p. The temperature level influences k considerably and c_p to a lesser degree.

The changes in the k value of aluminum 2024-T351 at the high temperatures were found to exhibit a pattern. This pattern begins with the k value of the specimen when it is quickly brought to its nominal temperature (in the range 350 to 425 °F). The thermal conductivity then increases to some maximum value while being maintained at the nominal temperature. The rate of increase depends on the temperature level with the higher temperatures causing more rapid changes in k. The thermal conductivity may dwell at the maximum for a very short time. After which it starts to drop until it reaches a certain value where it remains constant with time. At this stage the aluminum becomes over-aged.

It was found that the over-aged value of k for aluminum 2024-T351 at room temperature as well as the high temperatures (350 to 425 °F) is close to that obtained by the regular annealing process although it tends to be slightly higher.

In order to predict the k values of aluminum 2024-T351 for different temperatures and times, a mathematical model was developed based on the data obtained in this study.

An example was given in which the mathematical model was utilized to predict the k values and consequently

the temperature histories of an aluminum 2024-T351 plate while it is undergoing transient changes in its thermal properties.

5.1 Recommendations for further research

This study is the first step toward determining and understanding of the transient thermal properties of aluminum 2024-T351 and other materials that undergo changes in its microstructure at elevated temperatures.

Further research is needed to refine what has already been accomplished, and to extend the study to other related areas such as solid state physics and material science.

Some of the suggestions are:

1. Further study of the heat losses in the present experimental stystem is needed. Also, aluminum 2024-T351 need to be tested at temperatures other than the ones in this study (example: 360, 370, 380, 390, 410, 420, 430 °F). The specimens to be used should be prepared from the same aluminum 2024-T351 bar that was utilized in this study.

2. Develop techniques to take more rapid measurements; for example the use of the electric heater may provide a technique for more rapid measurements. See [1].

3. Extend the experimental techniques to other
    materials that undergo phase changes at the
    elevated temperatures.

4. Investigate the possible relationship between the
    above mentioned thermal conductivity pattern of
    aluminum 2024-T351 at the elevated temperatures and
    lattice dislocation, stored energy, and other
    related matters of concern to the solid state
    physicists and material scientists.

5. Investigate experimentally the key assumptions of
    the use of the mathematical model for transient
    temperature histories of the aluminum alloy.

BIBLIOGRAPHY

BIBLIOGRAPHY

1. Beck, J. V., and S. Al-Araji. "Investigation of a new simple transient method of thermal property measurement," to be published in the Journal of Heat Transfer.

2. Carslaw, H. S., and J. C. Jaeger. "Conduction of Heat in Solids." Oxford: Oxford University Press, 2nd ed., 1959, p. 261.

3. Taylor, J. R., and W. M. Underwood. "An improved line-source apparatus for measuring thermal conductivity of plastics." The 5th conference on thermal conductivity, Denver, Volume 1, 1965, p. II-C-1.

4. Wechsler, A. E., and M. A. Kritz. "Development and use of thermal conductivity probes for soils and insulations." The 5th conference on thermal conductivity, Denver, Volume 1, 1965, p. II-D-1.

5. Sidles, P. H., and G. C. Danielson. "Thermal Diffusivity Measurements at High Temperatures." Thermoelectricity. Paul H. Egli, editor. New York and London: John Wiley and Sons, 1960, p. 270.

6. Parker, W. J., and R. J. Jenkins, C. P. Butler, and G. L. Abbott. "Flash method of determining thermal diffusivity, heat capacity, and thermal conductivity." Journal of Applied Physics, 32, 1961, p. 1679.

7. Beck, J. V. "PROPERTY." Computer Center, Michigan State University, East Lansing, Michigan, 1969.

8. Klein, A. H., H. R. Shanks, and G. C. Danielson. "Thermal Diffusivity of Armco Iron by Three Methods." The 5th conference on thermal conductivity, Denver, Volume 1, 1965, p. II-G-1.

9. Carter, R. L., P. D. Maycock, A. H. Klein, and G. C. Danielson. "Thermal Diffusivity Measurements with Radial Sample Geometry." Journal of Applied Physics, 36, 1965, pp. 2333-2337.

10. McElroy, D. L., and J. P. Moore. "Radial Heat Flow Methods for the Measurement of the Thermal Conductivity of Solids." Thermal Conductivity. R. P. Tye, editor. London: Academic Press, Volume 1, 1969, p. 185.

11. Flynn, D. R. "Measurement of Thermal Conductivity by Steady-State Methods in Which the Sample is Heated Directly by Passage of an Electric Current." Thermal Conductivity. R. P. Tye, editor. London: Academic Press, Volume 1, 1969, p. 241.

12. Powell, R. W. "Thermal Conductivity Determinations by Thermal Comparator Methods." Thermal Conductivity. R. P. Tye, editor. London: Academic Press, Volume 2, 1969, p. 275.

13. Laubitz, M. J. "Measurement of the Thermal Conductivity of Solids at High Temperatures by Using Steady-State Linear and Quasi-linear Heat Flow." Thermal Conductivity. R. P. Tye, editor. London: Academic Press, Volume 1, 1969, p. 111.

14. Null, M. R., and W. W. Lozier. "Measurement of Thermal Diffusivity by the Phase Shift Method." Thermal Conductivity. Ho and Taylor, editors. Proceedings of the Eighth Conference. New York: Plenum, 1969, p. 837.

15. Beck, J. V. "Analytical Determination of High Temperature Thermal Properties of Solids Using Plasma Arcs." Thermal Conductivity. Ho and Taylor, editors. Proceedings of the Eighth Conference. New York: Plenum, 1969, p. 1009.

16. Beck, J. V. "Calculation of Thermal Diffusivity From Temperature Measurements." Journal of Heat Transfer, 85, 1963, p. 181.

17. Beck, J. V. "Determination of Temperature-Variable Thermal Conductivity and Specific Heat From Transient Temperature Measurements." AVCO Corporation, Wilmington, Mass., 1961.

18. Beck, J. V. "Determination of Thermal Conductivity and Specific Heat From Transient Temperature Measurements, Part II." AVCO Corporation, Wilmington, Mass., 1961.

19. Beck, J. V. "Improved Methods to Calculate Thermal Diffusivity." AVCO Corporation, Wilmington, Mass., 1961.

20. Beck, J. V. "Methods to Simultaneously Determine Thermal Diffusivity and Heat Reaction From Experimental Data." AVCO Corporation, Wilmington, Mass., 1961.

21. Beck, J. V., and A. M. Dhanak. "Analytical Investigation of Optimum Heat-pulse Experiment for Determining Thermal Properties." The 5th Conference on Thermal Conductivity. Denver, Volume 1, 1965, p. I-A-1.

22. Beck, J. V. "Transient Sensitivity Coefficients for the Thermal Contact Conductance." Int. J. Heat Mass Transfer, Volume 10, 1967, pp. 1615-1617.

23. Beck, J. V. "Analytical Determination of Optimum, Transient Experiments for Measurement of Thermal Properties." Proceedings of the Third International Heat Transfer Conference, IV, Am. Inst. Chem. Engrs., New York, 1966, pp. 74-80.

24. Beck, J. V., and A. M. Dhanak. "Simultaneous Determinations of Thermal Conductivity and Specific Heat." ASME Paper No. 65-HT-14, 1965.

25. Beck, J. V. "Determination of Optimum, Transient Experiments for Thermal Contact Conductance." Int. J. Heat Mass Transfer. Volume 12, 1969, pp. 621-633.

26. Beck, J. V. "Nonlinear Estimation Applied to the Nonlinear Inverse Heat Conduct Problem." Int. J. Heat Mass Transfer, Volume 13, 1970, pp. 703-716.

27. Beck, J. V. "Sensitivity Coefficients Utilized in Nonlinear Estimation With Small Parameters in a Heat Transfer Problem." Transactions of the ASME, J. of Basic Engineering, Volume 92D, 1970, pp. 215-222.

28. Beck, J. V. "Transient Determination of Thermal Properties." Nuclear Engineering and Design, Volume 3, 1966, pp. 373-381.

29. Beck, J. V. "The Optimum Analytical Design of Transient Experiments for Simultaneous Determinations of Thermal Conductivity and Specific Heat." Ph.D. Thesis, Michigan State University, East Lansing, Michigan, 1964.

30. Pfahl, R. C., Jr., and B. J. Mitchel. "Simultaneous Measurement of Six Thermal Properties of a Charring Plastic." Int. J. Heat Mass Transfer, 13, 1970, pp. 275-281.

31. Van Fossen, G. J. "Model Building Including Discrimination Between Rival Mathematical Models in Heat Transfer." Ph.D. Thesis, Michigan State University, East Lansing, Michigan, 1973.

32. Kavianipour, A. "Analytical Estimation of Thermal Properties and Variation of Temperature in Asphaltic Pavements." Ph.D. Thesis, Michigan State University, East Lansing, Michigan, 1971.

33. Touloukian, Y. S. "Thermophysical Properties of High Temperature Solid Materials." New York: The MacMillan Co., 1967.

34. Lucks, C. F., and H. W. Deem. "Thermal Properties of Thirteen Metals." ASTM special technical publication No. 227, 1958.

35. Carslaw, H. S., and J. C. Jaeger. "Conduction of Heat in Solids." Oxford: Oxford University Press, 2nd ed., 1959, p. 59.

36. "Aluminum Standards and Data." New York: The Aluminum Association, 1970-1971, 2nd ed.

37. Henning, C. D., and R. Parker. "Transient Response of an Intrinsic Thermocouple." Journal of Heat Transfer, 1967, p. 146.

38. Beck, J. V. "Parameter Estimation in Engineering and
     Science." Bound notes at Michigan State Uni-
     versity for ME 818, 1972.

39. Dye, J. L., and V. A. Nicely. "A general purpose
     curve-fitting program for class and research
     use." Journal of Chemical Education, Volume
     48, 1971, pp. 443-448.

40. Frame, J. S. Private communication, Michigan State
     University, East Lansing, Michigan, 1973.

41. Arpaci, V. "Conduction Heat Transfer." Reading,
     Mass.: Addison-Wesley, 1966.